ISSN 1173-5996

Flammability of Upholstered Furniture Using the Cone Calorimeter

by
Andrew R Coles

Supervised by

Dr Charley Fleischmann

Fire Engineering Research Report 01/1

March 2001

This report was presented as a project report as part of the
M.E. (Fire) degree at the University of Canterbury

School of Engineering
University of Canterbury
Private Bag 4800
Christchurch, New Zealand

Phone 643 364-2250
Fax 643 364-2758
www.civil.canterbury.ac.nz

ABSTRACT

With the development of modern materials, upholstered furniture posses a high fuel load and life safety threat. Due to the rapid growth rate of the organic material and the toxic combustion products, these fires usually lead to hazardous conditions and uncontrollable fires.

The heat release of a burning item is considered as the most important property in fire hazard analysis. The application of the European CBUF programme to New Zealand upholstered furniture is an ongoing initiative of the University of Canterbury.

The combustion behaviour of 3 foams combined with 14 fabrics were analysed using the cone calorimeter to provide data to predict full scale furniture fires. The major results that were derived form the Cone Calorimeter results is there is a pronounced fabric effect with regard to flammability and combustion characteristics.

Model I from the CBUF programme was applied to New Zealand furniture as to predict potential fire hazards from these small-scale results. It was found that fabrics that posed the greatest fire hazard were PE, PP, olefin and viscose which consistently produced high peak HRR, high total heat released and fast times to peak HRR and times to untenable conditions. The foams that posed the greatest fire hazard when coupled with these fabrics was a standard polyurethane foam and a high density polyurethane foam.

The ability of Model I to compensate for foam and fabric chemical compositions was limited which was reflected throughout the results. Its dependence on various experimentally variables limit its ability and power to predict various parameters if unattainable. Model I can be considered a conservative design model with resect to peak HRR, total heat released and time to peak HRR.

ACKNOWLEDGMENTS

Charley Fleischman for his persistence and help throughout his research, especially when there was trouble with the Cone Calorimeter.

Dominic Mahoney and Flora Chen for there help in the specimen preparation stage. If it was not for their help this process would have taken forever.

Thanks is extended to Grant Dunlop for his expertise and help with setting up the Cone Calorimeter, and Mike (the electrician) for setting up the new data logging equipment.

Thanks must be extended to the New Zealand Fire service for their interest in the ME Fire programme at the University of Canterbury. Thanks are also extended to Cosgrove Major Lincolne Scott for the part time employment throughout the year and technical advice.

NZFSC for their financial support throughout this project and to the ME Fire program at the University of Canterbury.

Thanks must go to Ashley T Petersen for his time and advice proofreading this report.

Thanks to fellow students of the ME Fire class of 2000. Many fun times have been had that will be reflected on in the future.

Finally, a debt of gratitude is owed to my parents for their support and help throughout, which made this year worth while. Kia ora.

TABLE OF CONTENTS

LIST OF FIGURES

LIST OF TABLES

NOMENCLATURE

Notation	Description	Units
A_0	Area of orifice plate	m^2
C	Calibration constant	--
$C'M$	Flow coefficient of the orifice plate	--
g_c	Dimensionless gravity constant (1.0 kg.m/N.s^{-2})	--
q''_{total}	Total heat released during the entire test	MJ/m^2
$\dot{q}''_{peak}$	Peak HRR from cone calorimeter curve	kW/m^2
$\dot{q}''_{pk\#2}$	Second peak HRR at 35 kW/m^2 exposure	kW/m^2
$\dot{q}''_{trough}$	Trough of Cone Calorimeter HRR curve	kW/m^2
$\dot{q}''_{60}$	Average heat release rate from time of ignition to 60 s later	kW/m^2
$\dot{q}''_{120}$	Average heat release rate from time of ignition to 120 s later	kW/m^2
$\dot{q}''_{180}$	Average heat release rate from time of ignition to 180 s later	kW/m^2
$\dot{q}''_{300}$	Average heat release rate from time of ignition to 300 s later	kW/m^2
HRR	Heat Release Rate	kW/m^2
$\Delta h_{c,eff}$	Effective heat of combustion	kJ / kg
m_i	Initial specimen mass (with foil)	g
m_f	Final specimen mass (with foil)	g
$\dot{m}_e$	Mass flow rate of exhaust products	kg/s
m_{soft}	Mass of the soft combustible parts of the full-scale item which includes foam, fabric, interliners etc., but does not include rigid support pieces.	kg
$m_{comb,total}$	Entire combustible mass (kg)	kg
M_i	Molecular weight of species i	g / mol
P_a	Atmospheric pressure	Pa
Δp	Pressure differential across orifice plate in exhaust duct	Pa
r_0	Stoichiometric oxygen to fuel ratio	--
RH	Relative humidity of ambient air	%

Style factor A and B	Style factors for the full-scale furniture.	(--)
t_{ig}	Time to ignition from the start of the test.	s
$t_{pk\#1}$	Time to first peak of the Cone Calorimeter HRR curve, from start of test	s
Δt	Sampling time interval	s
T_e	Temperature of the exhaust	°C
T_{ref}	Temperature of ambient air	°C
x_i^o	Ambient mole fraction of species i	--
x_i^a	Measured mole fraction of species i (by analyser)	--

Greek Notation	**Description**	**Units**
α	Expansion factor ≈ 1.105	--
β	Stoichiometric expansion factor	--
ϕ	Oxygen depletion factor	--
ρ_{ref}	Density of ambient air	kg/m^3

1 INTRODUCTION

1.1 General introduction

As part of a larger research project on domestic furniture, this project will look at the fire growth potential of several foam and fabric combinations used in common NZ furniture. An extensive series of cone calorimeter experiments on several foam and fabric combinations were conducted to determine the combinations posing the greatest fire hazard.

1.2 Impetus for this research

With the development of modern materials, upholstered furniture posses a high fuel load and life safety threat. Due to the rapid growth rate of the organic material and the toxic combustion products, these fires usually lead to hazardous conditions and uncontrollable fires.

The research presented here is part of an ongoing initiative of the University of Canterbury (UC) Fire Engineering group in assessing the flammability and combustion characteristics of NZ upholstered furniture materials. Previous research conducted at the University of Canterbury (see section 2.3) studied the *Combustion Behaviour Of Upholstered Furniture (CBUF) Research Programme* [6] conducted in Europe, and the application of various derived models to New Zealand upholstered furniture.

1.3 Direction of this work

The body of this research extends from Denize's research [7] where three foams that were previously used will be examined and compared with a variation of fabrics to assess fabric flammability and the most potentially hazardous foam fabric combination. The foams selected were deemed common construction foams utilised in commercial furniture and seating padding.

Determination of the test fabrics involved surveying a local furniture supplier to assess the range and blends of fabrics that are on offer to the consumer. This produced a better representative sample of the fabrics available and thus meaningful experimental results.

Testing of the specimens were conducted at the Fire Testing laboratory, University of Canterbury, New Zealand. Bench scale tests were conducted in the Cone Calorimeter to determine the most hazardous foam and fabric combination. Application of Model I of the CBUF research programme was applied to the small-scale results to provide predictions of potential fire hazards of full-scale furniture.

1.4 Outline of this report

The body of this report gives a qualitative outline of the steps taken throughout this research project. Chapter 2 gives an overview of the previous research at both the University of Canterbury and abroad. Guidelines to the selection of the foams and fabrics are provided in Chapter 3. The equations used in *Oxygen Consumption Calorimetry* and their application to the UC Cone Calorimeter are provided in Chapter 4. Chapters 5 and 6 describe the experimental facilities used and the experimental procedure that was followed. Chapter 7 discusses and summarises the observed combustion behaviour from the cone calorimeter with the conclusions of this section outlined in chapter 8. Chapter 9 of this research examines the application of Model I from the CBUF programme to exemplary New Zealand furniture, implementing the small-scale combustion test results. The overall conclusions and recommendations are provided chapter 10.

2 PREVOIUS RESEARCH

2.1 Introduction

The basis of this research is centred on the experimental practices and techniques of the European CBUF Research Programme [6]. Other postgraduate studies carried out at the University of Canterbury related to the CBUF research was by Tony Enright [8], James Firestone [9] and Hamish Denize [7]. This chapter provides a summary of these research topics and their conclusions.

2.2 European CBUF Project

In the United Kingdom (UK), regulations address the combustion behaviour of upholstered furniture. When they came into force, they introduced a major change of acceptance level in the UK. The UK regulations were adopted hastily, therefore validations and precision studies are lacking. The European Commission, facing the same issue, had the opportunity to ask for a general study of the combustion behaviour of upholstered furniture.

The CBUF (Combustion Behaviour of Upholstered Furniture) Research Programme [6] on the fire safety of upholstered furniture began in early 1993. This was in response to alarming reviews of the European statistics for fire fatalities associated with burning upholstered furniture. The aim was to provide a foundation for the development of test methods for measuring the burning behaviour of upholstered furniture. These test methods would then be needed either for the implementation of possible European Union legislation or standardisation. The intention of the CBUF project was to develop a useful design procedure for hazard assessment based on a limited number of typical items. From these results a series of three mathematical models were derived to predict the burning characteristics for furniture designs and fire room atmospheres.

The test methods used in the CBUF programme are the Cone Calorimeter (ISO 5660), the Room/Corner test (ISO 9705), and the Furniture Calorimeter (NT FIRE 032). The main issue therefore was to develop quality assured test protocols that were suitable and robust enough for routine testing.

The CBUF Programme consisted of five series' of test furniture. Series 1 represented the European marketplace, domestic type seating furniture and mattresses purchased in the UK, Eire, France, Germany, Spain and Sweden. Series 2, 3, 4 and 5 were "custom made" furniture. The furniture was designed to study the effect of material type, construction and ventilation conditions. The designs also facilitated the formation of predictive mathematical models.

The Cone Calorimeter (ISO 5660) tested bench scale items consisting of composite materials with various interliners and padding. The data was then used to develop three mathematical models to predict the burning behaviour of full-scale furniture. The Furniture Calorimeter was used for testing of full-scale furniture and the prediction of various room scenarios. These room scenarios were then compared with computer modelling packages CFAST (a zone model) and JASMINE (a field model).

Collation of the CBUF data was assembled in a FDMS data base and presently contains over 1500 tests of various types such as room tests, furniture calorimeter tests, cone calorimeter tests on composites and components, and LIFT tests.

2.3 Other CBUF work at the University of Canterbury

2.3.1 Enright's research

Enright's research [8], conducted at the University of Canterbury Fire Testing Laboratory, focused on calorimetric techniques, uncertainty analysis of calorimetric techniques, and instrumentation. The validation of furniture modelling and the application of CBUF Model I and II to New Zealand furniture were also investigated.

The extent of this research examined two techniques of measuring heat release, oxygen consumption and thermochemistry, as well as a comparison. This was achieved by burning a series of small-scale furniture composites and 13 full-scale furniture items in the UC Cone Calorimeter and Furniture Calorimeter. The results were used to validate the applicability of the CBUF Furniture fire models to typical New Zealand furniture.

The data showed that the application of Model I to New Zealand Furniture proved to give a poor representation of the burning characteristics especially the "goodness of fit" for the heat release rate. The model tended to pronounce the peak HRR and produce an extended burning period. The application of Model II proved to be a better predictor, compared to Model I, as it characterises the HRR history rather than the furniture properties.

2.3.2 Firestone's research

Firestone [9] analysed the prediction of "full scale" combustion behaviour from bench-scale test data. The prediction analysis was based on *Model I* from the CBUF Research Programme [6]. The foams and fabrics used were those typically found on the market. *High Resilience Polyurethane* and *Standard Polyurethane* foams were combined with a 100% polypropylene and 100% cotton/linen fabrics.

Data used from the fire-testing laboratory at CSIRO, in Melbourne, included 141 full-scale furniture tests and 33 bench scale tests. In addition to this, 22 bench-scale tests were conducted in the UC Fire Testing Laboratory, Christchurch.

Major findings of Firestone's research showed that *Model I* is a good predictor of the full-scale results for the *Standard Polyurethane* foam with both fabric combinations. The *High Resilience Polyurethane* foam was over predicted by the model. It also showed that the foam/fabric interaction was a crucial factor that determined combustion severity.

2.3.3 Denize's research

Denize's research [7] evaluated the combustion severity of New Zealand upholstered furniture materials with 7 different polyurethane foams (including two fire retardant) and two fabrics, 100% polypropylene and 95% wool, 5% synthetic. Testing involved 63 bench-scale Cone Calorimeter tests and 10 full-scale armchair Furniture Calorimeter tests which were conducted at the Fire-testing Laboratory, University of Canterbury. All experimental procedures followed the methods and protocol of the European CBUF Research Programme [6].

Major observations were; the woollen fabric was able to withstand the radiant heat for longer periods compared to the polypropylene fabric. This had the effect of prolonging ignition times and increasing times to the peak heat release for both the cone and furniture calorimeter tests.

The fire retardant foams tended to show combustion characteristics significantly "out of character" compared with the other foams. They had prolonged ignition times and time to peak HRR in the Cone and Furniture Calorimeters.

Model I of the CBUF Research Programme was applied to the New Zealand furniture materials. This model compares the peak heat release rate (kW/m^2), the time to this peak (sec), and the total amount of heat released (MJ), from burning tests conducted on full-scale armchairs. It was concluded that the model does not accurately predict the full scale burning characteristics, but more of a conservative design model.

3 MATERIAL SELECTION

3.1 Introduction

This section details the examination process of the materials that were selected for investigation of their flammability behaviour. The foams used are an extension of previous research conducted by Denize [7]. The purpose is to compare the behaviour of three common foams combined with other common retail fabrics. The fabrics examined are a selection of blends and designs retailers have available to the public.

3.2 Polyurethane Foam Selection

The selection of the foams analysed was as a continuation of Denize's [7] research. The criteria used to determine the foams was

- Foam grade and its applications
- Common usage by manufacturers
- Availability of the product

The denser foams of each application category were selected, along with a *fire retardant foam* (J). The codes assigned to each foam, basic colour, density and application are listed in Table 3-1. The coding systems used are to remain consistent with other CBUF research previously conducted at the University of Canterbury.

Table 3-1: Tabulated data of foam code, colour, density and their applications

Foam Code	*Colour*	*Density (kg/m^3)*	*Application*
J	Yellow	38	Public auditoriums; Public transport seating
K	Green	29	Domestic and commercial seat-backs, cushions
L	Grey	38	Public auditoriums; Maritime berths and seating

3.3 Fabric Selection

Most of the materials that are found in modern upholstery are a combination of thermoplastic fibres woven together with other inorganic cellulose blends to provided physical properties such as texture and durability. The major types of thermoplastic fibres of concern are olefin (including polyethylene and polypropylene), vinyl (including acrylic) polyamide (nylon), acetal, and thermoplastic polyester. Non-thermoplastics used are cellulosics such as cotton and viscose rayon.

Fabric selection was done by examining a local retail furniture store for the most common materials available to the consumer. A range of suppliers and designs were found that consisted of different compositions and blends of organic and inorganic polymer fibres. Three hundred and forty 'different' compositions were found. Denize investigated the behaviour of 2 fabric compositions, 100% polypropylene and 95% wool, 5% Synthetic.

The fabrics available to the consumer all have a combination of organic polymers. The examination process also indicated that it was typical for a furniture designer to use a common fabric supplier for its products.

The criteria used to select the fabrics were based on

- The composition of the fabric
- The recurrence of the blend and composition in fabric manufacturers designs
- The similarity of fabric compositions between each manufacturer
- A general representation of the fabrics used in the New Zealand furniture industry

A fabric blend is a combination of the type of weave that is used in the fabric, whether it is the thickness of the weave or the way that it is constructed, and the combination of the polymers used. The way that a fabric is blended influences the texture of the fabric and its aesthetic appeal to the consumer.

The final 13 fabrics selected were determined to give a good representation of what is commonly used in the furniture industry. Fabric 28 has been specified to exceed BS

5852 [4]. The purpose of this fabric selection was to gauge how the other fabrics behaved in comparison to a "standard" flame resistant fabric. Table 3.2 indicates the codes, general colours and composition of each fabric.

Table 3-2: Tabulated data of fabric code, colour, and composition

Fabric	Colour	Composition
23	Multi colour pattern	100% Polypropylene
24	Grey	100% Polyester
25	Yellow	100% Acrylic Chenille
26	Royal blue + black stripes	100% Olefin
27	Gold	100% Nylon Pile
28	Red felt	100% Cotton
29	Ivory with blue checked weave	42% Polyester, 58% Acrylic
30	Light blue with yellow pattern	51% Polyester, 49% Cotton
31	Green	50% Polyester, 50% Olefin
32	Blue	51% Polyester, 49% Viscose
33	Dark green	60% Polypropylene, 40% Polyester
34	Light and Dark blue	31% Polyester, 21% Acrylic, 48% Cotton
35	Off yellow with blue background	43% Polyester, 41% Acrylic, 16% Olefin
36	Light brown with black weave	39% Polyester, 40% Acrylic, 21% Viscose

3.4 Specimen codes.

The codes assigned to each sample include the foam code, fabric code and the sample number. The CBUF protocol specifies that three samples be tested for each composite combination. Hence, for a specimen that consists of foam J and fabric 23 the corresponding codes assigned to the triplicate batch are J-23-1 through to J-23-3. This system is developed to enable easy recognition of each specimen for the purpose of data collection. Appendix A provides details of each specimen and the masses of each constituent in the composite.

4 OXYGEN CONSUMPTION CALORIMETRY

4.1 Introduction

This chapter gives an overview of the oxygen consumption technique[1] and the general equations and assumptions used in the analysis of heat release rate, HRR. Section 4.2; Calculation of Heat Release Rate, is a summary of the expressions developed in Enright's research [8] which have been implemented in the use of the UC Cone Calorimeter. The remaining sections summarise the assumptions and generalisations associated with oxygen consumption calorimetry.

4.2 Calculation of Heat Release Rate

Traditionally, heat release rates have been measured using a thermochemistry technique by examining the heat lost by the system and through a total system energy balance. A new technique developed referred to as "Oxygen Consumption Calorimetry" looks at the amount of heat released per unit of oxygen consumed. The technique requires two simple measurements, the volumetric flow of air and combustion products through the system, and the concentration of oxygen in the exhaust duct. By comparing the inflow of ambient oxygen to the outflow in the exhaust, the amount of oxygen consumed is found. The generalised heat release rate in equation 4.1 shows the linearly proportional relationship between these two variables.

$$\dot{q} = \frac{\Delta h_c}{r_0}\left(\dot{m}_{O_2}^{o} - \dot{m}_{O_2}\right) \qquad [4.1]$$

This relationship can then be reduced to equation 4.2 by considering the oxygen depletion factor, ϕ.

$$\dot{q} = \frac{\Delta h_c}{r_0}\left(\dot{m}_{O_2}^{o} - \dot{m}_{O_2}\right) \qquad [4.2]$$

[1] Oxygen Consumption Calorimetry examines the amount of energy released per unit of oxygen consumed. This technique is used for examination of organic liquids or solids.

The oxygen depletion factor is an expression of the fraction of incoming air that is fully depleted of its oxygen during the process. Equation 4.3 shows the equality between the required mass flows and the measurable mole fractions recorded by the analysers.

$$\phi = \frac{\dot{m}^o_{O_2} - \dot{m}_{O_2}}{\dot{m}^o_{O_2}} = \frac{\left(x^o_{O_2} - x^a_{O_2}\right)}{x^o_{O_2}\left(1 - x^a_{O_2}\right)} \qquad [4.3]$$

The oxygen mass flow can then be determined by equation 4.4.

$$\dot{m}^o_{O_2} = x^o_{O_2}\left(1 - x^o_{CO_2} - x^o_{H_2O}\right)\frac{M_{O_2}}{M_a}\dot{m}_a \qquad [4.4]$$

To obtain an expression for the flow rate of incoming air, in terms of measurable variables, it is related to the mass flow rate of the exhaust gas by equation 4.5.

$$\dot{m}_a = \frac{\dot{m}_e}{1 + \phi(\alpha - 1)} \qquad [4.5]$$

The combustion factor α is expressed as a function of the stoichiometric expansion factor β, by equation 4.6.

$$\alpha = 1 + x^o_{O_2}(\beta + 1) \qquad [4.6]$$

By combining equations 4.2 through 4.6, an expression for the heat release rate is given in equation 4.7 in terms of measurable and known variables.

$$\dot{q} = \frac{\Delta h_c}{r_0}\frac{M_{o_2}}{M_a}\frac{\phi}{1 + \phi(\alpha - 1)}x^o_{O_2}\left(1 - x^o_{CO_2} - x^o_{H_2O}\right)m_e \qquad [4.7]$$

4.2.1 Other governing equations

The remaining equations used to calculate the heat release rate are provided below. The mass flow in the exhaust duct is given in equation 4.8. It relates the pressure differential across the orifice plate in the exhaust duct, the temperature of the exhaust gases calibration constant, C.

$$m_e = C\sqrt{\frac{\Delta p}{T_e}} \qquad [4.8]$$

The calibration constant, C given by equation 4.9 represents a mass flow constant that is characteristic for each individual apparatus. It is a constant experimentally determined

from the methane HRR calibration. This constant is compared at the start of each day testing and is compared to the previous constant and modified accordingly.

$$C = C' M A_0 \sqrt{2.g_c.T_{ref}.\rho_{ref}} \qquad [4.9]$$

Ambient water vapour concentration is required to determine the dry mole fraction of oxygen after combustion. Equation 4.10 shows the relationship between the ambient pressure, temperature and relative humidity, RH.

$$x^0_{H_2O} = 1.19\times10^8 \frac{RH}{P_a} e^{\left(\frac{-3816}{T_{ref}-46}\right)} \qquad [4.10]$$

4.3 Assumptions

Because oxygen consumption method only requires measurements of the exhaust flow, and its associated oxygen concentration, no thermal insulation is required, compared to a thermochemistry where often-cumbersome enthalpy conservation is required.

The combustion factor, α, and the stoichiometric expansion factor β, are related to each other by equation 4.6. The stoichiometric expansion factor β is defined as the ratio of moles of products to the number of moles of oxygen consumed in a stoichiometric equation. A minimum value is, β=1 for pure carbon and β=2 for pure hydrogen. Unless the fuel composition is known, an average value of β=1.5 is used which corresponds to α = 1.105. For more values of α and β see Babrauskas [1].

4.3.1 Huggett's Constant

The heat release rate of an organic liquid or solid can be determined by measuring the amount of oxygen consumed during combustion. It was reported by Huggett [12] that most organic compounds have an average of 13.1 MJ/kg of O_2 consumed, which varied by $\pm$4% for a range of organic liquids, polymers and fuels. Methane has a value of $\Delta h_c / r_0$=12.54 MJ/kg which was used in the calibration procedure. For more information on expected values for $\Delta h_c / r_0$ see Huggett [12].

5 EXPERIMENTAL FACILITIES

5.1 Introduction

This chapter provides an overview of the equipment used at the University of Canterbury Fire testing laboratory. Details of the testing apparatus and components are outlined in the following chapter. The UC Cone Calorimeter was characterised by Enright [8] to comply with ISO 5660.1 and the standard test method as amended in Appendix A6 of the final CBUF report.

5.2 University of Canterbury Cone Calorimeter

The proceeding section outlines the components that are installed on the UC Cone Calorimeter. Figure 5-1 below is a schematic of the UC Cone Calorimeter sampling apparatus.

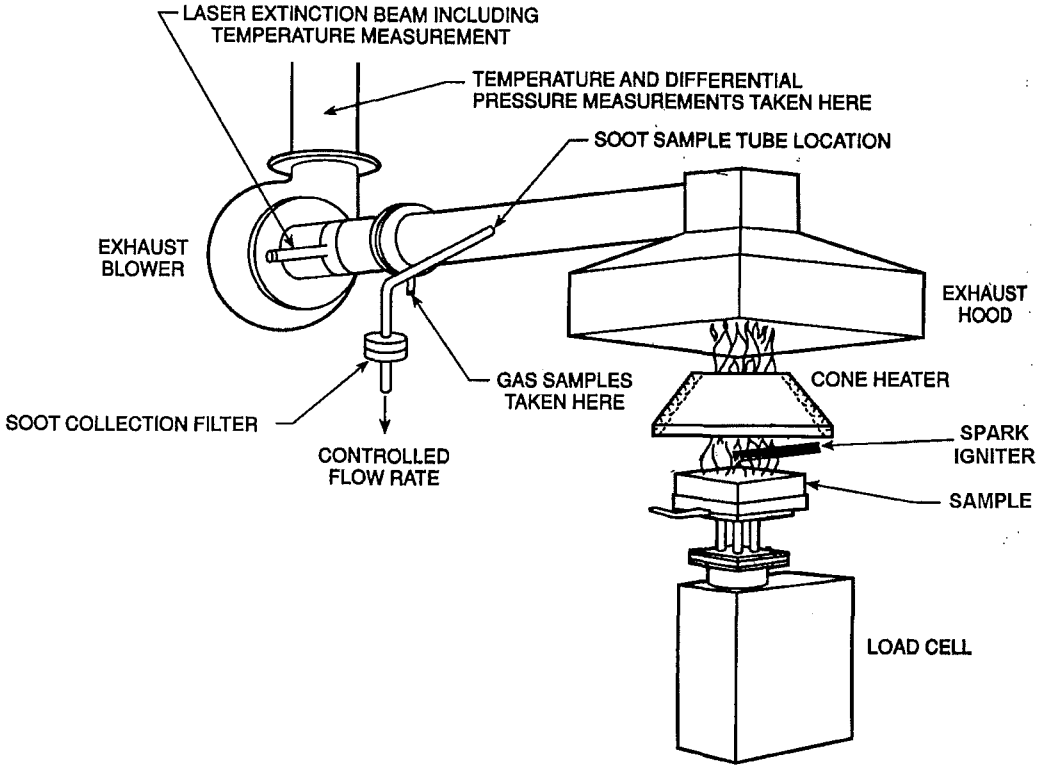

Figure 5-1: Schematic of horizontal Cone Calorimeter set-up adopted from Babrauskas [2].

5.2.1 Cone heater

The purpose of the heating element is to improvise heat fluxes that items would be exposed to in realistic fires. This may range up to 150 kW/m^2. The term "cone" is derived from the conical shape that the heating element is wound. The purpose of using an electrically powered heating element is to ensure the specimen is exposed to a constant radiant flux throughout burning. The element temperature is measured by three thermocouples across the heater coil and is monitored by an electronic controller that averages the three-thermocouple readings to ensure the element temperature remains constant. The corresponding temperatures are converted to a heat flux using a heat flux gauge (see section 6.2.2.3 of the Final CBUF report)

5.2.2 Specimen mounting

Specimens are mounted on a horizontal orientation pedestal on the mass scale. The height of each specimen can be altered by adjusting the pedestal height to ensure there is a 25mm gap between the top of the specimen and the bottom of the cone element.

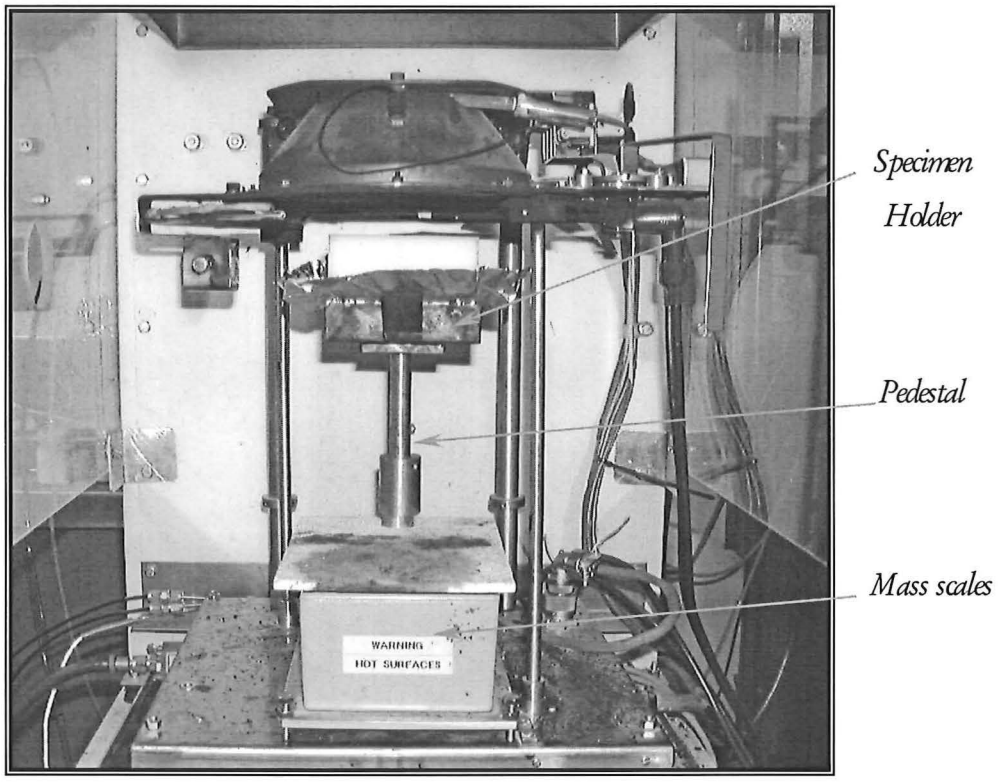

Figure 5-2: Depiction of how specimens were mounted on the UC Cone Calorimeter.

A 12mm thick Kaowool blanket is located underneath the specimens, which fits inside the horizontal specimen holder. For more details refer to paragraph A6: 1.3.2.1 of the CBUF final report and figure 2 of ISO 5660-1:1993 respectively. Figure 5-2 is an indication of how specimens are mounted. It is important to ensure the aluminium foil is removed from the sides of the specimen once placed in the specimen holder.

5.2.3 Spark Igniter and Specimen Shield

The spark igniter and specimen shield are located directly below the opening in the heater base plate. The spark igniter consists of two spark plug powered tungsten electrodes that produce a spark at one-second intervals. The spark igniter is located such that the source of ignition is situated approximately 13mm above the centre of the specimen.

The "Specimen shield" is used to prevent radiation exposure to the specimen before the start of the test (t=0). In the closed position, it completely covers the opening in the heater base plate. The specimen shield is manually opened via a mechanical lever.

5.2.4 Gas Sampling Apparatus

The gas analysing component of the sampling train includes a Servomex 540A paramagnetic oxygen analyser for O_2, and a Siemens ULTRAMAT 6.0 NDIR gas analyser (dual-cell, dual-beam) for CO_2 and CO. The exhaust blower, as indicated in Figure 5-1, provides a steady flowrate of exhaust gases in the sampling port. The pressure differential and temperature are recorded downstream of the exhaust fan to obtain a corresponding exhaust flowrate.

The gas analysers incorporate other support components, which can be seen in Figure 5-3. These include:

- A pump to provide negative pressure within the system to draw sampling gas from the exhaust flute
- A soot filter
- A cold trap which condenses out the moisture in the exhaust gas

- Dryrite crystals upstream of the cold trap to remove any remaining moisture that may pass through the cold trap
- Serial data boxes that are used in conjunction with computer software to log recorded data

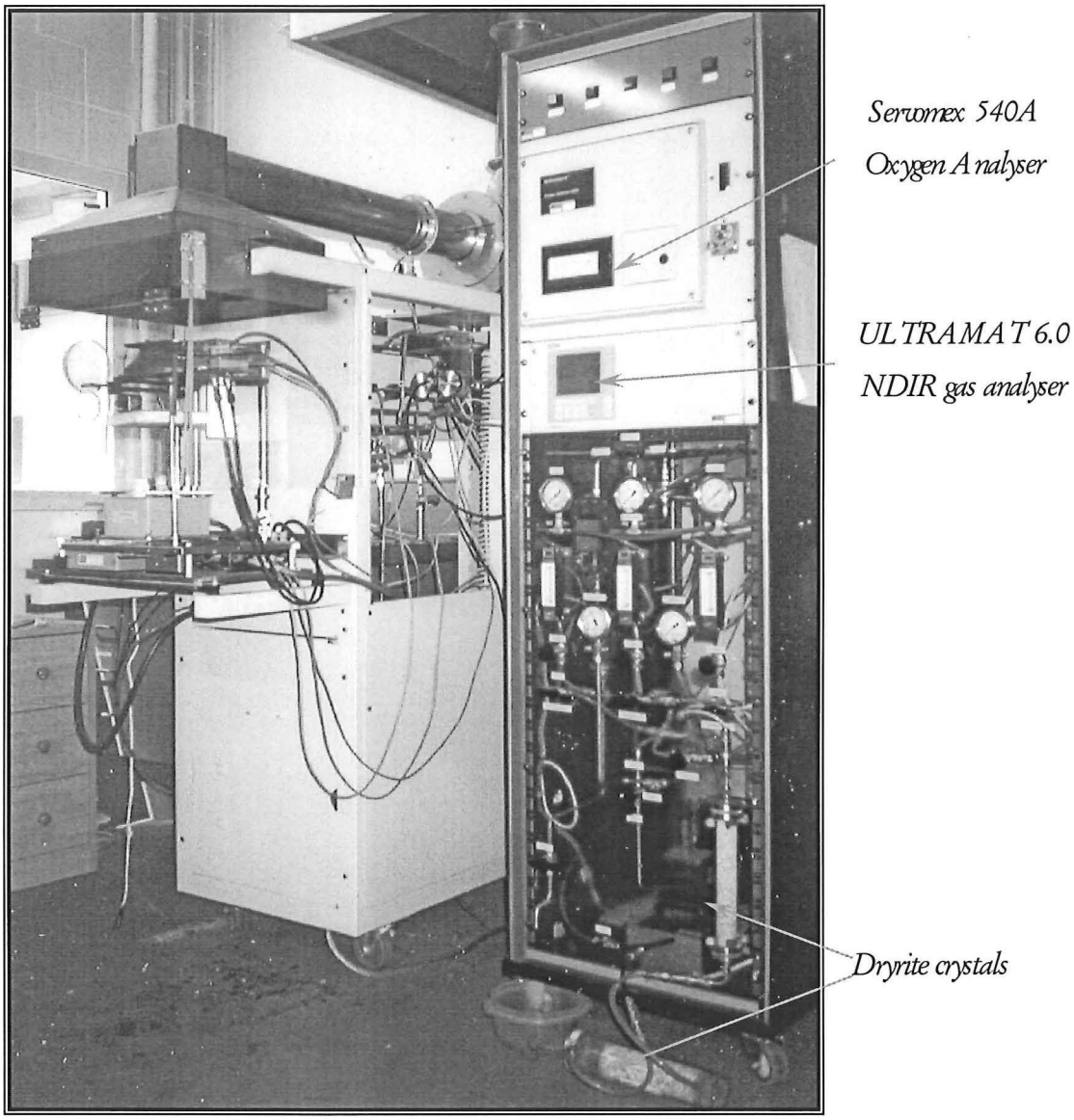

Figure 5-3: Photograph of gas analyser instrumentation and the Cone Calorimeter.

As water vapour concentration is not measured, Dryrite crystals are used to remove the water from the atmospheric air. The ambient water vapour concentration is then found using equation 4.10.

The output is recorded in "*.csv" spreadsheet format which is then edited and reduced in an Excel spreadsheet specifically developed for the UC Cone Calorimeter.

6 EXPERIMENTAL PROCEDURE

6.1 Introduction

The CBUF developed Cone Calorimeter test protocol for conducting a standardised test on furniture composites is in accordance to ISO 5660-1:1993 [13], with amendments outlined in *Appendix A 6; Cone Calorimeter testing* of the final CBUF report [6].

6.2 Specimen preparation and testing procedure

This section summarises the testing procedure and protocol that has to be adhered to with regard to preparation and burning of specimens in the Cone Calorimeter. The specimen preparation and testing procedure as are outlined in ISO 5660-1:1993 and Appendix A6 of the CBUF Programme.

6.2.1 Specimen preparation

All foam samples were cut using a band saw and a specified foam-cutting blade. Each sample was cut to have a square face of 102.5mm x 102.5mm ± 0.5mm, with a nominal thickness of 50 mm. The acceptance of each foam specimen is done by comparing the mass of each triplicate batch. The mass of the three samples must not vary more than ± 5% of the arithmetic mean.

The fabric pieces are prepared by first cutting a 200mm x 200mm square. Three samples are then weighed to ensure that the mass variation is within ± 5% of the arithmetic mean. The samples are then cut into the designated shape (see *Figure 48: Fabric cutting shape*, Appendix A6 of the CBUF final report).

The fabric shells are constructed using a non acrylic-based adhesive and masking tape. The glue is allowed to cure for a period of 24 hours and is then removed and the final composite specimen constructed. An aluminium foil tray is constructed to collect residue and by-products from the testing procedure.

The completed specimens and the foil tray are placed in a conditioning chamber at 23 ± 2°C and 50% relative humidity (RH) for a minimum of 24 hours.

6.2.2 Testing procedure

The testing procedure followed was the specifically written "UC Cone Calorimeter Test Procedure" [16], which is based on the CBUF Protocol and ISO 5660-1:1993. All Cone Calorimeter tests were conducted at a uniform radiant flux of 35 kW/m^2 in a horizontal orientation. Tests were carried out in a draught free environment at 20-80% RH and temperature between 15°C - 30°C.

The top of the specimen is located 25mm from the base plate of the heating element. A two-minute base line is run before each test. The specimen shield is then closed and the specimen is placed on the specimen holder at approximately 110 secs. The shield is then opened exposing the specimen to the radiant heat flux, and the spark igniter moved into position. Once the specimen ignites the time is recorded and the spark igniter is removed 4 seconds after sustained flaming is verified.

The end of the test is declared when

1. Flaming has stopped *and* the mass loss rate drops below 150g/m^2 per minute or
2. No ignition has occurred *and* 10 minutes has elapsed since the start of the test.

Data is collected for a minimum of 2 minutes beyond the end of the test while conditions return to ambient.

Each set of triplicate tests is conducted in quick succession as to reduce drifting calibration changes between tests. The triplicate test values of $\dot{q}''_{180}$ (180-second HRR average) were compared. If a differential of more than ± 10% from their arithmetic mean existed, a further three tests are required from the protocol (Clause 11.2.9, ISO 5660-1:1993).

6.3 Calibration Procedure

The UC Cone Calorimeter was calibrated as by the procedure layed out in the University of Canterbury Cone Calorimeter Calibration procedure [15]. The important

aspects of the Cone Calorimeter that require accurate calibrations are the conical heater and gas analysers. At the start of each day's testing all of these apparatus are tested and calibrated. For detailed calibration details consult in the University of Canterbury Cone Calorimeter Calibration procedure [15].

6.3.1 Gas Analysers calibration

The gas analysers are calibrated using gases of known concentrations. The gases used are 99.99% Nitrogen and a combination of 16% O_2, 4.51% CO_2 and 0.794% CO (7940 ppm). First, the apparatus is calibrated using atmospheric oxygen to ensure the oxygen analyser gives a voltage corresponding to 21% atmospheric O_2. The O_2, CO_2 and CO analysers are then "zeroed" using Nitrogen. Subsequently, the CO_2 and CO analyser span is then calibrated using the combined gases by ensuring instrument readings give correct corresponding gas percentages.

6.3.2 Heat release rate calibration

The heat release rate is calibrated with a 5 kW Methane flame. The proportionality constant, $\Delta h_c / r_o$, for methane is 12.54 MJ/kg of O_2 consumed. Knowing the required flow rate for a 5 kW flame, when the calibration data is reduced the results can be verified to ensure a constant HRR curve of 5 kW is produced. C values are then compared to the previous days testing. If the error is not within $\pm 5\%$ of the previous day then the calibration procedure must be repeated.

6.3.3 Heat Flux calibration

The heat flux from the conical element is calibrated using a heat flux gauge. Each gauge has a specific calibration curve that converts a voltage to a corresponding heat flux. For the UC Cone Calorimeter, a heat flux of 35 kW/m^2 corresponds to a cone element temperature of 678 °C.

6.4 Data reduction

The raw data output is reduced in a standard Excel spreadsheet developed by Enright for the UC Cone Calorimeter. The average, triplicate test results are compared to ensure compliance to the CBUF protocol.

6.4.1 Test periods

The start of the test, t = 0 is defined by the moment the specimen shield is opened exposing the specimen to the radiant heat flux. The time to ignition is measured from the start of the test. The end of the test is determined from one of the two defined conditions and is measured from t = 0. The *"test period"* is measured from the time to ignition to the end of the test.

6.4.2 Effective heat of combustion

The effective heat of combustion, $\Delta h_{c,eff}$, is a mean value derived over the whole test period. Equation 6.1 is the recommended method used to calculate the mean effective heat of combustion.

$$\Delta h_{c.eff} = \frac{\sum \dot{q}(t)\Delta t}{m_i - m_f} \qquad [6.1]$$

6.4.3 Time delays and response times

The calculated HRR is a function of time dependent measured variables. There are time delays that exist between each property being produced and it's value being measured. The time delays are not uniform for when the property is produced to when it is recorded. Therefore, at any time-step recorded the properties correspond to different relative events. An example of such is between the measurement of the specimen mass and species concentrations. The mass scale measures the instantaneous mass of the specimen, where the gas analyser has to wait for the combustion products to travel down the ducting and sample lines to the analyser.

Time delay, t_d is a function of two different types of lag, transport lag and response time lag. *Transport lag* is the physical time taken for the specimen to actually reach the analyser. The *Response time lag* is the time taken for the instrument to read and register the measurement. The Excel spreadsheets used to derive the HRR curves have the corresponding time lags incorporated into the data reduction process. For further information on time lags for the UC Cone Calorimeter, consult Enright's [8] work.

7 CONE CALORIMETER RESULTS AND DISCUSSION

7.1 Introduction

The testing procedure consisted of the three individual foams and fourteen foam/fabrics combinations giving 135 bench-scale tests. All HRR curves for the individual foams and the composite specimens can be found in *Appendix B: HRR Curves*, which combines each triplicate HRR curve for the same composite. All data sets for each composite are summarised in Table D-1 of *Appendix D: Averaged Data* as required by ISO 5660-1:1993 and Appendix A6 of the final CBUF report. This tabulated data corresponds to averages of each triplicated test. A description of this calculation can be found in *Appendix C: Averaging triplicate runs*. Throughout testing there were noticeable differences between the foam burning behaviour and the composite specimens. The results are divided into three categories, "Melting fabrics", "Charring fabrics", and "Charring/melting fabrics" which are defined in the proceeding section 7.3; Fabric burning behaviour.

7.2 Foam Combustion Characteristics

The combustion behaviour of the individual foams is detailed in this section. Table 7-1 summarises the foam mass and density, time to ignition, peak HRR, total heat released, and effective heat of combustion. The actual foam densities are calculated from the foam mass and volume of each sample cut and compared to the tabulated manufacturer densities.

Table 7-1: Tabulated data of mass, density, t_{ig}, peak HRR, total heat released, and $\Delta h_{c,eff}$ for the individual foams

Foam	m (g)	ρ (kg/m^3)	t_{ig} (s)	q''_{peak} (kW/m^2)	q''_{tot} (MJ/m^2)	$\Delta h_{c,eff}$ (MJ/kg)
J	23.8	44.9	18.7	489	41	18.6
K	15.0	28.3	4.0	578	31	20.9
L	21.1	39.8	5.0	655	44	21.1

Foam J is sold as a fire retardant foam, with an average density of 44.9 kg/m^3. The general trend that this foam displayed (through all tests) was that the HRR's were significantly less than its other counterparts. Consequently, this caused longer decomposition periods. The HRR curves show two phases of burning, an initial peak followed by a recession that subsequently increases to another peak with a slow decline. The flame height tended to be significantly smaller than the other foams, with production of excessive soot and a pungent aroma. The remanent in the Aluminium (Al) tray was the insulating char layer that formed during the burning phase (see Figure 7-3 (a).). This typical burning behaviour is depicted in Figure 7-1.

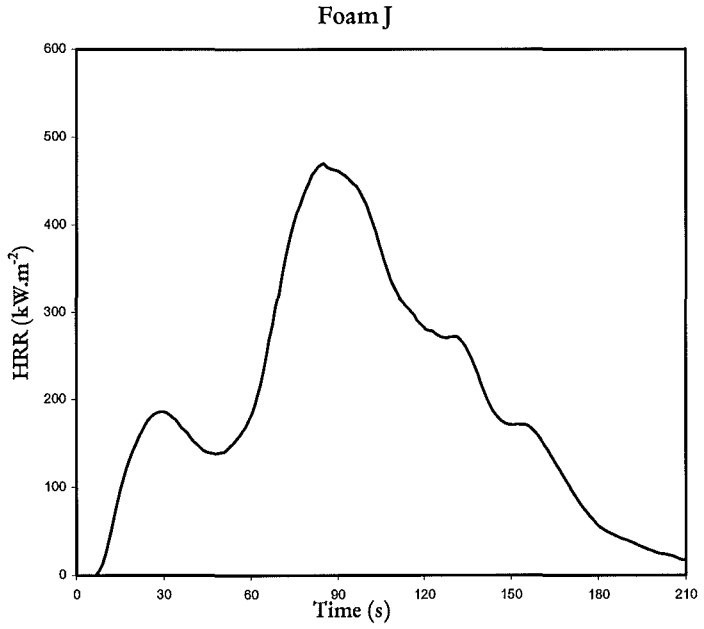

Figure 7-1: HRR history of foam J.

Foams K and L (density of 28 kg/m^3 and 39 kg/m^3 respectively) show very similar trends in their burning behaviour. There is a fast growth to a plateau early after ignition, which is followed by a fast progression to a peak HRR. The plateau results from the foam forming into a liquid phase (approximately 35-40 seconds). Once this transformation has completed, burning tends to accelerate as the decomposing material vaporises quicker compared to the solid state foam. The decay after the peak is very rapid with all material being decomposed leaving a thin layer of char remaining in the tray (see Figure 7-3 (b).) This typical burning behaviour is graphically depicted in Figure 7-2.

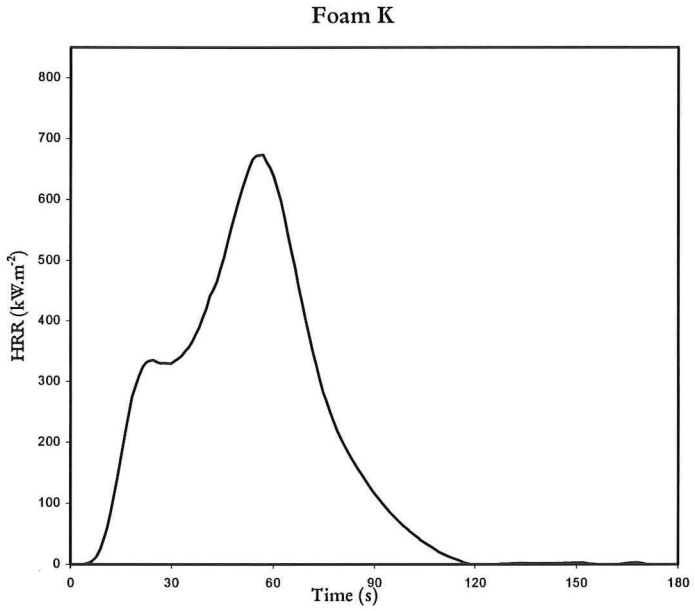

Figure 7-2: HRR history of foam K

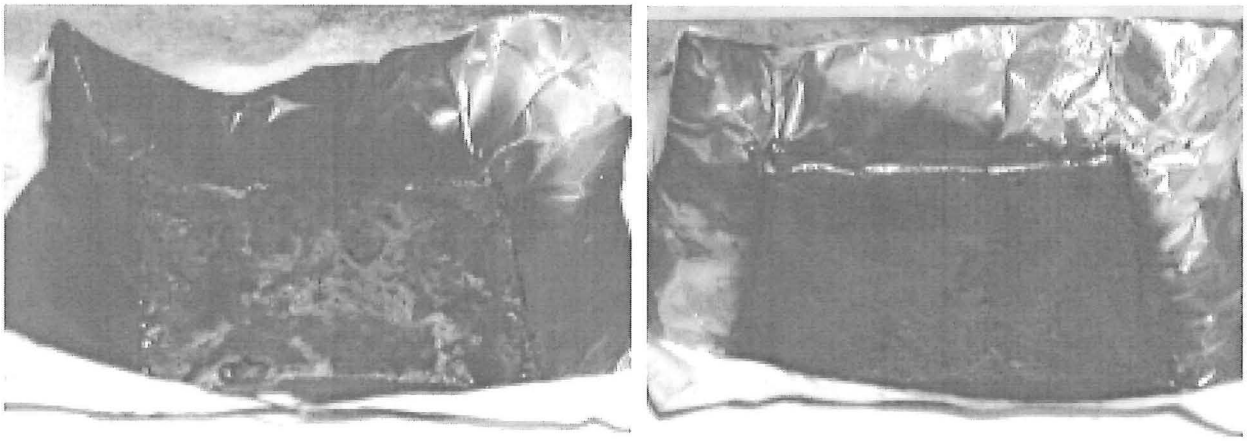

(a) Foam J remnants (b) Foam L remnants

Figure 7-3: Photographs of the remnants that foam J and foam L produce.

The total energy released by Foam J is equivalent to Foam L but Foam J tends to release all of its energy at lower levels over longer periods, where Foam L has higher rates of energy released over shorter periods. Foam K exhibits the similar behaviour to that of Foam L where it expels the majority of its energy at higher rates over a shorter period.

The ignition times observed with Foam J tended to be very erratic ranging between 6-28 seconds. This trend seemed to be prevalent throughout most of the tests. This behaviour is related to the fire retardant properties of the fabric where the vapour being expelled past the spark-igniter is borderline of being flammable, causing the discrepancies between ignition times (This is further discussed in section 7.7). The ignition behaviour

of foams K and L were very consistent with mean ignition times of 4 and 5 seconds respectively.

The heat of combustion for the three foams examined ranged between 18.6-21.1 MJ/kg. Foams J and L have very similar total heat outputs, but difference exists between their respective heat of combustion, $\Delta h_{c,eff}$. Whereas foams K and L tend to completely decompose, foam J forms an insulating char that primarily contributes to the remaining mass. Although foam J is the heavier specimen, the actual mass consumed to produce the same amount of energy is relatively equivalent. Foam K, the lightest of the 3 foams, produces the least amount of heat. Contrary to this, although foam K is the lightest, the amount of energy stored per unit mass consumed results in a high heat of combustion (ie equivalent to foam L)

7.3 Fabric Burning behaviour

Fabric burning behaviour and the technical terms applied will be defined in the following two sections. That forms the basis of the fabric flammability categories for the resutls.

7.3.1 Melting fabrics

Organic thermoplastics, such as *Flame Resistant* (FR) polyester and FR modacrylic, when subjected to a heat source *do not readily ignite but melt and shrink away from the heat source.* This tends to leave the underlying surface exposed and the possibility of the molten polymer sticking to the underlying surface. The heat flux actually reaching the top part of the foam is reduced by the energy consumed in the vaporisation of the fabric pool during the early part of the test. Fabrics which belong to this group are FR viscose, polyester and acrylic.

7.3.2 Char forming fabrics

Char forming fabrics do not melt or shrink when exposed to heat and flames but *convert to an insulating char, thus creating a barrier and preventing further exposure of the material to the heat source.* These are often termed *Heat resistant* textiles [10]. These fabrics typically have a low heat of combustion due to the carbon being retained in the

char forming process. Glowing is a typical combustion characteristic due to char oxidation.

For man-made fibres (eg polyester and polypropylene), this behaviour can be achieved by chemically treating the fibre either before, or after spinning. Other non-thermoplastic fabrics such as FR cotton and viscose are flame retarded the in the same way. It is advantageous that the presence of cellulose in the chemical structure provides an inherent form of fire retardancy.

7.4 Melting fabrics.

7.4.1 Fabric flammability

As previously defined, *melting fabrics* or *flame resistant fabrics* are those that, when subjected to a heat source, do not readily ignite but melt and shrink away from the heat source. This behaviour is inherent in most thermoplastic fibres such as olefin (including polypropylene and polyester) and acrylic. The observed behaviour was that fabrics inclined to billow, shrink, and then melt exposing the underlying surface. The fabrics typically fractured from the centre and proceed to melt radially outward to the edges of the specimen. Typical remnants after burning are depicted in Figure 7-4.

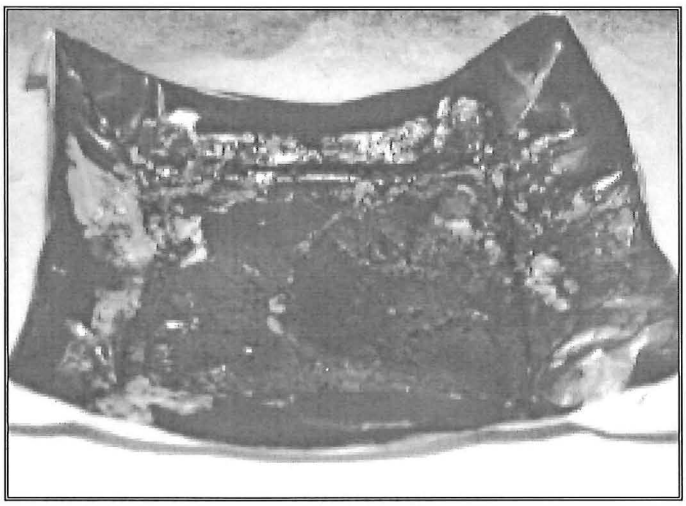

Figure 7-4: Photograph depicting the remnants of composite L-23 after burning.

Table 7-2 lists the fabrics categorised as *meting fabrics, also* the composite mass, density, time to ignition, time for the fabric to melt, peak HRR, total heat released, and effective heat of combustion for respective fabric/foam combinations.

Table 7-2: Tabulated data of mass, density, t_{ig}, t_{melt}, peak HRR, total heat released, and $\Delta h_{c,eff}$ for melting fabrics.

Fabric	Foam	m (g)	ρ_{com} (kg/m^3)	t_{ig} (s)	t_{melt} (s)	$\dot{q}''_{peak}$ (kW/m^2)	q''_{tot} (MJ/m^2)	$\Delta h_{c,eff}$ (MJ/kg)
23	J	32.88	64.5	16.0	6	709	69.0	22.3
	K	24.29	47.6	9.7		742	52.3	22.0
	L	30.67	60.1	11.7		730	67.3	22.3
24	J	35.32	69.3	16.0	8	384	55.0	17.4
	K	30.25	59.3	12.0		729	46.4	18.2
	L	33.06	64.8	12.7		742	59.8	19.0
25	J	35.06	68.7	26.7	8	520	53.6	17.6
	K	26.58	52.1	13.7		676	46.6	19.8
	L	32.19	63.1	13.0		642	58.2	20.0
26	J	30.99	60.8	17.7	5	576	60.7	20.9
	K	22.92	44.9	10.7		714	53.5	23.6
	L	28.50	55.9	9.7		781	64.9	23.0
29	J	32.75	64.2	14.7	8	604	53.2	18.4
	K	24.75	48.5	11.3		603	43.0	19.3
	L	30.39	59.6	11.7		657	55.2	19.9
31	J	30.59	60.0	10.7	8	650	56.9	20.3
	K	22.71	44.5	9.0		660	45.9	21.1
	L	28.34	55.6	12.7		664	57.7	21.1
33	J	31.94	62.6	12.7	7	629	60.3	20.4
	K	24.40	47.8	11.0		706	51.8	22.3
	L	29.84	58.5	9.7		723	63.6	22.2
35	J	34.62	67.9	22.3	10	523	58.1	19.3
	K	27.57	54.1	14.7		602	49.9	20.3
	L	32.60	63.9	14.7		661	61.1	20.5

7.4.2 Combustion behaviour of melting fabrics

The general combustion behaviour exhibited by flame resistant composites exhibit two trends (see Appendix A for HRR curves). Composites that include foam K and foam L display a fast growth and decay period. The growth phase was very quick, which tended to gradually decrease. The decay phase for these foam composites is very quick.

Composites that consist of foam J have similar HRR curves to the preceding foam composites, but tended to burn at lower HRR's for longer periods. The decay phase is not as fast, as decomposition recedes into a smouldering phase.

Proceeding the growth rate, the composites exhibits one of two types of behaviour.

1. A gradual growth and recession to and from the peak HRR or (refer Figure 7-5),
2. Fluctuating HRR that include growth and recession periods. This may be very repetitive. (refer Figure 7-6)

Proceeding the decay phase, there is a period of smouldering combustion as the flame broke into isolated areas. It was common for the residue to glow after flaming had ended.

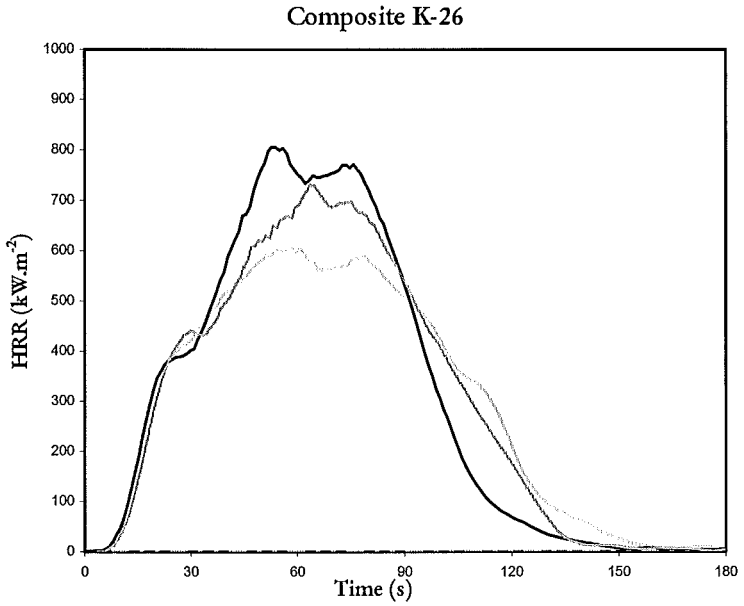

Figure 7-5: HRR curve of composite K-26

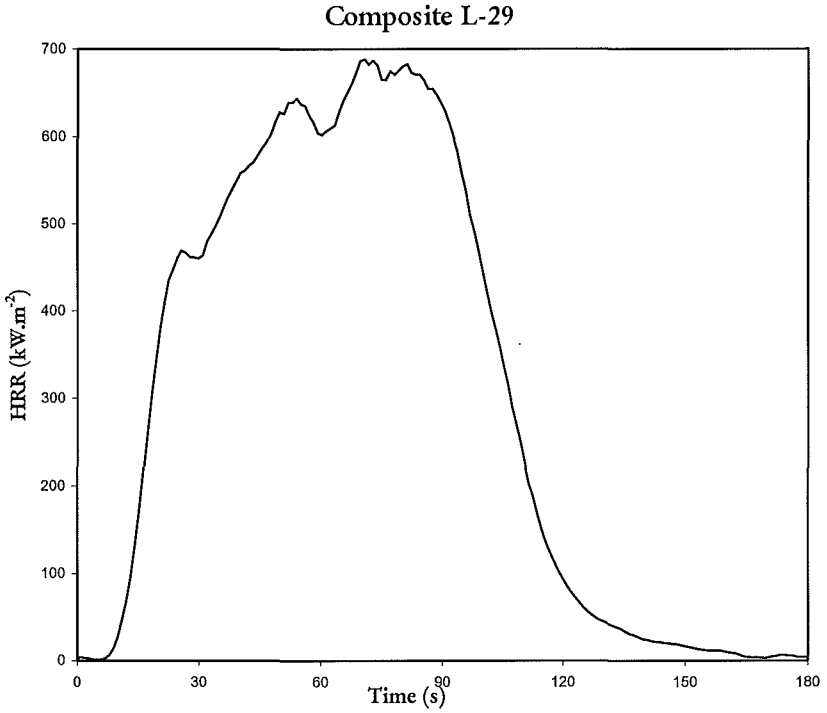

Figure 7-6: HRR history of composite L-29

Foam J composites:

All composites that included foam J displayed lower HRR's and longer burning duration's compared to the other foam composites. The decay phases are thus slower and longer. These characteristics were also observed in the combustion behaviour where symptoms included low flame heights and smouldering combustion after decay. The only exceptions to this are composites consisting of fabric 31 and fabric 33. Their trends depicted an increase of the HRR to a magnitude similar to the other composites in each respective foam/fabric category (refer to Table 7-2

Foam K composites:

Composites that include foam K tend to produce a "rounder" HRR curve where there is a distinctive growth phase, a defined increase to a peak followed by a decay phase. The only exception to this are composites K-24, K-25, K-29, and K-35, which tend to be inherent with fabric compositions (discussed later).

Foam L composites:

Most flame resistant composites that contained foam L displayed similar behaviour. After the initial growth period, fluctuating HRR's with a defined peak were common.

For some composites (eg L-29 and L-35) the burning behaviour for each of the three specimens did not tend to agree definitively, but did display similar trends. Composites with foam L are inclined to burn for longer duration's at these higher HRR. Compared to the other respective foam composites the decay phase is a lot later. Combustion features of these composites exhibit a high proportion of soot in the flame.

7.4.3 Fabric effect on composite flammability

Common symptoms of composites with fabrics constructed of acrylic and polyester (ie fabrics 24, 25, 29 and 35) showed an adverse effect on the HRR curve whereby, after the growth phase, the HRR tends to fluctuate at high levels. For most of these composites, the HRR increases to a peak, recedes, and then increases to a second peak HRR. The peak HRR produced from these composites had a mean of 612 kW/m^2 and ranged between 384-742 kW/m^2. Both extremity values derived from composites with fabric 24. The minimum value was obtained from composite J-24 that only included the two specimens tested.[2] The fabrics that consistently produced the highest HRR were those that included polypropylene and olefin fabric (ie fabrics 23, 26, 31, 33). The composite that has the highest HRR was L-26 at 781 kW/m^2. For composites J-31 and J-33, the addition of the fabric had the effect of enhancing the peak HRR to a magnitude similar to the other composites.

The total heat released by flame resistant fabrics is the highest of all three categories with an average of 56 MJ/m^2. This was comparative to the individual foams (not bounded by fabric), which release an average 38.4 MJ/m^2, the additional energy is derived from the addition of the molten fabric as it forms into the foam pool. Predominantly all of the flame resistant fibres used are thermoplastics, which will contribute additional energy throughout the combustion process. This heat is expelled from the polymer melt stage as the liquid pyrolyzates are vaporised.

Of all ignition times observed, melting fabrics were the quickest of all three categories. Composites with foam J tend to have longer ignition times compared to its counterparts because of the chemical nature of the solid state foam (as discussed in section 7.7). Compared with the individual foams, the ignition times increase due to the presence of

[2] This discrepancy is discussed in section 7.7: Flammability of foam J

the fabric. Some heat resistant composites ignited as early as 9 seconds compared with 4 seconds for foam K. It was typical for fabrics that contained olefin to ignite quicker than other composites (eg fabrics 26 and 31). Although fabric 35 includes olefin, the presence of other fibres such as acrylic had the adverse effect of slightly delaying ignition.

Flame resistant fabrics tended to have the highest heats of combustion of all three categories ranging between 17.4 - 23.6 MJ/kg. Since the consumable mass is larger than the individual foams, there is more stored energy. Because most of this mass is consumed the relative difference between the total energy produced and the mass consumed is inherently the same. Fabric composites that tend to have high heats of combustion are those that contain olefin and polypropylene. Adversely, fabric composites that exhibit lower heats of combustion are those which contain acrylic and polyester fibres.

7.5 Charring fabrics

7.5.1 Fabric flammability

As previously defined, *charring fabrics* or *heat resistant fabrics* (typically non-thermoplastic organic materials such as FR cellulose and FR wool) do not melt or shrink but convert to an insulating char, thus creating a barrier. The behaviour typically observed was for the fabrics to shrink a small amount and then the exposed top surface began to char. As the foam ignites and begins to melt, the remaining part of the fabric shell forms a crust layer in unison with the decreasing foam height. The char layer remains throughout the entire burning period tending to restrict the radiant heat flux and slow decomposition rates. An example of this char layer can be viewed in Figure 7-7.

Figure 7-7: Photograph depicting the remaining char layer formed by composite L-28.

The two materials that exhibited this behaviour were fabric 27 and fabric 28. They consisted of 100% Nylon pile and 100% Cotton respectively. Tabulated data of the foam/fabric mass and density, time to ignition, time for fabric to melt, peak HRR, total heat released, and effective heat of combustion is provided in Table 7-3. Fabric 28 was certified to meet BS 5852 in terms of flammability. (Note: t_{melt} in Table 7-3 refers to the time required for the fabric to char on the top of the specimen).

Table 7-3: Tabulated data of mass, density, t_{ig}, t_{melt}, peak HRR, total heat released, and $\Delta h_{c,eff}$ for charring fabrics.

Fabric	Foam	m (g)	ρ_{com} (kg/m^3)	t_{ig} (s)	t_{melt} (s)	$\dot{q}''_{peak}$ (kW/m^2)	q''_{tot} (MJ/m^2)	$\Delta h_{c,eff}$ (MJ/kg)
27	J	33.37	65.4	31.0	10	570	48.2	16.6
	K	24.67	48.4	16.0		573	44.7	19.1
	L	30.56	59.9	17.3		626	55.8	19.3
28	J	36.10	70.8	19.0	10	624	58.2	18.2
	K	28.19	55.3	17.7		658	50.1	19.5
	L	33.41	65.5	18.7		681	60.6	19.7

7.5.2 Combustion behaviour of charring fabrics

The combustion behaviour of these composites follows a "general" trend for the foam/fabric combinations in this category (refer to Appendix A for a full list of the

HRR curves). The trend displayed is in two stages. The first stage has a rapid increase of HRR to an initial peak. Subsequently, there is a fast decay into a trough[3]. The second phase of burning shows a slower progression to a lower peak followed by a gradual decay. This generally occurs over a relatively longer periods compared to the first stage. This trend is depicted in Figure 7-8.

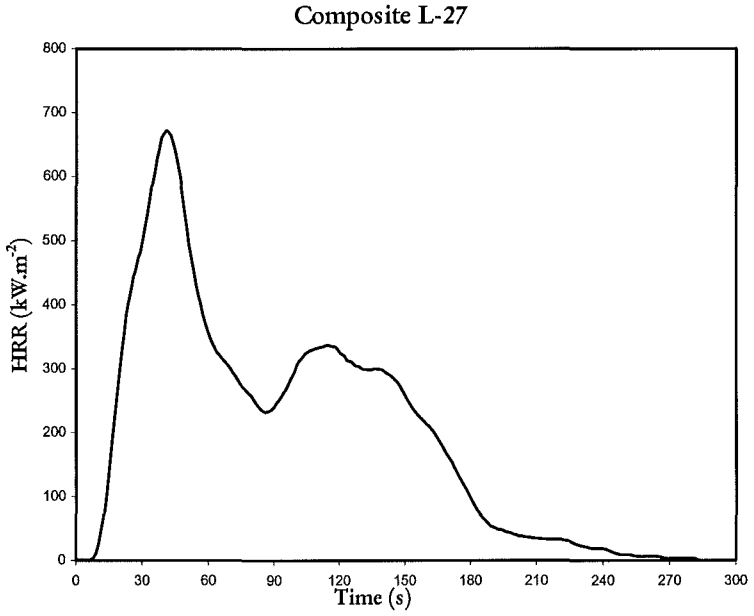

Figure 7-8: HRR history of composite L-27.

The initial peak develops from the rapid combustion of the readily available pyrolyzates from the fabric and foam. Once the char layer has formed over and its combustible material is exhausted, energy is now developed from the liquid pool, which drives the second peak. Because of the insulating char, decomposition rates reduce thus lengthening burning periods.

The combustion behaviour of foam J combined with charring fabrics burn longer than other composites similarly categorised. Composites J-27 and J-28 rapidly increase, shortly after ignition, to a peak HRR and then rapidly decay. This is evident with the quick progression of the flame height that extends into the ducting immediately after ignition. A lot of soot is emitted from the flame. Burning begins to increase after a short period once the polymer melt has formed. Composite K-27 and L-27 showed that the

[3] A "trough" when describing HRR curves, is where there is a noticeable hollow. It is typically preceded by a decay phase and before another growth phase.

progression to the peak HRR had a spike in the curve. One specimen of composite K-27 shows an initial peak and a series of stepwise declines. Both specimens show the very similar trend of, progressional decays into a trough followed by a similar second burning phase. The decay of these composites tend to be shorter than J-27. Composites K-28 and L-28 depict the same general characteristics where an initial peak HRR is rapidly reached followed by a fast decay. The second burning phases consist of a moderate growth to a second peak subsequently followed by a steady decay. The initial plateau, characteristic of the individual foams, is no longer present with the addition of the fabric. Typical values of HRR for heat resistant fabrics range between 570-681 kW/m^2. Fabric 28 (100% cotton) consistently had higher peak HRR for respective foam composites.

The total heat released by charring fabrics ranged between 44.7 - 60.6 MJ/m^2. It appeared that the extra energy was obtained from the combustion of the solid-state char formed by the fabrics during decomposition. Table 7-3 shows the higher total heat released is derived from composites including foam L. It is also evident that fabric 28 produces more energy than fabric 27 does for all of the composite combinations.

The benefit of charring fabrics is their ability to delay ignition. For all of the respective foam/fabric combinations, charring fabrics inherently have longer ignition times. Table 7-3 summarises the average ignition times of charring fabrics (for comparisons see Table D-1). Due to the formation of the insulating char over the foam, taking approximately 10 seconds (ie t_{melt}), the heat flow is hindered to the underlying foam resulting in longer ignition times. Adversely, these longer ignition times are then followed by some of the shortest times to peak HRR's for all of the respective flammability categories.

The effective heat of combustion for charring fabrics ranged between 16.6-19.7 MJ/kg. If compared to the individual foams, these composites exhibit less energy per unit mass than the foams alone.

7.6 Charring/melting fabrics

7.6.1 Fabric flammability

This section has been derived whereby the fabric flammability characteristics exhibit both melting and charring phenomena. Typical fabric compositions include a cellulose material such as cotton (and/or viscose rayon) blended with other thermoplastic fibres such as polyester and acrylic. When exposed to a radiant heat, the fabric appears to delaminate longitudinally as the interwoven thermoplastics begin to melt. The remaining cellulose fibres begin to char, forming an intertwined shell over the melting foam sample as depicted in Figure 7-9. The remaining charred fibres become very brittle and have a tendency to glow. The brittleness emanates due to the lack of stability in the structure from degradation of the cellulose material.

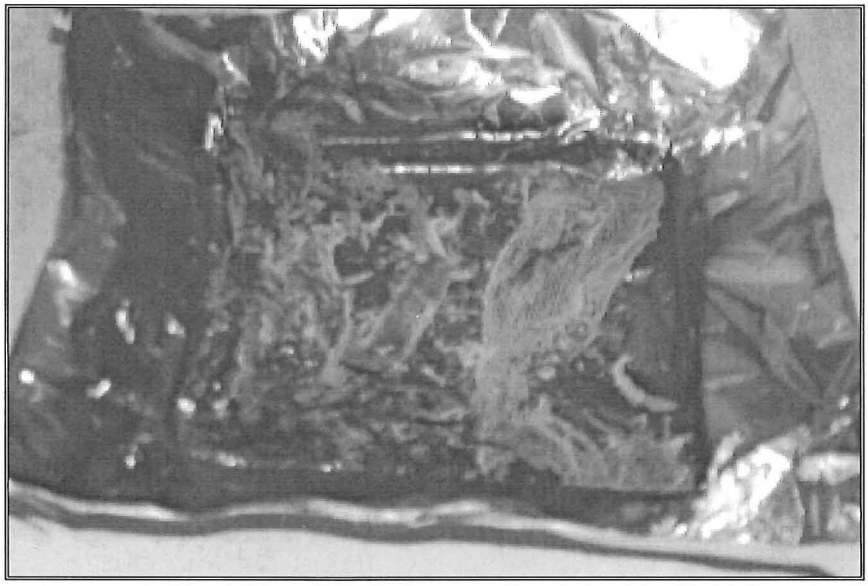

Figure 7-9: Photograph depicting the charred cellulose fibre strand that formed during the burning of composite K-34

Tabulated data of composite mass, density, time to ignition, time to melt, peak HRR, total heat released, and effective heat of combustion for charring/melting fabric composites.

Table 7-4: Tabulated data of mass, density, t_{ig}, t_{melt}, peak HRR, total heat released, and $\Delta h_{c,eff}$ for charring/melting fabric composites.

Fabric	Foam	m (g)	ρ_{com} (kg/m^3)	t_{ig} (s)	t_{melt}* (s)	$\dot{q}''_{peak}$ (kW/m^2)	q''_{tot} (MJ/m^2)	$\Delta h_{c,eff}$ (MJ/kg)
30	J	32.00	62.8	16.0	8	462	50.3	16.9
	K	24.11	47.3	11.3		611	40.7	17.2
	L	29.53	57.9	14.7		637	51.6	17.7
32	J	34.38	67.4	16.0	10	426	52.1	16.5
	K	26.72	52.4	13.0		645	44.9	17.2
	L	31.85	62.4	14.3		671	54.7	17.7
34	J	30.55	59.9	13.0	8	463	50.7	17.8
	K	23.14	45.4	10.3		619	41.2	18.2
	L	28.53	55.9	12.3		664	52.9	18.8
36	J	33.42	65.5	12.7	10	580	53.8	17.3
	K	26.50	52.0	15.3		659	42.7	16.3
	L	31.66	62.1	14.7		678	53.6	17.1

7.6.2 Combustion behaviour of charring/melting fabrics

The combustion behaviour of these composites follows a "general" trend for all foam/fabric combinations in this category. The HRR rapidly increases to an initial peak as readily available pyrolyzates from the fabric ignite, and vaporise. Subsequently burning recedes into a trough. This recess in HRR is then followed by an increase to a second peak HRR, in some cases higher than the first. Once the predominant bulk of the material has decomposed, burning progresses to a smouldering phase. The burnout period tended to be prolonged where flaming required a long time to extinguish as it broke into isolated corners, accompanied with glowing of the remaining cellulose material. A typical HRR history depicting this trend is provided in Figure 7-10.

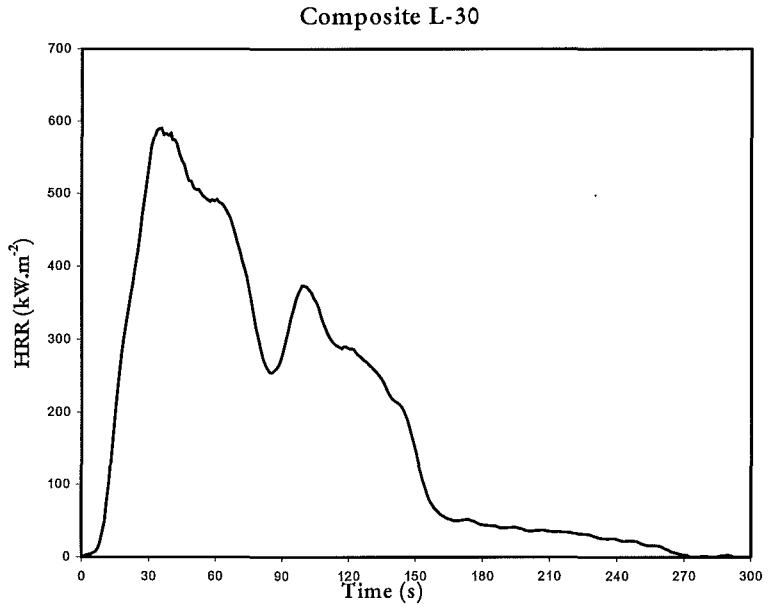

Figure 7-10: HRR history of composite L-30

Composites that consisted of foam J tended to burn at lower HRR rates for longer periods, which was evident in the trends displayed for the charring/melting fabric composites. Observations from composites including foam J were small flame heights (protrusion slightly above the top of the cone element) and a lot of soot. Composites with foam J have peaks considerably less than the other composites (approximately 200 kW/m^2). Composite J-30 tended to burn at a steady state for a brief period after the first peak is reached, and then recedes into a trough. Composite J-32 shows consistency between two specimens but the third seems to be an anomaly where no second peak HRR was present, but a steady burning period followed with a longer decay phase. Composite J-34 is very consistent through all three specimens where the second peak HRR is of the same magnitude as the first (463 kW/m^2). Composite J-36 had an increase after the trough to a point where a steady state burning period is briefly sustained for 30 seconds followed by decay. One specimen seemed to show behaviour abnormal to the other two where the second peak is approximately 130 kW/m^2 greater.

Composites consisting of foams K and L all depict the general burning trends. All HRR curves show a high first peak followed by a lower second peak after a recession to a trough. Foam L composites displayed higher HRR than foam K composites. Composites K-32 and L-32 recede into a trough but as the HRR began to increase, they tended to

burn for longer duration's at these steadier rates. Once the predominant portion of the material is consumed, there was a generally fast decay.

The fabric fibres that tended to produce the higher HRR rates were those consisting of polyester and viscose (fabrics 32 and 36, which had peaks HRR's of 678 kW/m^2 and 671 kW/m^2 respectively).

The total heat released from charing/melting fabrics shows a general trend where composites consisting of foams J and L are very similar with values ranging between 50-55 MJ/m^2. Generally, composites with foam J have a lower peak HRR and longer burning periods compared to foam L composites where peak HRR's are higher with shorter burning periods. Composites with foam K release a total energy between 41-45 MJ/m^2. The HRR is similar to foam L composites, but the composite density is less than its counterparts.

Ignition times for charring/melting fabrics tend to be somewhat longer than melting fabrics, but shorter than charring fabrics. The effect these types of fabrics have on the ignition times is dependent on the fabric fibres. The effect of including FR viscose in the fabric composition tends to delay the fabric from melting as quick as other fabrics in this category. This is also reflected in the times to ignition for the composites that have a fabric partially constructed from viscose (fabrics 32 and 36) where ignition is delayed for approximately two seconds longer. The presence of FR cotton also has this same effect, but not to the same degree as viscose.

Given that foam L is one of the denser specimens, it is expected that composites comprising of this foam will have a higher heat of combustion. The effective heat of combustion indicated that charring/melting fabrics tend to have the lowest heats of combustion of all three categories ranging between 16.3-18.8 MJ/kg.

7.7 Flammability of Foam J

The flammability of foam J proved to be questionable from the derived results. Not only did some specimens fail to ignite (eg J-23-1 and J-24-3) but also ignition times for some specimens tended to differ by 10 seconds (eg foam J, J-23, J-27, J-35). Not only were

ignition times an issue, but the burning behaviour of some specimens (eg J-23, J-27, J-28, J-32, and J-36) varied from what was otherwise expected. This associated inconsistent behaviour gave rise to errors in results that otherwise would not be pertinent, such as verification of 180 second average HRR's. The composites evident of this were J-23, J-27 and J-28. These arose due to the inconsistency in the burning behaviour of each composite where certain characteristics were not present or differed from what was otherwise typical. Composite J-23 displayed the same burning characteristics but peak HRR differed more than 200 kW/m^2. Composites J-27 and J-28 both had two specimens which the HRR somewhat differed from the norm, resulted in 180 second averages greater than 10%.

The thermal decomposition[4] of polymers may proceed by oxidation or by the application of heat. Chemical processes are responsible for the generation of flammable volatiles while physical changes, such as melting and charring can markedly alter the decomposition and burning characteristics. Figure 7-11 is a representation of the physical and chemical process that occurs during thermal decomposition.

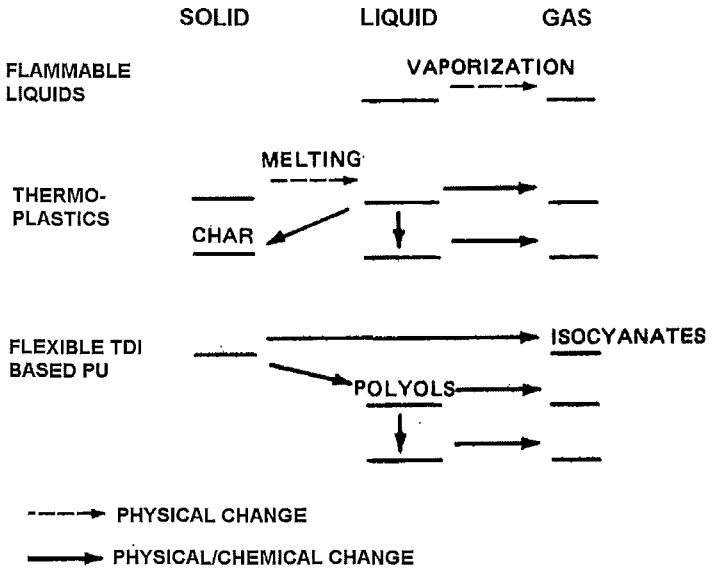

Figure 7-11: Physical and chemical changes during thermal decomposition adopted from Beyler et al, Fig-7.3 [3].

[4] Thermal decomposition is the breaking down of large polymer molecules into smaller monomers allowing vaporisation.

The mechanism that governs whether a solid will ignite is *lean flammability limit*[5]. The production of volatiles is both physical and chemical in polymeric solids. The rate, mechanism and product composition depend both on the physical properties and on the chemical composition. If a polymer transforms from a solid state to a liquid state below the decomposition temperature the material is likely to drip or flow. For the specimens that failed to ignite, this behaviour was evident where the foam sample continued to melt into a liquid phase. The concentration of volatiles in the pyrolyzate was below the lean flammability limit, yielding non-ignition. This behaviour would be inherent for fire retardant foams where additives prevent the onset of ignition and further fire growth.

If this behaviour were consistent throughout there would be no concern, but since the inconsistent behaviour of the foam caused such discrepancies further investigation is required into the presence and concentrations of additives that are attributed to this behaviour. Because of such discrepancies, the conclusions made will neglect the composites that include these errors as to produce consistent recommendations.

[5] The lean flammability limit is defined as a lower limit of combustible volatiles in the pyrolyzate to enable flaming propagation possible.

8 CONE CALORIMETER CONCLUSIONS

This section is a summary of the major results and observations made from the previous investigations. Tabulated ranges of t_{ig}, peak HRR, total heat released $\Delta h_{c,eff}$ are provided in Table 8-1 for individual foams, melting, charring, and charring/melting flammability categories.

Table 8-1: Tabulated ranges for t_{ig}, peak HRR, total heat released, and $\Delta h_{c,eff}$ for individual foams, melting, charring, and charring/melting fabrics.

	FOAMS	MELTING FABRICS	CHARRING FABRICS	CHARRING/MELTING FABRICS
t_{ig} (s)	18.7-4.0	9.0-26.7	16-31	10.3-16.0
$\dot{q}''_{peak}$ (kW/m^2)	655-489	384-781	570-681	426-678
q''_{tot} (MJ/m^2)	43.7-30.9	43.0-69.0	44.7-60.6	40.7-54.7
$\Delta h_{c,eff}$ (MJ/kg)	21.1-18.6	17.4-23.6	16.6-19.7	16.3-18.8

8.1 Foam flammability

The foam that tended to produce the greatest amount of energy, consistently have the highest peak HRR, and ignite very quickly was foam L. Foam J showed the tendency to release a lot of energy over longer periods. The charring tendency of the foam causes the onset of smouldering combustion. Since this decomposition rate is slower the burning duration's are longer. Foam K has the tendency to release comparatively smaller amounts of energy, over shorter periods.

8.2 Fabric flammability

There is a pronounced fabric effect demonstrated in the small-scale tests. The presence of fabric over the foams has the effect of increasing ignition times. The fabric composition also has the effect of changing the burning characteristics of the foam composite.

8.2.1 Melting fabrics

Fabrics constructed of acrylic and polyester have adverse effects on composite combustion causing fluctuating HRR. Fabrics that consistently produce the highest HRR were those constructed of polypropylene and olefin (781 kW/m^2, L-26). The presence of these fibres also has the effect of enhancing the burning characteristics of foam J.

The total heat released by melting fabric composites was consistently the highest of all three categories that ranged between 43-69 MJ/m^2 where composite L-26 produced the most energy. Olefin fabrics characteristically released higher amounts of energy than the other fabrics.

Melting fabrics display faster ignition times of the three categories. Some composites ignite as early as 9 seconds. Results indicate fabrics that include olefin have a tendency to ignite quicker than other flame resistant fabrics. Adversely, acrylic has the effect of delaying ignition.

The effective heat of combustion for melting fabric composites ranged between 17.4 - 23.6 MJ/kg. Composites that displayed high heats of combustion were fabrics that included olefin (eg 23.6 MJ/kg, for K-26). Fabrics composed of acrylic and polyester fibres typically displayed lower heat of combustion (eg 17.4 MJ/kg for J-24) in this category.

8.2.2 Charring fabrics

Heat resistant fabrics display the tendency to form an insulating char layer that decreases decomposition rates causing longer burning periods. The fabric that produced the highest HRR's was fabric 28, 100% cotton. Composite L-28 gave the highest HRR at 681 kW/m^2.

The total heat released by charring fabric composites range between 44.7-60.6 MJ/m^2. Additional energy is released from further combustion of the insulating char layer. The 100% cotton fabric consistently produced more energy than the 100% nylon fabric.

Charring fabrics displayed the longest ignition times of the three categories. The effective heat of combustion for heat resistant composites ranged between 16.6-19.7 MJ/kg.

8.2.3 Charring/melting fabrics

Fabrics in this category displayed the tendency to smoulder. The fabric fibres that produced the highest HRR rates were those that consist of polyester with viscose. Fabrics 32 and 36 had peaks HRR's of 678 kW/m^2 and 671 kW/m^2 respectively.

The total heat released from charring/melting fibre composites ranged between 40.7-54.7 MJ/m^2 where the maximum of 54.7 MJ/m^2 was from composite L-32.

Charring/melting fabrics display ignition times similar to flame resistant. No particular fabric composite showed a tendency to ignite any quicker. The effective heat of combustion for charring/melting composites ranged between 16.3-18.8 MJ/kg.

8.3 Combinations posing the highest flammability.

The previous investigation showed the foam with the most potentially hazardous flammability characteristics was foam L, which consistently had the highest peak HRR, total heat released and effective heat of combustion. Conversely, although foam J burns at lower rates, there is presence of a smouldering combustion phase and the volatile products from the fire-retarding chemicals.

The most flammable foam/fabric combination was composite L-26. This fabric consistently had the highest peak HRR, and total energy released.

Melting fabrics composed of polypropylene, olefin displayed characteristics with high HRR's, and production of large amounts of energy when combined with any of the three foams.

9 PREDICTING FULL-SCALE FURNITURE BURNING BEHAVIOUR FROM BENCH SCALE TEST DATA

9.1 Introduction

Full scale fire testing of furniture, as a hazard predictor is a much more costly and time-consuming process than bench scale testing. The CBUF programme developed three useful predictive models to analyse and predict full-scale furniture scenarios from bench scale data. Enright investigated/tested eight exemplary chairs and five two-seat sofas representative of typical NZ domestic furniture in order to validate the applicability of Model I to exemplary NZ furniture.

Model I of the CBUF programme will be used to provide full scale burning behaviour estimates of peak HRR, time to peak HRR, total heat released, and time to untenable conditions in a standard room. Conclusions and recommendations regarding the potentially hazardous foam/fabric combination will be derived from these results. No full-scale furniture testing was examined in this research so conclusions will be made with respect to past NZ-CBUF results.

9.2 CBUF Model I

Model I is a "factor based" method that uses statistically correlated data to predict full scale burning behaviour from small-scale tests. The purpose of this research is to predict the flammability characteristics of the foam and fabrics examined in the Cone Calorimeter tests. The results obtained from the small-scale tests are used to provide predictions of the peak HRR, total heat released, time to peak HRR, and the time to untenable conditions.

The mass of the "soft combustible components" (m_{soft}) includes fabric, foam, interliner and other components, it does not include the frame or any support pieces. As no full-scale furniture has been examined in this research, data from past CBUF researchers at the University of Canterbury (ie Enright and Denize) has been used to estimate quantitative frame masses and foam/fabric composite densities. Predicted values of m_{soft} are extrapolated using the average small-scale composite densities (Appendix E

provides a detailed description of the assumed frame mass and fabric volumes used for each chair style).

The *style factors* incorporated in the predictive equations are numeric expressions representing different styles or physical characteristics of upholstered furniture in the CBUF data base. The style factor modifies the HRR that would otherwise not be resolved by the Cone Calorimeter test method. Style factors presented in Model I are used for two purposes: for prediction of peak HRR (Style factor A) and for prediction of time to peak (Style factor B). For a complete list of the style factors consult the CBUF Final Report [6]. Previous research conducted by Denize [7] and Enright [8] examined the full-scale combustion characteristics of fully upholstered armchairs and two-seat sofa's from series 2 of the CBUF research programme. Table 9-1 provides the style factors used by the aforementioned researchers.

Table 9-1: Furniture styles used in the CBUF and NZ-CBUF programmes.

CBUF STYLE	STYLE FACTOR A	STYLE FACTOR B	TYPE OF FURNITURE
1	1	1	Armchair, fully upholstered, average amount of padding
2	1	0.8	Sofa, two-seat
3	0.8	0.9	Sofa, three-seat
4	0.9	0.9	Armchair, fully upholstered, high amount of padding

The NZ-CBUF series 2 items tested included single seat armchairs and two seat sofas with average to high amounts of padding. Style 3 is included for completeness.

9.2.1 Propagating/Non-propagating Behaviour

The basic determination made when modelling a furniture item is whether the item will support the propagation of fire over its surface once an ignition source is removed. *Non-propagating* items exhibit behaviour where once the ignition source is removed burning can not be sustained, in contrast furniture items that experience flame spread over most of the surface once the ignition source is removed are *propagating* items.

The European CBUF programme investigated the full-scale combustion behaviour of chair/sofa specimens and derived a critical heat flux of $\dot{q}''_{180} = 65$ kW/m^2 as a transition

point between propagation and non-propagation. Comparisons made with earlier investigations at the time-suggested values of $\dot{q}''_{180} = 75$ kW/m^2 were consistent with the limiting value derived. Model I is relevant to chairs that display propagating fire behaviour.

9.2.2 Prediction of Peak Heat Release Rate

As described in detail in the final report [6], CBUF Model I is a factor based method that uses a series of statistically correlated variables, x_1 and x_2, to predict the peak HRR. These are valid expressions for different HRR magnitudes indicated in equations 9.1 and 9.2.

$$x_1 = \left(m_{soft}\right)^{1.25} (style\,fac.A)\left(\dot{q}''_{pk} + \dot{q}''_{300}\right)^{0.7}\left(15 + t_{ig}\right)^{-0.7} \quad [9.1]$$

$$x_2 = 880 + 500\left(m_{soft}\right)^{0.7} (style\,fac.A)\left(\Delta h_{c,eff} / q''_{tot}\right)^{1.4} \quad [9.2]$$

Determination of which correlating variable to use is decided by the following conditions.

1) If (x_1 >115) or (q''_{tot} >70 and x_1 >40) or (style ={3,4} and x_1 >70) then $\dot{Q} = x_2$ [9.3]

2) If, x_1 <56 then $\dot{Q}$ =14.4 x_1 [9.4]

3) Otherwise $\dot{Q}$ =600 + 3.7714.4 x_1 [9.5]

9.2.3 Prediction of total heat released.

The total heat released is determined from the actual mass of the furniture item and small-scale effective heat of combustion. It is necessary to consider that an upholstered chair will have two main components that burn: the soft parts (ie. Foam, interliner, fabric etc.) and the frame, the latter of these is not seen until nearly all of the 'soft' materials are consumed. The predicted total heat released is provided in equation 9.6.

$$Q = 0.9 m_{soft} \Delta h_{c,eff} + 2.1\left[m_{comb,tot} - m_{soft}\right]^{1.5} \qquad [9.6]$$

The effective heat of combustion comes from the Cone Calorimeter test data. Estimates of m_{soft} are from full-scale furniture items based on previous researchers data [7,8]. A detailed calculation of m_{soft} can be found in Appendix E.

9.2.4 Prediction of time to peak HRR

Predicting the time to peak HRR is an important modelling parameter in fire scenarios. It is recognised that often other variables are maximised at, or near the time of peak HRR. The expression developed for predicting the time to peak HRR is given in equation 9.7.

$$t_{peak} = 30 + 4900\,(style\,fac.\,B)\left(m_{soft}\right)^{0.3}\left(\dot{q}''_{pk\#2}\right)^{-0.5}\left(\dot{q}''_{trough}\right)^{-0.5}\left(t_{pk\#1} + 200\right)^{0.2} \qquad [9.7]$$

9.2.5 Time to untenable conditions

The time to untenable conditions in a standard room[6] is given in equation 9.8. Untenability is defined by the time from 50 kW HRR to 100°C temperature, 1.1 to 1.2 m above floor level. Although compartment fires are not part of this research, an investigation into the effects the respective materials may have on tenability times may be pertinent to conclusions regarding the potentially most hazardous fabric.

$$t_{UT} = 1.5\times10^{5}(style\_fac.B)\left(m_{soft}\right)^{-0.6}\left(\dot{q}''_{trough}\right)^{-0.8}\left(\dot{q}''_{pk\#2}\right)^{-0.5}\left(t_{pk\#1} - 10\right)^{0.15} \qquad [9.8]$$

The pertinent nomenclature for Model I are as follows. Figure 9-1 shows the relevant nomenclature that refers to the Cone Calorimeter HRR histories.

[6] The ISO 9705 Standard room dimensions are 3.6 m x 2.4m x 2.4m high.

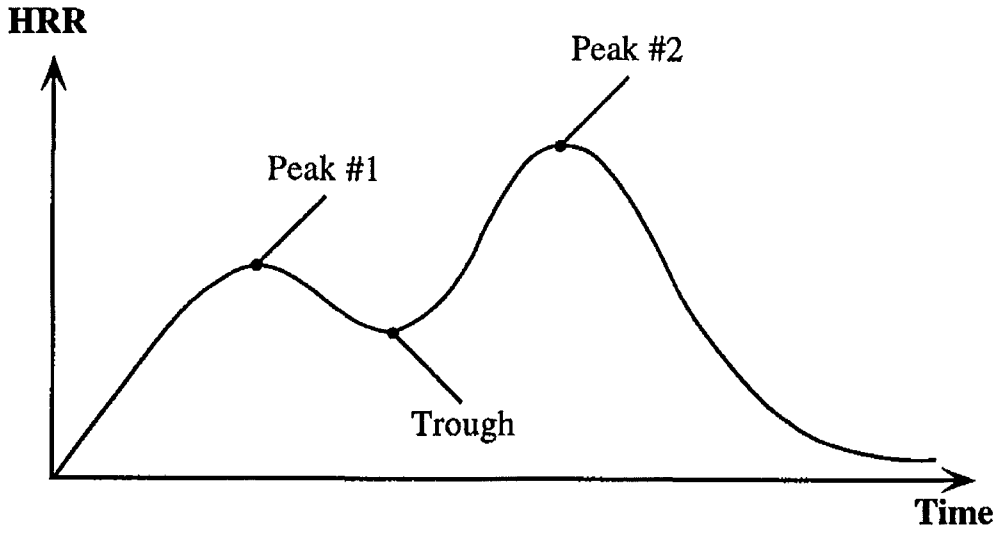

Figure 9-1: Schematic view of a Cone Calorimeter HRR curve indicating nomenclature used in Model I [6].

m_{soft}	Mass of the soft combustible parts of the full-scale item (kg) which includes foam, fabric, interliners etc., but does not include rigid support pieces.
$m_{comb,total}$	Entire combustible mass (kg)
$\dot{q}''_{peak}$	Peak HRR (kW/m^2) at 35 kW/m^2 exposure
$\dot{q}''_{300}$	300 second average HRR (kW/m^2) at 35 kW/m^2 exposure
q''_{total}	Total heat released (MJ/m^2)at 35 kW/m^2 exposure
t_{ig}	Cone Calorimeter time to ignition (s)
$t_{pk\#1}$	Time to first peak of the Cone Calorimeter HRR curve, from start of test (s)
$\dot{q}''_{pk\#2}$	Second peak HRR (kW/m^2) at 35 kW/m^2 exposure
$\dot{q}''_{trough}$	Trough of Cone Calorimeter HRR curve (kW/m^2)
$\Delta h_{c,eff}$	Test average effective heat of combustion in the Cone Calorimeter (MJ/kg)
Style fac. A and B	Style factors for the full-scale furniture.

9.2.6 Input parameters

The required input variables V_{soft}, m_{frame}, Style factor. A and Style factor. B for Model I are summarised in Table 9-2. The values of V_{soft} and m_{frame} are averages for the respective chair styles.

Table 9-2: Input variables for Model I for an armchair and a two-seat sofa.

	ARMCHAIR		TWO-SEAT SOFA
STYLE CODE(--)	{1}	{4}	{2}
Style factor. A (--)	1.0	0.9	1.0
Style factor. B (--)	1.0	0.9	0.8
V_{soft} (m^3)	0.133	0.112	0.188
m_{frame} (kg)	19.54	16.42	24.36

Equations 9.1-9.8 used in Model I for calculating peak HRR, total heat released, time to peak HRR, and time to untenable conditions requires the mass of the soft combustible components (m_{soft}) and the total combustible mass ($m_{comb,total}$). The mass of the soft combustible components is given in equation 9.9 utilises the small-scale composite density and the volume of soft components for the respective chair styles.

$$m_{soft} = \rho_{com} V_{soft} \qquad [9.9]$$

The total combustible mass is given in equation 9.10 combines the frame mass and the mass of the soft combustible components.

$$m_{comb,total} = m_{soft} + m_{frame} \qquad [9.10]$$

9.3 Model I results

9.3.1 Armchair (styles 1 and 4) and Two-seat sofa (style 2)

The proceeding tabulated data is a summary of the results obtained from CBUF Model I for armchair styles 1 and 4. Table 9-3 summarises the values of peak HRR, and total heat released predicted by Model I for flame resistant foam/fabric composites. The time to peak HRR and time to untenable conditions are unattainable as these values are dependent on $\dot{q}''_{trough}$ and $\dot{q}''_{pk\#2}$ which are not discernible in the HRR histories for each composite. These values have been omitted from the table for clarity, however they are

included in other tables elsewhere. Composites J-23 and J-24 have been omitted as their $\dot{q}''_{180}$ average exceeded ± 10 % of the arithmetic mean.

Table 9-3: Model I predictions of peak HRR, and total heat released, for armchair styles 1 and 4, and a two-seat sofa, style 2, for melting fabric/foam composites.

	ARMCHAIR				TWO-SEAT SOFA	
FOAM/ FABRIC	{1}		{4}		{2}	
	$\dot{Q}_{peak}$ (kW)	Q_{total} (MJ)	$\dot{Q}_{peak}$ (kW)	Q_{total} (MJ)	$\dot{Q}_{peak}$ (kW)	Q_{total} (MJ)
K-23	1011	307	1311	245	1571	430
L-23	1338	342	1244	274	1464	480
K-24	1455	311	1337	248	1613	436
L-24	1334	329	1241	263	1458	461
J-25	1033	326	1274	261	1511	458
K-25	988	305	1346	243	1627	427
L-25	1378	333	1276	267	1515	467
J-26	1364	333	1265	267	1498	467
K-26	962	309	861	246	1592	433
L-26	1357	335	1259	269	1488	470
J-29	1390	323	1286	259	1530	453
K-29	948	294	851	234	1646	411
L-29	1390	324	1286	259	1531	453
J-31	1386	327	1282	262	1525	459
K-31	955	294	856	234	1627	412
L-31	1026	322	1273	257	1511	451
J-33	1365	335	1266	268	1498	469
K-33	985	310	1328	247	1598	434
L-33	1360	337	1262	270	1492	472
J-35	1379	338	1276	271	1516	474
K-35	1445	313	1329	250	1601	439
L-35	1365	339	1266	271	1498	475

Table 9-4 summarises the results of CBUF Model I, armchair styles 1 and 4 charring fabrics. Composites J-27 and J-28 have been omitted because their $\dot{q}''_{180}$ average exceeded ± 10 % of the arithmetic mean

Table 9-4: Model I predictions of peak HRR, total heat released, time to peak HRR, and time to untenable conditions for armchair styles 1 and 4, and a two-seat sofa, style 2, for charring and charring/melting fabric/foam composites.

	ARMCHAIR								TWO-SEAT SOFA			
FOAM/ FABRIC	{1}				{4}				{2}			
	$\dot{Q}_{peak}$ (kW)	Q_{total} (MJ)	t_{peak} (s)	t_{UT} (s)	$\dot{Q}_{peak}$ (kW)	Q_{total} (MJ)	T_{peak} (s)	t_{UT} (s)	$\dot{Q}_{peak}$ (kW)	Q_{total} (MJ)	t_{peak} (s)	t_{UT} (s)
CHARRING FABRICS												
K-27	950	292	139	73	853	233	123	73	1597	409	127	47
L-27	1363	320	139	62	1264	256	123	62	1496	448	126	40
K-28	1419	310	144	68	1308	248	127	68	1567	435	131	44
L-28	1350	336	106	32	1254	269	95	32	1480	471	98	21
CHARRING/MELTING FABRICS												
J-30	1360	308	114	46	1261	246	102	46	1492	432	105	30
K-30	939	279	94	41	845	221	85	41	1572	390	87	27
L-30	1014	304	97	36	1250	242	87	36	1474	426	89	23
J-32	1344	315	137	53	1249	251	121	53	1472	441	125	34
K-32	1390	290	121	53	1285	230	107	53	1530	406	110	34
L-32	1333	314	123	49	1240	251	110	49	1457	440	113	32
J-34	1375	309	112	44	1274	247	100	44	1512	433	103	28
K-34	934	280	125	63	841	222	111	63	1593	392	114	41
L-34	1033	307	114	45	1260	245	101	45	1490	430	104	29
J-36	1345	317	112	36	1249	253	100	36	1472	444	103	23
K-36	965	283	132	62	863	225	117	62	1523	396	120	40
L-36	1323	309	134	56	1233	246	119	56	1445	432	122	36

Table 9-5 and Table 9-6 are summary tables of ranges for peak HRR, total heat released, time to peak HRR, and the time to untenable conditions for the three fabric flammability categories and the respective armchair and sofa styles.

Table 9-5: Range of Model I predictions of peak HRR, total heat released, time to peak HRR, and time to untenable conditions for armchair styles 1 and 4 for melting, charring, and charring/melting composites.

	Melting Fabrics		Charring Fabrics		Charring/Melting Fabrics	
ARMCHAIR	1	4	1	4	1	4
$\dot{Q}_{peak}$ (kW)	948-1455	851-1346	950-1419	853-1308	853-1308	841-1285
Q_{total} (MJ)	294-342	234-274	292-336	233-269	279-317	221-253
t_{peak} (s)	N/A[7]	N/A	106-144	95-127	94-137	85-121
t_{UT} (s)	N/A	N/A	32-73	32-73	36-63	36-63

Table 9-6: Range of Model I predictions of peak HRR, total heat released, time to peak HRR, and time to untenable conditions for a two-seat sofa (style 2) using melting, charring, and char/melting composites.

	Melting Fabrics	Charring Fabrics	Char/Melting Fabrics
TWO-SEAT SOFA	{2}	{2}	{2}
$\dot{Q}_{peak}$ (kW)	1458-1646	1480-1597	1445-1593
Q_{total} (MJ)	411-480	409-471	390-444
t_{peak} (s)	N/A	98-131	87-125
t_{UT} (s)	N/A	21-47	23-41

Figure 9-2 and Figure 9-3 are graphical depictions of the tabulated results of the times to peak HRR for charring and char/melting fabrics, armchair style 1. Other chair styles have not been included as Style factor. B is only a scalar variable that will have the effect of moving the points up or down. The purpose of the graphs is to display the trends evident with the foam and fabric compositions.

[7] N/A in the tables indicates that the predicted value is not applicable. This arrises because of the dependence on $\dot{q}''_{trough}$ and $\dot{q}''_{pk\#2}$ which are not discernible in the HRR histories for each composite.

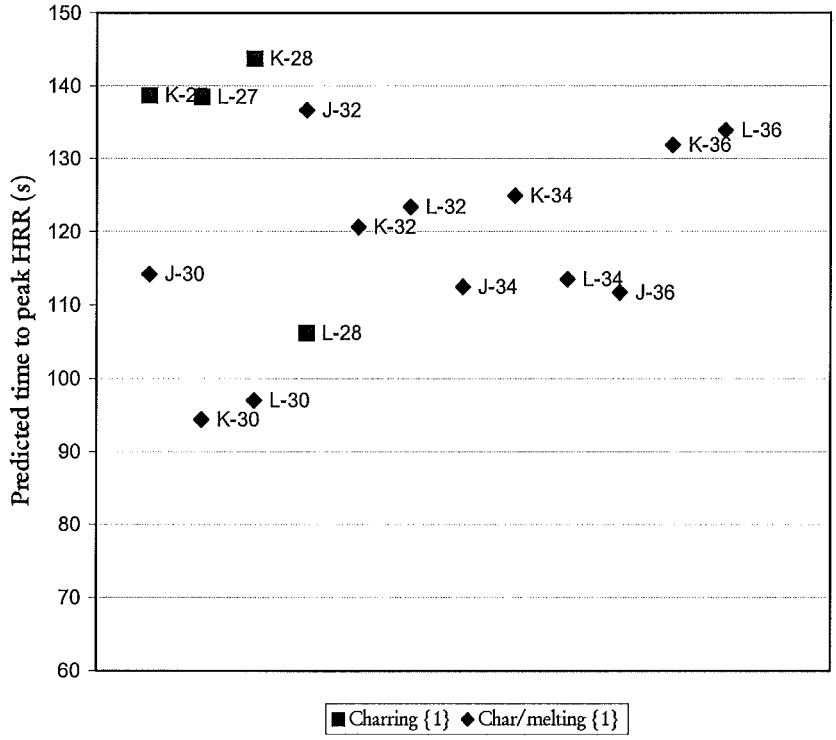

Figure 9-2: Graphical depiction of times to peak HRR for charring and char/melting fabrics for armchair style {1}

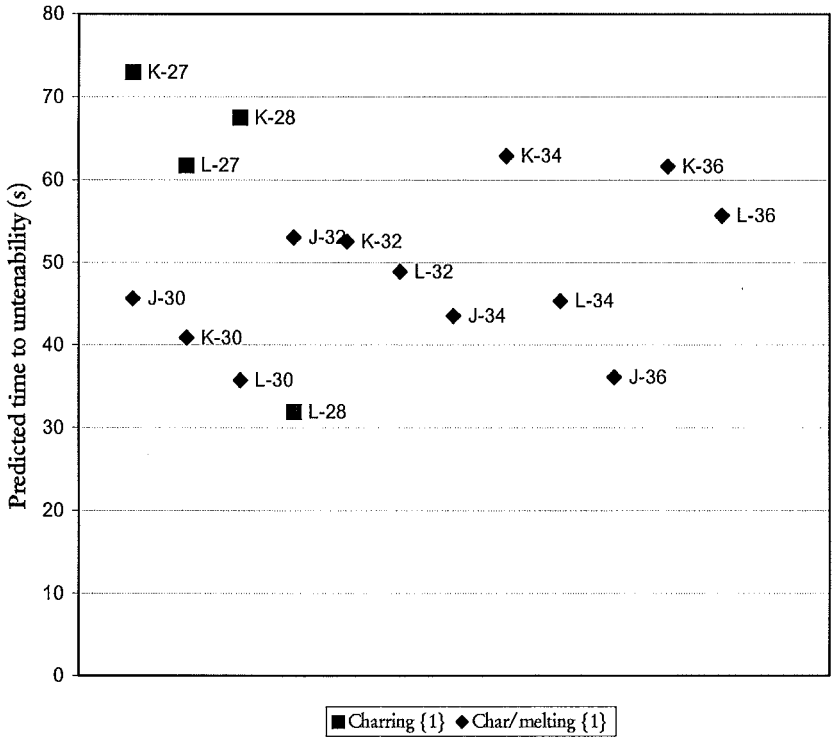

Figure 9-3: Graphical depiction of times to untenable conditions for charring and char/melting fabrics for armchair style {1}

9.4 Discussion of results of Model I

Because no full-scale furniture items were tested in this research, the results are compared with previous NZ-CBUF work conducted at the UC. If trends can be developed for how Model I predicts the peak HRR, total heat released, and the time to peak HRR for NZ-CBUF items, meaningful conclusions can be made with regard to the accuracy of the model and the applicability of the results.

9.4.1 Previous NZ-CBUF research at UC

Previous CBUF research conducted at the UC by and Denize [7], Enright [8], and Firestone [9], concluded that Model I tended to be a poor predictor of NZ furniture in terms of peak HRR, total heat released and the time to peak HRR.

NZ-CBUF foams and fabrics examined by Enright consisted of polyether and generic polyurethane foams, with a blend of polyester, nylon and cotton fabrics. Eight armchairs (styles 1 and 4) and five two-seat sofas (style 2) were used as a basis for the conclusions.

Enright concluded that Model I was a poor predictor, especially for the peak HRR rate where values were significantly under-predicted by the model. The time to peak HRR also showed under-prediction whereas the total heat released showed relatively good interpretation, but tended to be over predicted for certain items. Statistical correlations, provided in Table 9-7 for each parameter, were prepared which indicates the degree of accuracy Model I was able to produce. The correlation coefficient 'R' and coefficient of determination 'R^2' were calculated for the sample set.

Table 9-7: Correlation statistics, Model I (Table 11, Enright)

	Correlation 'R'	Determination 'R^2'
Peak HRR (kW)	57%	32%
Total heat (MJ)	87%	76%
Time to peak (s)	75%	57%
Peak $HRR_{modified}$ (kW)	74%	54%

As the values converge to 100%, the accuracy of the prediction increases. It is important to note that these do not indicate bias such as over prediction or under-prediction.

Enright elaborated on the high dependence of the partial correlating variable, x_1, to the measured peak HRR in the determination regimes. Neglecting this partial dependence had the effect of improving the "goodness of fit" as indicated in Table 9-7, Peak $HRR_{modified}$. As the correlating variable x_1 is strongly coupled to the mass of soft combustibles, the peak HRR prediction is more or less linearly proportional to x_1. This trend was displayed whereby varying fabrics caused differing cone and furniture HRR histories suggesting an over dependence on mass of combustibles, rather than fabric composition.

Firestone's observations from the bench-scale tests applied to Model I indicated that a pronounced foam and fabric effect exist on the combustion behaviour of the full-scale furniture and the predicted results obtained from Model I. The peak HRR tended to be over predicted for both foam and fabric combinations, more so for the high resilience foam. For predicted times to reach peak HRR, the model tended to under-predict times for the standard polyurethane foam/fabric combinations, but over-predicted times for the high resilience foam/ fabric combinations. The total heat released tended to be over-predicted, except for the standard foam and cotton/linen fabric, which was under-predicted. One composition that was notable was the high resilience foam and the polypropylene fabric, which was poorly predicted by Model I. Major findings were the difficulty of the model to accurately predict the full-scale burning characteristics of the combustion modified foam.

Denize conversely showed that Model I predicted the peak HRR with some degree of accuracy whereby there was both under-prediction and over-prediction of the peak HRR. The total heat released values obtained by Model I indicated an over prediction. Conversely, the time to peak HRR predicted by the model tended to show an under-prediction of times. From a design perspective these results could be considered as a conservative approach, but the variation and spread of data points indicate a poor representation of NZ furniture (for detailed results consult figures 10.1, 10.3 and 10.4 of Denize's research).

Table 9-8 summarises the previous researchers results regarding how Model I predicts the peak HRR, total heat released, and the time to peak HRR.

Table 9-8: Summary of Denize, Enright, and Firestones results indicate how Model I predicted the peak HRR, total heat released, and the time to peak HRR.

	Peak HRR	Total Heat Released	Time to peak
Denize	Good*	Over	Under
Enright	Under	Average (over)**	Under
Firestone	Over	Over	Under/Over***

* Denize's results show a good correlation, but a small tendency for the model to over predict the peak HRR.

** Enright's results show a good interpretation but a tendency to over predict.

*** Firestone indicated by varying the foam effected the models prediction capabilities whereby for standard foams times were under-predicted, and for combustion-modified foam the times were over predicted.

As a basis to draw conclusions by, a consensus must be made regarding the Model's capabilities of being able to predict the required parameters. Past results indicate Model I had the tendency to both over-predict and under-predict peak HRR's, but for clarity it will be considered that over-prediction is a common trend. It is unanimous that the total heat released is generally over-predicted and the time to peak HRR is under-predicted. The effect that combustion-modified foams had (ie foam J) on the results was considered. Firestone concludes the model has various inaccuracies regarding predicting peak HRR, and time to peak HRR where by exaggerated over prediction is common. Overall Model I can be considered as conservative where peak HRR's and total heat released are over-predicted and the time to peak HRR's are under-predicted.

9.4.2 Peak Heat Release Rate

Armchair style 1 has higher upper and lower bounds for the HRR compared with style 4 and for all HRR magnitudes, style 1 is noticeably greater that style 4. The two-seat sofa

typically had higher heat release rates because of the extra mass of soft combustible components, which is a heavily dependent component in the predictive equation.

Comparison of flammability behaviour observed from the Cone Calorimeter and the predicted values obtained from Model I show that there is no *direct* similarity between characteristics such as the peak HRR and the fabric composition. For example, it was observed that flame resistant fabrics that contained olefin (fabrics 26, 31, and 35) typically depicted high or the highest heat release rates, whereas compared to the full-scale peak HRR predicted by Model I, olefin containing fabrics are amongst the lowest peak HRR. It is also typical of the composites that exhibit the highest values for HRR are composites that included foam J, which tends to be the denser foam of the three examined. Because the values of m_{soft} are estimates from previous data, which incorporate the average small-scale specimen density, then the determination of the correlation coefficient x_1 becomes heavily dependent on this variable.

Other characteristics observed from the cone calorimeter that did not coincide with the predicted values were melting fabrics containing polyethylene (PE) and acrylic. They had lower peak HRR's but are considered by Model I to have the highest full-scale peaks. This is again related to the density of the composite, especially the fabric weight where PE fabrics tended to be heavier.

It was common to see predicted values for foam J to be one of the highest for the each foam/fabric composition. Since this is the heaviest foam examined, it will inherently have one of the highest predicted peaks, given the dependence of the correlating coefficient, x_1, with the mass of soft combustibles. Although the peak HRR, $\dot{q}''_{peak}$, is coupled into the equation, the effect of the combustion modified foam is not reflected clearly, where it was graphically shown, that composites consisted of foam J have significantly lower peak HRR, and longer burning periods.

Because the correlation coefficient x_1 is dependent on the 300 second HRR average, its emission resulted in a difference of up to approximately 200 kW in the final predicted result. The effect this may have on decisions regarding which is the potentially most

hazardous combination of foam and fabric may be of great importance. Because the test duration did not span this length, these values were otherwise unattainable.

For melting fabrics, olefin and/or PE consistently produce the highest peak HRR for both armchair styles and the two-seat sofa with maximum values of 1455 kW, 1337 kW and 1646 kW for the respective styles. For charring fabrics, cotton produced the highest peak HRR with maximum values of 1419 kW, 1308 kW for armchair styles 1 and 4 respectively. The only irregularity was the two-seat sofa where the nylon fabric (28) produced a peak HRR of 1597 kW. For the char/melting fabrics PE/viscose blends tended to produce the highest peak HRR with values of 1390 kW, 1285 kW and 1593 kW.

The foam that was most prominent in the previous results was foam K. Foam K is less dense than the other specimens, but the flammability concern arises due to the high heat of combustion it possesses. Although its density varies up to 28% compared to foams J and L, the amount of heat it releases is comparable to that of foam L.

9.4.3 Total Heat Released

The predicted total heat released provided in equation [9.6], is highly dependent on the mass of soft combustible components on the chair. The effective heat of combustion of the small-scale composite is also coupled to the mass of soft combustibles so this is the determining part of the equation. Subsequently, the remainder of the equation essentially remains constant for all chair styles since it only calculates the mass of the chair frame to an exponent.

The results show that the two-seat sofa consistently produces more energy than the armchairs, given the greater mass of soft combustibles on the frame and the larger overall mass. The tabulated results conclusively show that fabrics comprised of Polypropylene (PP), PE, olefin, and viscose release high amounts of energy. For melting fabrics, PP, PE, olefin or a combination of these three fabrics (eg. PE + olefin) proved to release the most energy. Fabrics 23, 24, and 26 comprised of 100% PP, 100% PE and 100% olefin respectively. Fabric 31and 33 comprised of 50/50 PE/olefin and 51/49 PP/PE respectively. Maximum values for the total heat released was 342 MJ, 274

MJ, and 480 MJ for the respective chair styles. For charring fabrics, fabric 28 (100% cotton) consistently produced the highest amount of heat for the armchair and the two-seat sofa with 336 MJ, 269 MJ, and 471 MJ for the respective styles. These values were obtained from combinations with foam L. For charring/melting fabrics the predominant fabrics that release larger amounts of energy are those that were comprised of PE and Viscose. The composite that produced the most energy in this category was J-36 with 317 MJ, 253 MJ, and 444 MJ for chair styles 1,4 and 2 respectively. Given all the charring/melting fabrics comprise of PE, the combination of PE with viscose proved to be a greater threat in terms of total heat released.

The reason why fabrics comprised of PP and PE release such high amounts of energy is the fibres high heat of combustion The heat of combustion of PP and PE are 46.2 - 46.5 MJ/kg and 46.37 MJ/kg respectively. These fabrics are inherently quite dense. This is to reduce flame spread across the surface [6], but it provides extra combustible mass.

For the fabrics outlined above, their combination with foam L tended to produce the largest amount of energy for the respective foam/fabric combinations. Because foam L is one of the heavier specimens (heat of combustion 21.1 MJ/kg) the total amount of heat released, coupled with high heat of combustion fabrics, will inherently be high.

9.4.4 Time to peak HRR

The time to peak HRR is dependant on the experimentally determined variables m_{soft}, $\dot{q}''_{pk\#2}$, $\dot{q}''_{trough}$, and $t_{pk\#1}$. The empirical law in equation [9.7] indicates the dependence on the mass of soft combustibles, is again a governing factor. Previous research indicated that predicted times to peak HRR were generally under-predicted by Model I, which is conservative, but also had the tendency of over-predicting times for combustion modified foams. The limitation of this derivation is the inability to predict times to peak HRR when these governing variables are unattainable.

Inspection of the tabulated results shows that charring/melting fabrics displayed shorter times to peak HRR than the charring fabrics did. The trends displayed that fabrics composed of PE tended to have faster times to peak HRR than other fabric compositions. Composition K-30 had the fastest time to peak HRR at 85 seconds for

armchair style 4. For charring fabrics, it was confirmed that the times to peak HRR are longer than their counterparts. No evidence of particular foams that effected the time to peak HRR, but more of a fabric effect.

If the Cone Calorimeter results are examined and compared to the output of Model I, the reason the predicted times to peak HRR are so rapid is the reliance on the time to the fist peak, $t_{pk\#1}$. Because charring/melting fabrics exhibit an ultra fast growth to the first peak, this caused the predicted values of the time to peak HRR to be very rapid as well. The fast growth rate was the result of the immediately combustible material been vaporised which causes this initial spike in the HRR histories.

9.4.5 Time to untenable conditions

The scope of this research does not include prediction of times to untenable conditions but these values would provide a good predictor of the potentially hazardous foam/fabric combinations in a room scenario. Equation [9.8] is the expression derived from the CBUF programme for Model I to predict the time to untenable conditions in the ISO 9705 standard room. This also is dependent on the experimentally determined variables m_{soft}, $\dot{q}''_{pk\#2}$, $\dot{q}''_{trough}$, and $t_{pk\#1}$. As with predictions of time to peak HRR, the empirical law's ability is restricted when these variables are unattainable. At present, no previous NZ-CBUF has been conducted regarding the validity of this model and the accuracy of the results, which would be a sound basis for future research.

Untenability is defined by the time from 50 kW HRR to 100°C temperature, 1.1 to 1.2 m above floor level. The results showed charring/meting fabrics to have faster times to untenable conditions than charring fabrics. It was common for fabrics composed of PE with viscose to produce faster times to untenability than other fabric compositions. This is evident due to the rapid combustion of the PE fibre in the weave. The fastest time to untenability was composite L-28 at 21 seconds for a two-seat sofa. It was expected that times to untenable conditions would be shorter for the two-seat sofa given the larger mass of the item. The times obtained from these results seem relatively short compared with the time to peak HRR. Again, there was no evidence of particular foams effecting the time to peak HRR, but more of a fabric effect.

9.4.6 Propagation of uncertainty through Model I

It is expected that with the dependence of Model I on experimentally determined variables and the highly empirical nature of the defining equations, uncertainty throughout the results is likely to occur. Various factors and variables that are prone to cause such uncertainty in the results are

1. The correlation coefficient x_1 and its dependence on the estimated values of the soft combustible mass, m_{soft}.
2. The inability of the model to predict fire scenarios when input variables such as $\dot{q}''_{pk\#2}$, $\dot{q}''_{trough}$, and $\dot{q}''_{300}$ are unattainable.
3. The inability to adjust to chemical changes in foams and the effect different fabric fibre compositions may have on the burning behaviour of various composites.

The correlation coefficient x_1 is strongly coupled to the mass of soft combustibles, and the peak HRR prediction is more or less linearly proportional to x_1. The derivation of the mass of soft combustibles was experimentally calculated from previous data to give a representation of the volume of foam and fabric on the armchairs and two-seat sofas. Given the small sample size of the data referenced, and the availability of the sample data, an interpretation of the mass of soft combustibles is given using an *average composite density* multiplied with this hypothetical volume. Upon inspection, calculated foam/fabric volumes for the armchair (styles 1 and 4) and the two-seat sofa (style 2) vary up to 36% and 38% of their arithmetic means respectively for different foam/fabric combinations. If it were possible in this situation for this variation to be propagated through the results, it could cause substantially different outcomes for the peak HRR, total heat released, time to peak HRR and the time to untenable conditions.

There are limitations in the model's ability to predict various parameters, such as time to peak HRR, and time to untenable conditions, because of their dependence on the variables $\dot{q}''_{pk\#2}$, $\dot{q}''_{trough}$, and $\dot{q}''_{300}$. It was found that certain HRR histories (ie those characteristic of melting fabrics) did not display the characteristics where these values could be distinguished. It was also noted that the duration of the test did not extend past 300 seconds from the start of the test, so values for $\dot{q}''_{300}$ could not be calculated (this

was prominent for 47% of the averaged triplicate samples). The impact this value may have on the peak HRR could be an extra 100 to 200 kW in the result.

The predicted results obtained from Model I show that there is lack of ability to account for difference in chemical composition of both foam and fabric throughout the model. It was shown that the effect certain foams and fabrics had on the HRR histories (ie lower peaks and prolonged burning periods, consistently high HRR and total heat released) were not prevalent in the predicted results.

9.5 Model I Conclusions

9.5.1 Peak Heat Release Rate

Melting fabrics, olefin and PE consistently produce the highest peak HRR for both armchair styles and the two-seat sofa with maximum values of 1455 kW, 1337 kW and 1646 kW for the respective chair styles. For charring fabrics, cotton produced the highest peak HRR with maximum values of 1419 kW, 1308 kW for armchair styles 1 and 4 respectively. For the two-seat sofa, the nylon fabric (28) produced a peak HRR of 1597 kW. For the charring/melting fabrics PE/viscose blends tended to produce the highest peak HRR with values of 1390 kW, 1285 kW and 1593 kW respectively.The foam that was most prominent in producing the high peak HRR was foam K.

9.5.2 Total heat released

Melting fabrics, PP, PE, olefin or a combination of these three proved to release the most energy. Maximum values for the total heat released was 342 MJ, 274 MJ, and 480 MJ for the respective chair styles. For charring fabrics, cotton consistently produced the highest amount of heat with 336 MJ, 269 MJ, and 471 MJ for the respective styles. For char/melting fabrics the predominant fabrics that release larger amounts of energy are those that comprised of PE and viscose. The composite that produced the most energy in this category was J-36 with 317 MJ, 253 MJ, and 444 MJ for chair styles 1,4 and 2 respectively. For the fabrics outlined above, their combination with foam L tended to produce the largest amount of energy for the respective foam/fabric combinations.

9.5.3 Time to peak heat release rate

Charring/melting fabrics displayed shorter times to peak HRR. Fabrics composed of PE tended to have faster times to peak HRR than the other fabric compositions. Composition K-30 had the fastest time to peak HRR at 85 seconds for armchair style 4. There was no evidence of particular foams effecting the time to peak HRR, but more of a fabric effect.

9.5.4 Time to untenable conditions

Fabrics composed of PE with viscose tended to produce faster times to untenability than other fabric compositions. The fastest time to untenability was composite L-28 at 21 seconds for a two-seat sofa. It was expected that times to untenable conditions would be shorter for the two-seat sofa given the larger mass of the item.

9.5.5 Associated errors

The dependence of Model I on experimentally determined variables and the highly empirical nature of the equations, uncertainty throughout the results is unavoidable. Various factors and variables that are prone to cause such uncertainty in the results are

1. The correlation coefficient x_1 and its dependence on the estimated values of the soft combustible mass, m_{soft}.
2. The inability of the model to predict fire scenarios when input variables such as $\dot{q}''_{peak}$, $\dot{q}''_{trough}$, and $\dot{q}''_{300}$ are unattainable.
3. The inability to adjust to chemical changes in foams and the effect different fabric fibre compositions may have on the burning behaviour of various composites.

The derivation of the mass of soft combustibles was experimentally calculated from previous data to give a representation of the volume of foam and fabric on the armchairs and two-seat sofas. The lack of raw data to provide a precise estimate of m_{soft} will effect the results given the high reliance of the defining equations on this variable.

The models limitation to predict parameters such as time to peak HRR, and time to untenable conditions because of their dependence on the variables $\dot{q}''_{pk\#2}$, $\dot{q}''_{trough}$, and $\dot{q}''_{300}$ which were sometimes not discernible from various HRR histories (ie those characteristic of melting fabrics). The dependence of Model I on numerous parameters that are sometimes unattainable hinders the models performance and predictive power.

The lack of ability to account for differences in chemical composition of both foam and fabric throughout the model and the effect that certain foams and fabrics had on the HRR histories ie. Lower peaks and prolonged burning periods, consistently high HRR and total heat released were unaccounted.

10 CONCLUSIONS AND RECOMMENDATIONS

10.1 Cone Calorimeter conclusions

The foam that tended to produce the greatest amount of energy, consistently have the highest peak HRR, and ignite very quickly was foam L. Foam J (fire retardant) showed the tendency to release a lot of energy over longer periods. The combustion characteristics of foam J were dubious, which caused a lot of uncertainty in the results regarding ignition times and its ignitability. Foam K has the tendency to release comparatively smaller amounts of energy, over shorter periods.

There is a pronounced fabric effect demonstrated in the small-scale tests. The presence of fabric over the foams has the effect of increasing ignition times. The fabric composition also has the effect of changing the burning characteristics of the foam/fabric composite.

The most flammable foam/fabric combination was composite L-26. This fabric consistently had the highest peak HRR, and total energy released.

Melting fabrics composed of PP and olefin displayed characteristics where high HRR's, and large amounts of energy are produced when combined with any of the three foams.

10.2 Model I conclusions

Melting fabrics olefin and PE consistently produce the highest peak HRR for both armchair styles and the two-seat sofa. For charring fabrics, cotton produced the highest peak HRR with maximum values of 1419 kW, 1308 kW for armchair styles 1 and 4 respectively. For the two-seat sofa, the nylon fabric (28) produced a peak HRR of 1597 kW. For the charring/melting fabrics PE/viscose blends tended to produce the highest peak HRR with values of 1390 kW, 1285 kW and 1593 kW for the respective chair styles. The foam that was most prominent in the results was foam K. Model I had a tendency to over-predicting the peak HRR so the values obtained can be considered conservative from a design point.

Melting fabrics, PP, PE, olefin or a combination of these three proved to release the most energy. Maximum values for the total heat released was 342 MJ, 274 MJ, and 480 MJ for the respective chair styles. For charring fabrics, cotton consistently produced the highest amount of heat with 336 MJ, 269 MJ, and 471 MJ for the respective styles. For char/melting fabrics the predominant fabrics that release larger amounts of energy are those that comprised of PE and viscose. The composite that produced the most energy in this category was J-36 with 317 MJ, 253 MJ, and 444 MJ for chair styles 1,4 and 2 respectively. Generally, foam L combined with the above fabrics produce the larger amounts of energy for the respective foam/fabric combinations. Model I had a tendency to over-predicting the total heat released so the values obtained can also be considered conservative from a design point.

Fabrics composed of PE tended to have faster times to peak. Composition K-30 had the fastest time to peak HRR at 94 seconds for armchair style 1. There was no evidence of particular foams effecting the time to peak HRR, but more of a fabric effect.

Fabrics composed of PE with viscose tend to produce faster times to untenability than other fabric compositions. The fastest time to untenability was composite L-28 at 21 seconds for a two-seat sofa.

10.3 General Conclusion

1. The fabrics that pose the highest flammability are those that consist of PE, PP and olefin. These caused high peak HRR's, high total heat released and faster time to peak HRR and untenable conditions due to their high heats of combustion.

2. The foams that pose the highest flammability, when coupled with these fabrics, are foams K and L. Fire retardant foam J (ie combustion modified) produces large amounts of energy over longer periods, but tended to smoulder after flaming extinction.

3. The ability of Model I to accurately predict these values was not investigated but it was noted that there is a tendency to over predict HRR and total heat released and under predict time to peak HRR. The ability to compensate for foam and fabric

chemical compositions was limited which was reflected throughout the results. Its dependence on various experimentally variables limit its ability and power to predict various parameters if unattainable. Overall, Model I can be considered conservative from a design point with respect to peak HRR, total heat released and time to peak HRR.

10.4 Recommendations

1. Given the sample size of the NZ-CBUF data, it is recommended that further research be conducted to expand this. There is a need for full-scale furniture testing from series 2 of the CBUF programme to provide a better predictor of NZ furniture, and an improvement of the regimes used to predict full-scale furniture burning behaviour. It was shown that there is a heavy dependence on the mass of the combustible components instead of the type of foam and the fabric composition. Differences in the accuracy of the values predicted were prevalent whereby as the foam and/or fabric was changed the accuracy of the predicted values became larger, which was shown by Firestone.

2. Investigations into the burning behaviour of flame resistant foams and their possible impact on fire growth and severity, especially ignition times.

3. The application of fire scenarios in an ISO-9705 standard room for the further development of Model I as a predictor of time to untenable conditions for NZ-CBUF furniture items.

4. Further application of Model II to NZ-CBUF furniture where fabric effects can be accounted for, which was prevalent throughout these results and unaccountable for.

REFERENCES

1. BABRAUSKAS, V "Development of the Cone Calorimeter-A bench scale Heat release Rate Apparatus Based on Oxygen Consumption" Fire and Materials, Vol 8. (1984)

2. BABRAUSKAS, V "The Cone Calorimeter" SFPE Handbook of Fire Protection Engineering, Second Edition, Society of Fire Protection Engineers, Boston USA (1995), Chapter 3, Section 3.

3. BEYLER, C. L, HIRSCHLER, M. M "Thermal decomposition of polymers" SFPE Handbook of Fire Protection Engineering, Second Edition, Society of Fire Protection Engineers, Boston USA (1995), Chapter , Section 7

4. BS 5852: Methods of test for assessment of the ignitability of upholstered seating by smouldering and flaming ignition sources.

5. BUCHANAN, A "Fire Engineering Design Guide" Center for Advanced Engineering, University of Canterbury (1994).

6. "CBUF. Fire Safety of Upholstered Furniture- the final report on the CBUF research programme". Edited by B. Sundstorm, Interscience Communication Limited, London, UK. (1995)

7. DENIZE, H.A "The Combustion Behaviour of Upholstered Furniture Materials in New Zealand" A thesis in Masters of Fire Engineering at University of Canterbury.

8. ENRIGHT P.A "Heat Release and the Combustion Behaviour of Upholstered Furniture" Thesis in Doctor of Philosophy at University of Canterbury.

9. FIRESTONE, J "An Analysis of Furniture Heat Release Rates by the Nordtest" A thesis in Masters of Fire Engineering at University of Canterbury.

10. HALL, M.E. et al "The flammability of Lyocell" Polymer Degradation and Stability v 54 n 2-3 Nov-Dec 1996.

11. HILADO, C.J "Flammability Handbook for Plastics, 4th Edition" Technomic Publishing Co. Inc (1990)

12. HUGGETT, C "Estimation of Rate of Heat Release by Means of Oxygen Consumption Measurements" Fire and Materials, Vol 4. No 2 (1980).

13. ISO 5660-1 (1993) Fire tests-Reaction to fire-Part 1: Heat release rate from building Products (Cone Calorimeter Method), ISO 5660-1:1993 (E). International Organisation for standardisation, Geneva, 1993.

14. MURTY KANURY, A. "Ignition of Liquid fuels" SFPE Handbook of Fire Protection Engineering, Second Edition, Society of Fire Protection Engineers, Boston USA (1995), Chapter 10, Section 2.

15. University of Canterbury Cone Calorimeter Calibration Procedure, (1999) Edited by Frank Greenslade, University of Canterbury.

16. University of Canterbury Cone Calorimeter Test Procedure, (1999) Edited by Frank Greenslade, University of Canterbury.

17. WILLIAMS, S.S "Flammability regulations and standards in the United States for upholstered furniture" Fire Technology v 22, Nov 1986, p. 349-51.

APPENDIX A: FOAM AND FABRIC SPECIMEN MASSES

Table A-1: Foam and fabric masses

Fabric Type	Fabric Mass (g)	Mean fabric Mass (g)	% Diff	Foam Type	Foam Mass (g)	Mean Foam Mass (g)	% Diff	Total Sample Mass (g)	Total Sample Mean (g)	% Diff	Specimen Code Foam/Fab/S#
23	9.75		0.1	J	23.66		-0.2	32.59		-0.9	J-23-1
	9.75	9.74	0.1	Yellow	23.80	23.71	0.4	33.05	32.88	0.5	J-23-2
	9.73		-0.1		23.68		-0.1	33.01		0.4	J-23-3
	9.63		0.5	K	15.25		0.1	24.2		-0.4	K-23-1
	9.55	9.59	-0.4	Green	15.23	15.24	-0.1	24.42	24.29	0.5	K-23-2
	9.58		-0.1		15.24		0.0	24.25		-0.2	K-23-3
	10.06		0.8	L	20.94		0.0	30.75		0.3	L-23-1
	9.91	9.98	-0.7	Grey	20.93	20.94	0.0	30.63	30.67	-0.1	L-23-2
	9.97		-0.1		20.94		0.0	30.63		-0.1	L-23-3
24	12.96		0.2	J	23.46		-0.2	35.31		0.0	J-24-1
	12.94	12.93	0.1	Yellow	23.54	23.52	0.1	35.31	35.32	0.0	J-24-2
	12.90		-0.3		23.55		0.1	35.34		0.1	J-24-3
	13.16		0.4	K	15.22		0.1	26.8		-0.4	K-24-1
	13.10	13.11	-0.1	Green	15.20	15.21	0.0	26.75	26.91	-0.6	K-24-2
	13.07		-0.3		15.20		0.0	27.19		1.0	K-24-3
	13.17		-0.4	L	20.99		0.2	33		-0.2	L-24-1
	13.25	13.22	0.2	Grey	20.88	20.94	-0.3	33.28	33.06	0.7	L-24-2
	13.24		0.2		20.95		0.0	32.91		-0.5	L-24-3
25	13.00		0.0	J	23.58		0.0	34.99		-0.2	J-25-1
	12.99	13.00	-0.1	Yellow	23.55	23.57	-0.1	35.05	35.06	0.0	J-25-2
	13.00		0.0		23.59		0.1	35.14		0.2	J-25-3
	13.01		0.0	K	15.25		0.0	26.63		0.2	K-25-1
	13.03	13.01	0.2	Green	15.21	15.24	-0.2	26.54	26.58	-0.2	K-25-2
	12.99		-0.2		15.27		0.2	26.58		0.0	K-25-3
	12.89		-0.1	L	20.82		0.0	32.18		0.0	L-25-1
	12.85	12.90	-0.4	Grey	20.83	20.82	0.0	32.25	32.19	0.2	L-25-2
	12.95		0.4		20.81		0.0	32.13		-0.2	L-25-3
26	7.91		0.2	J	23.37		-0.3	30.98		0.0	J-26-1
	7.88	7.89	-0.2	Yellow	23.47	23.45	0.1	31.01	30.99	0.1	J-26-2
	7.89		0.0		23.50		0.2	30.97		-0.1	J-26-3
	8.01		0.1	K	15.29		0.3	22.84		-0.4	K-26-1
	8.00	8.00	0.0	Green	15.26	15.25	0.1	22.87	22.92	-0.2	K-26-2
	7.99		-0.1		15.19		-0.4	23.06		0.6	K-26-3
	8.08		-0.9	L	20.75		-0.2	28.3		-0.7	L-26-1
	8.20	8.16	0.5	Grey	20.80	20.79	0.0	28.58	28.50	0.3	L-26-2
	8.19		0.4		20.83		0.2	28.61		0.4	L-26-3
27	11.06		0.3	J	23.30		-0.1	33.31		-0.2	J-27-1
	11.04	11.02	0.2	Yellow	23.32	23.33	0.0	33.35	33.37	0.0	J-27-2
	10.97		-0.5		23.36		0.1	33.44		0.2	J-27-3
	10.84		-0.2	K	15.11		-0.1	24.38		-1.2	K-27-1
	10.91	10.86	0.4	Green	15.13	15.13	0.0	25	24.67	1.3	K-27-2
	10.84		-0.2		15.14		0.1	24.64		-0.1	K-27-3
	10.94		-0.1	L	20.76		0.1	30.51		-0.2	L-27-1
	10.94	10.95	-0.1	Grey	20.74	20.74	0.0	30.66	30.56	0.3	L-27-2
	10.97		0.2		20.73		-0.1	30.52		-0.1	L-27-3

Table A-1 (Continued)

Fabric Type	Fabric Mass (g)	Mean fabric Mass (g)	% Diff	Foam Type	Foam Mass (g)	Mean Foam Mass (g)	% Diff	Total Sample Mass (g)	Total Sample Mean (g)	% Diff	Specimen Code Foam/Fab/S#
28	14.84		0.0	J	23.26		0.1	36.05		-0.1	J-28-1
	14.84	14.84	0.0	Yellow	23.29	23.25	0.2	36.36	36.10	0.7	J-28-2
	14.84		0.0		23.19		-0.2	35.89		-0.6	J-28-3
	14.81		-0.4	K	15.15		0.1	28.89		2.5	K-28-1
	14.88	14.86	0.1	Green	15.14	15.13	0.1	27.83	28.19	-1.3	K-28-2
	14.90		0.2		15.10		-0.2	27.86		-1.2	K-28-3
	14.92		-0.2	L	20.69		0.0	33.52		0.3	L-28-1
	14.92	14.95	-0.2	Grey	20.69	20.69	0.0	33.34	33.41	-0.2	L-28-2
	15.00		0.4		20.69		0.0	33.38		-0.1	L-28-3
29	10.81		-0.3	J	23.08		-0.2	32.85		0.3	J-29-1
	10.86	10.84	0.2	Yellow	23.17	23.13	0.2	32.72	32.75	-0.1	J-29-2
	10.86		0.2		23.14		0.0	32.69		-0.2	J-29-3
	11.00		0.3	K	15.08		-0.2	24.77		0.1	K-29-1
	10.94	10.97	-0.3	Green	15.09	15.10	-0.1	24.73	24.75	-0.1	K-29-2
	10.97		0.0		15.14		0.2	24.76		0.0	K-29-3
	10.91		0.1	L	20.70		-0.1	30.45		0.2	L-29-1
	10.85	10.90	-0.5	Grey	20.75	20.72	0.1	30.35	30.39	-0.1	L-29-2
	10.94		0.4		20.72		0.0	30.38		0.0	L-29-3
30	10.32		-0.1	J	22.86		0.0	32		0.0	J-30-1
	10.34	10.33	0.1	Yellow	22.86	22.86	0.0	31.95	32.00	-0.2	J-30-2
	10.34		0.1		22.85		0.0	32.06		0.2	J-30-3
	10.24		-0.1	K	15.11		0.2	24.12		0.1	K-30-1
	10.26	10.25	0.1	Green	15.02	15.07	-0.4	24.04	24.11	-0.3	K-30-2
	10.26		0.1		15.09		0.1	24.16		0.2	K-30-3
	10.21		0.0	L	20.62		0.0	29.47		-0.2	L-30-1
	10.21	10.21	0.0	Grey	20.61	20.61	0.0	29.67	29.53	0.5	L-30-2
	10.22		0.1		20.60		0.0	29.45		-0.3	L-30-3
31	8.65		0.0	J	22.85		-0.5	30.53		-0.2	J-31-1
	8.67	8.65	0.3	Yellow	23.03	22.95	0.3	30.61	30.59	0.1	J-31-2
	8.62		-0.3		22.98		0.1	30.62		0.1	J-31-3
	8.74		-0.1	K	15.08		0.2	22.72		0.1	K-31-1
	8.72	8.75	-0.3	Green	15.05	15.05	0.0	22.71	22.71	0.0	K-31-2
	8.78		0.4		15.01		-0.2	22.69		-0.1	K-31-3
	8.73		-0.6	L	20.52		-0.2	28.18		-0.6	L-31-1
	8.76	8.78	-0.2	Grey	20.57	20.55	0.1	28.38	28.34	0.1	L-31-2
	8.85		0.8		20.57		0.1	28.47		0.4	L-31-3
32	13.41		0.0	J	22.75		-0.1	34.26		-0.4	J-32-1
	13.42	13.41	0.0	Yellow	22.80	22.78	0.1	34.44	34.38	0.2	J-32-2
	13.41		0.0		22.79		0.0	34.45		0.2	J-32-3
	13.44		0.0	K	15.04		-0.1	26.7		-0.1	K-32-1
	13.42	13.44	-0.1	Green	15.06	15.05	0.1	26.77	26.72	0.2	K-32-2
	13.46		0.1		15.05		0.0	26.69		-0.1	K-32-3
	13.45		0.1	L	20.42		0.2	31.87		0.1	L-32-1
	13.39	13.43	-0.3	Grey	20.37	20.38	-0.1	31.82	31.85	-0.1	L-32-2
	13.46		0.2		20.36		-0.1	31.85		0.0	L-32-3

Table A-1 (Continued)

Fabric Type	Fabric Mass (g)	Mean fabric Mass (g)	% Diff	Foam Type	Foam Mass (g)	Mean Foam Mass (g)	% Diff	Total Sample Mass (g)	Total Sample Mean (g)	% Diff	Specimen Code Foam/Fab/S#
33	10.83		-0.1	J	22.47		-0.4	31.76		-0.6	J-33-1
	10.84	10.84	0.0	Yellow	22.56	22.56	0.0	32.05	31.94	0.3	J-33-2
	10.86		0.2		22.64		0.4	32.02		0.2	J-33-3
	10.92		0.7	K	15.07		0.2	24.44		0.2	K-33-1
	10.81	10.84	-0.3	Green	15.01	15.04	-0.2	24.4	24.40	0.0	K-33-2
	10.80		-0.4		15.03		0.0	24.36		-0.2	K-33-3
	10.88		-0.1	L	20.38		-0.2	29.8		-0.1	L-33-1
	10.84	10.89	-0.5	Grey	20.42	20.42	0.0	29.78	29.84	-0.2	L-33-2
	10.96		0.6		20.45		0.2	29.93		0.3	L-33-3
34	9.48		0.3	J	22.43		0.2	30.61		0.2	J-34-1
	9.47	9.45	0.2	Yellow	22.43	22.38	0.2	30.58	30.55	0.1	J-34-2
	9.41		-0.5		22.29		-0.4	30.46		-0.3	J-34-3
	9.46		0.5	K	15.03		-0.2	23.19		0.2	K-34-1
	9.40	9.41	-0.1	Green	15.06	15.06	0.0	23.16	23.14	0.1	K-34-2
	9.37		-0.4		15.08		0.2	23.06		-0.3	K-34-3
	9.53		0.0	L	20.21		-0.2	28.5		-0.1	L-34-1
	9.52	9.53	-0.1	Grey	20.29	20.26	0.1	28.56	28.53	0.1	L-34-2
	9.53		0.0		20.28		0.1	28.54		0.0	L-34-3
35	14.54		0.0	J	22.29		0.5	34.82		0.6	J-35-1
	14.48	14.53	-0.4	Yellow	22.16	22.17	0.0	34.58	34.62	-0.1	J-35-2
	14.58		0.3		22.06		-0.5	34.46		-0.5	J-35-3
	14.65		-0.4	K	15.03		0.1	27.5		-0.3	K-35-1
	14.78	14.71	0.5	Green	15.00	15.01	-0.1	27.59	27.57	0.1	K-35-2
	14.70		-0.1		15.00		-0.1	27.62		0.2	K-35-3
	14.42		-0.6	L	20.10		-0.1	32.4		-0.6	L-35-1
	14.53	14.50	0.2	Grey	20.12	20.12	0.0	32.72	32.60	0.4	L-35-2
	14.55		0.3		20.15		0.1	32.68		0.2	L-35-3
36	13.51		0.1	J	22.03		0.1	33.64		0.6	J-36-1
	13.48	13.49	-0.1	Yellow	22.02	22.00	0.1	33.4	33.42	-0.1	J-36-2
	13.49		0.0		21.96		-0.2	33.23		-0.6	J-36-3
	13.76		0.5	K	14.97		0.1	26.41		-0.3	K-36-1
	13.66	13.69	-0.2	Green	14.92	14.96	-0.2	26.51	26.50	0.0	K-36-2
	13.64		-0.3		14.98		0.2	26.58		0.3	K-36-3
	13.61		-0.1	L	20.15		-0.3	31.63		-0.1	L-36-1
	13.67	13.62	0.4	Grey	20.20	20.21	0.0	31.74	31.66	0.2	L-36-2
	13.58		-0.3		20.27		0.3	31.62		-0.1	L-36-3

Foams alone

J	21.92		0.2	24.05		0.9	J-1
Yellow	21.88	21.88	0.0	22.86	23.84	-4.1	J-2
	21.83		-0.2	24.6		3.2	J-3
K	14.92		-0.2	15		-0.2	K-1
Green	14.95	14.95	0.0	15.01	15.02	-0.1	K-2
	14.98		0.2	15.06		0.2	K-3
L	21.01		0.0	21.09		-0.1	L-1
Grey	21.04	21.02	0.1	21.15	21.11	0.2	L-2
	21.00		-0.1	21.08		-0.1	L-3

APPENDIX B: HRR CURVES

Individual foams:

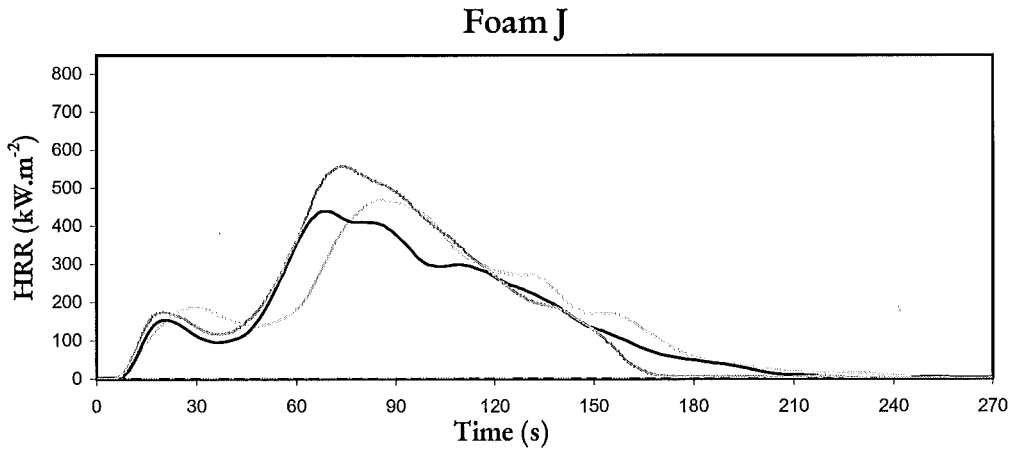

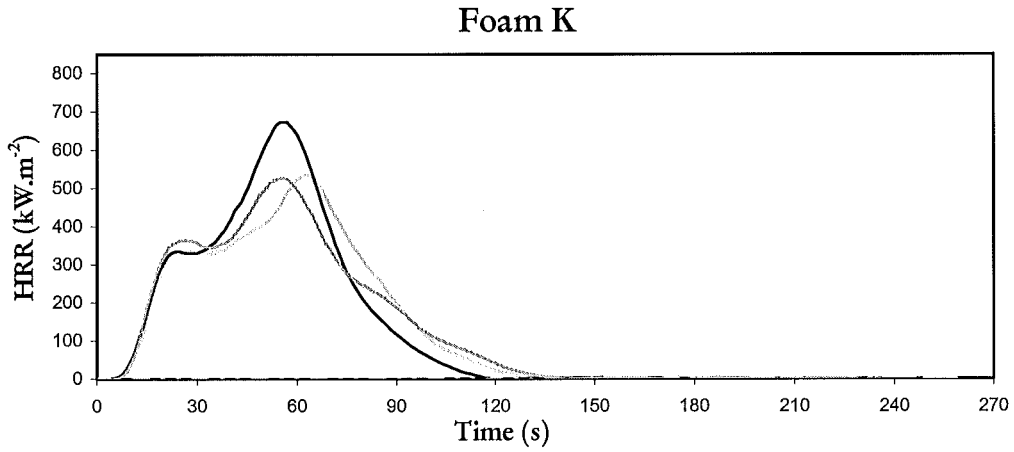

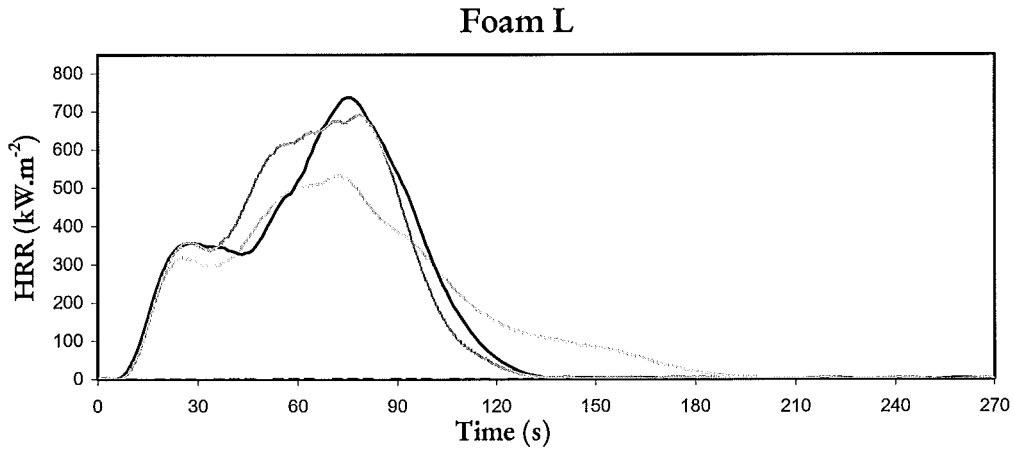

Melting fabrics

Fabric 23:

Composition: 100% Polypropylene

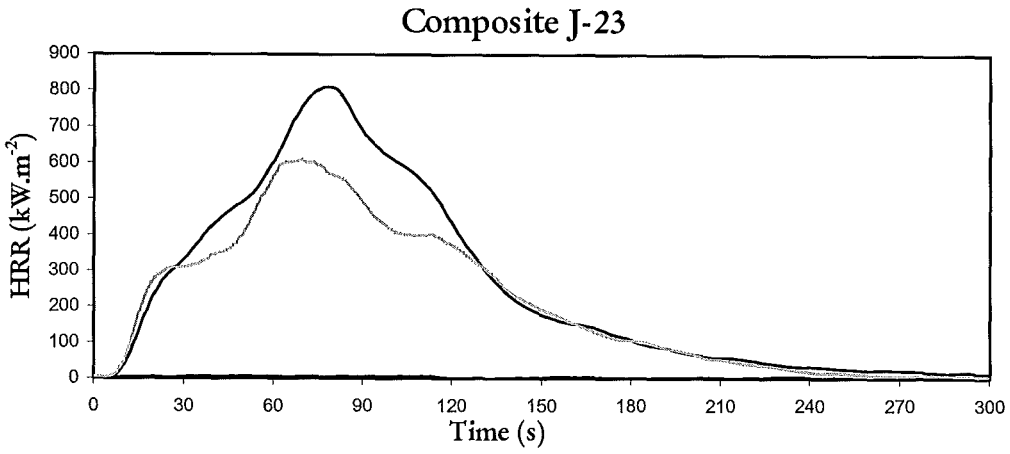

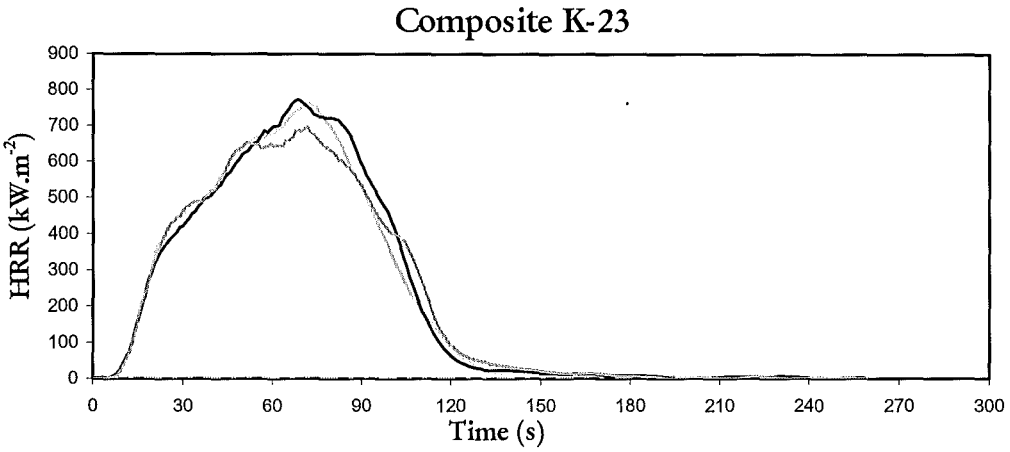

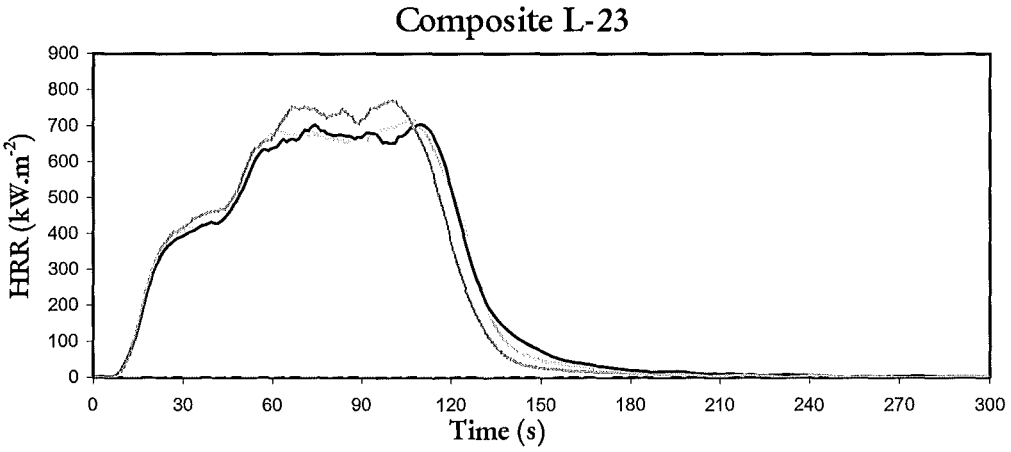

Fabric 24:

Composition: 100% Polyester

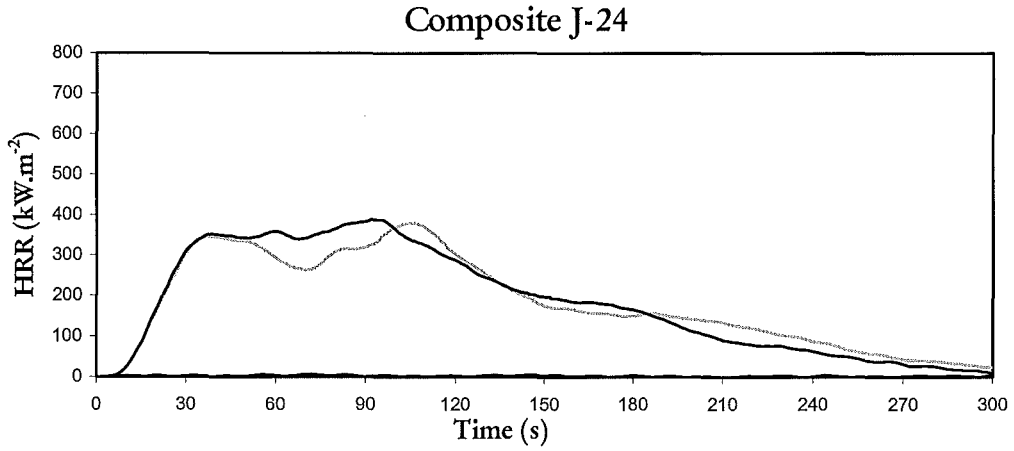

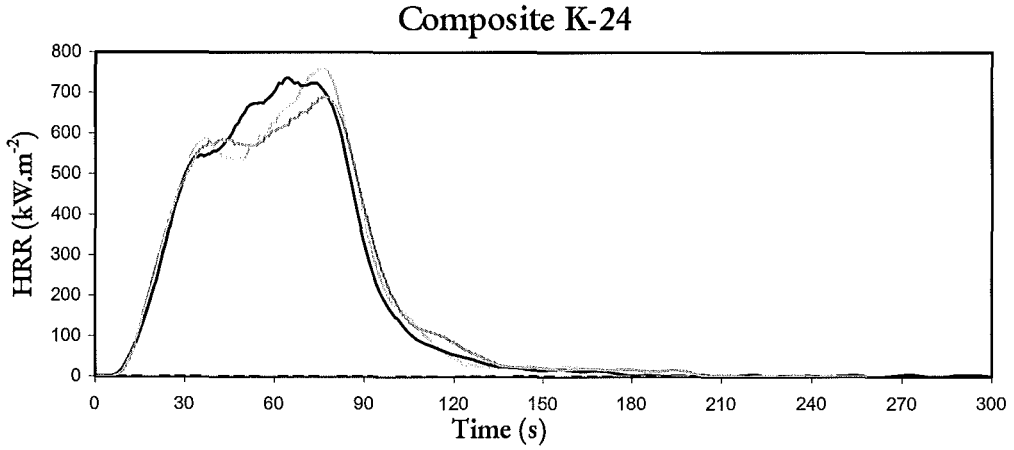

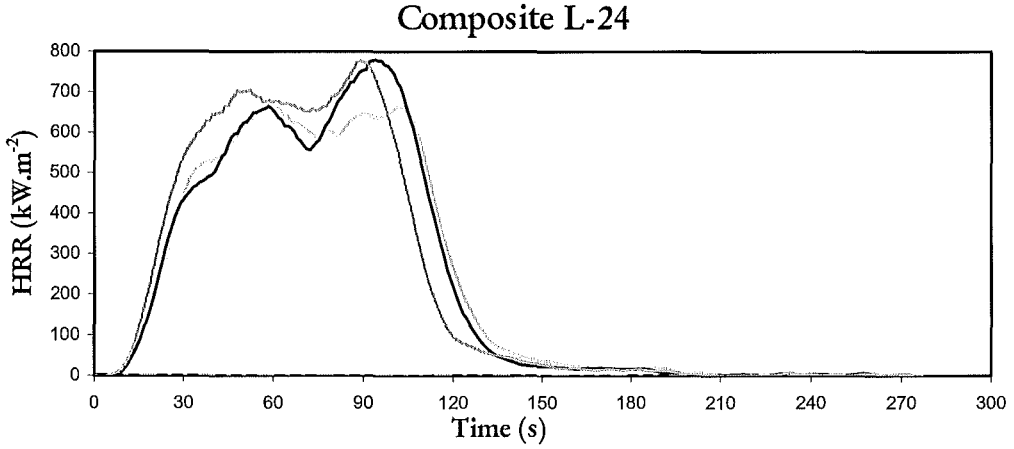

Fabric 25:

Composition: 100% Acrylic Chenille

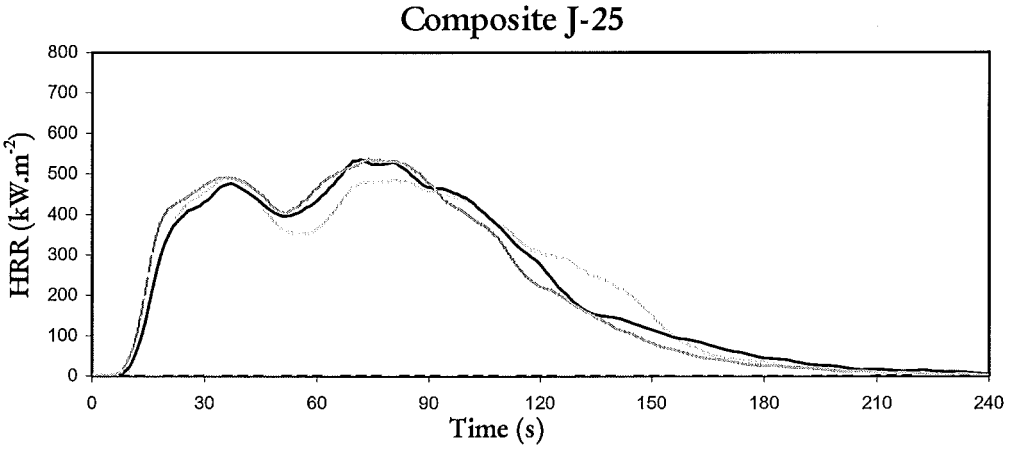

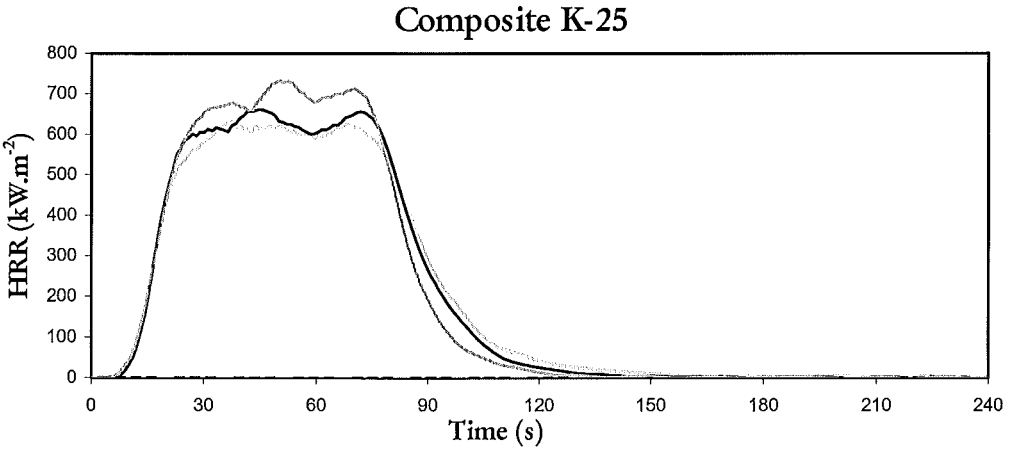

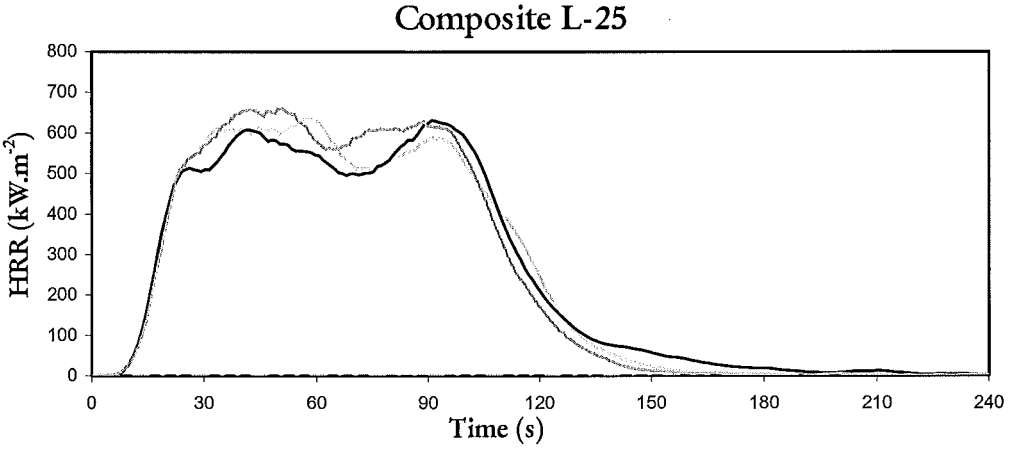

Fabric 26:

Composition: 100% Olefin

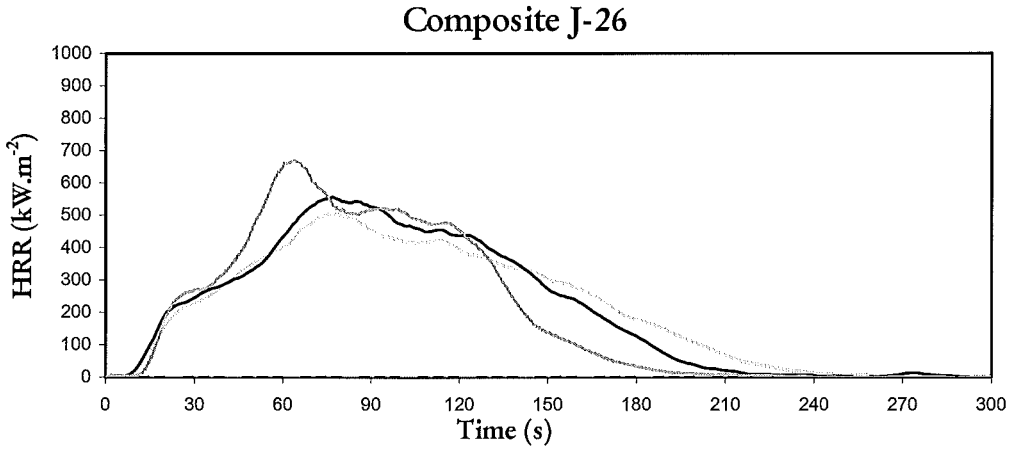

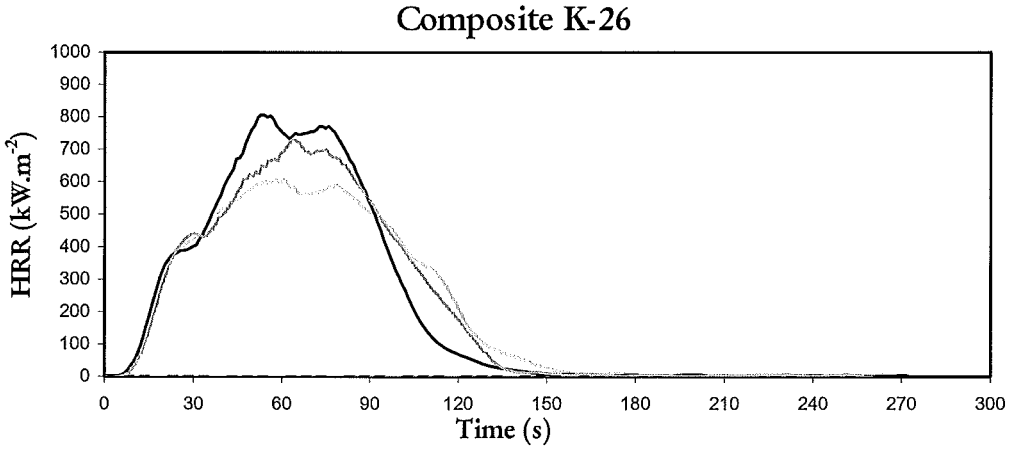

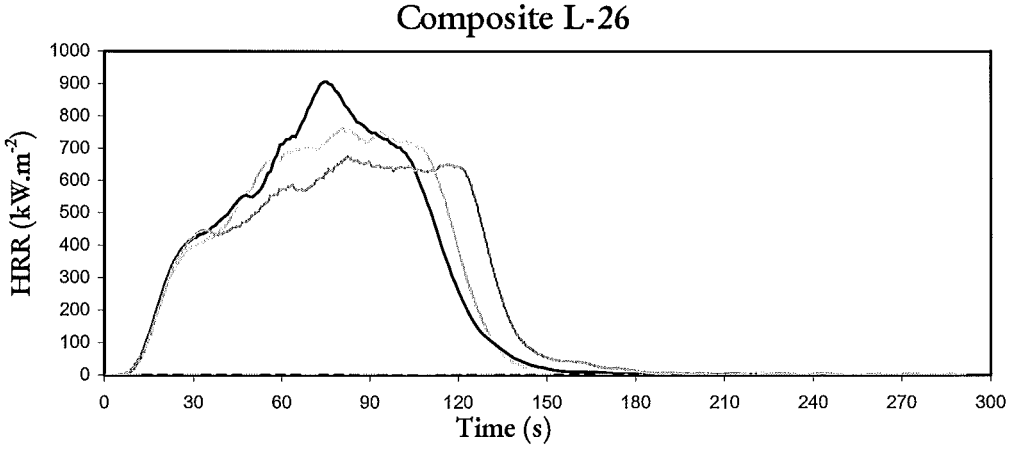

Fabric 29:

Composition: 42% Polyester; 58% Acrylic

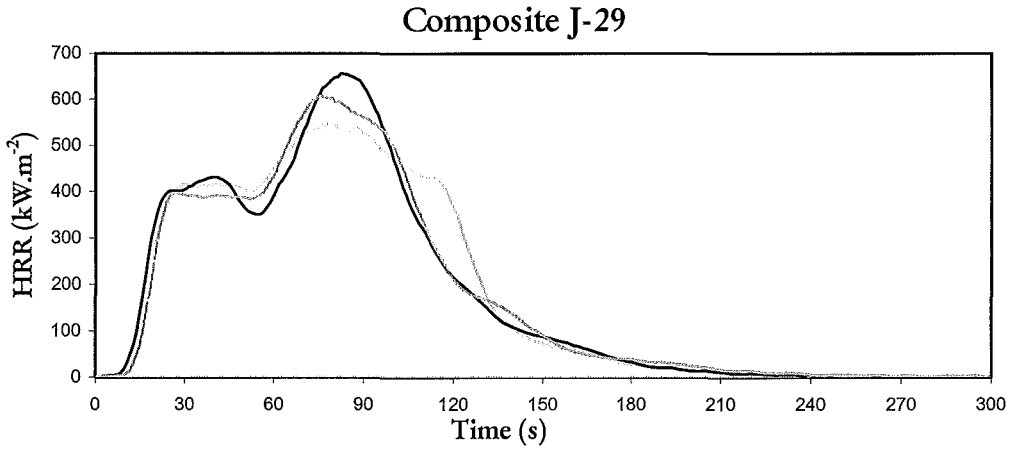

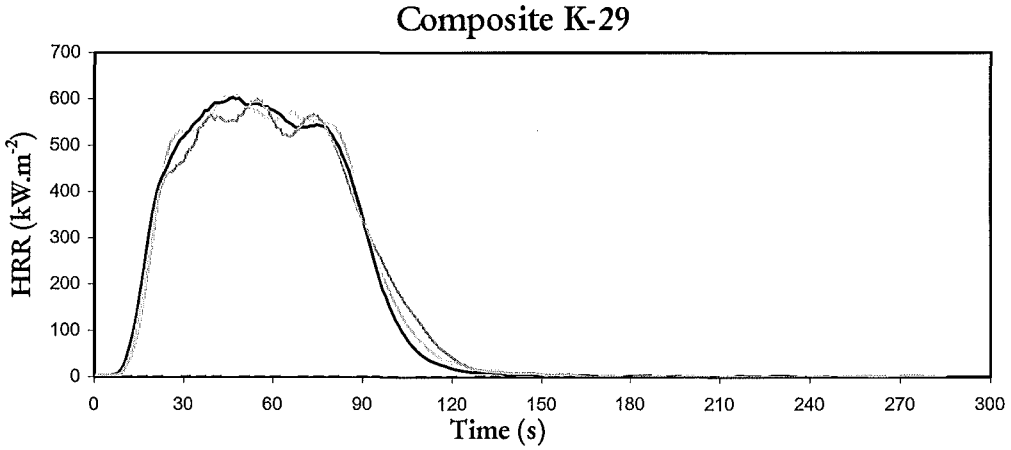

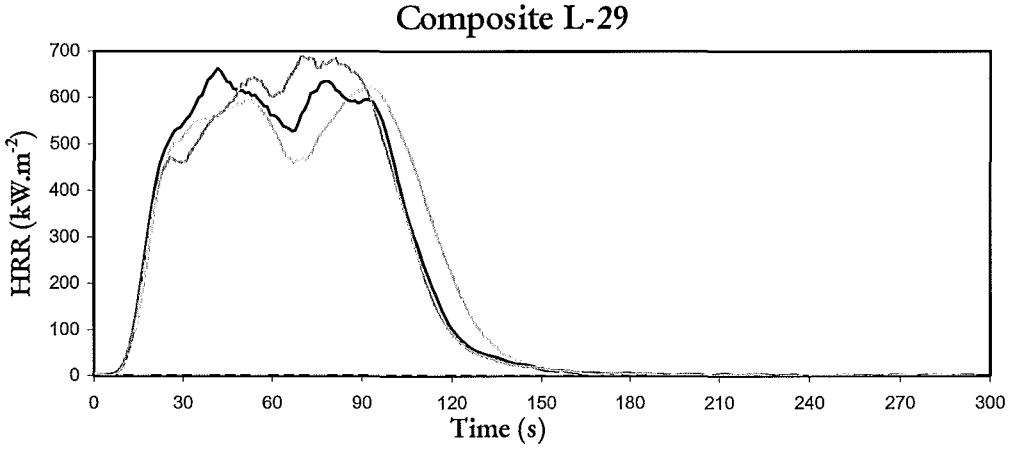

Fabric 31:

Composition: 50% Polyester, 50% Olefin

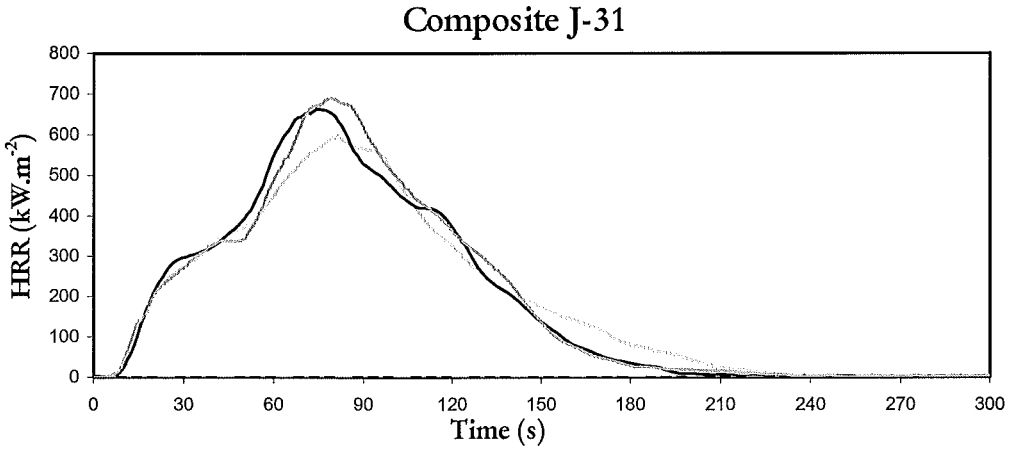

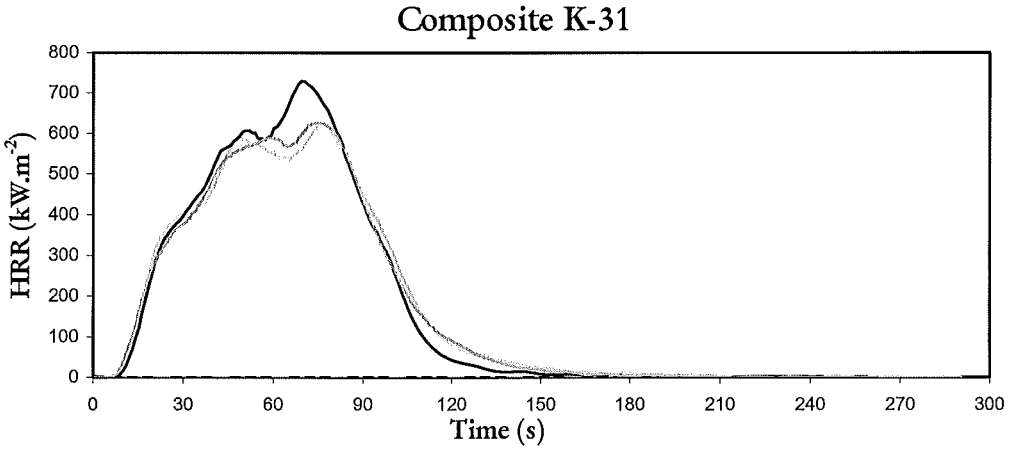

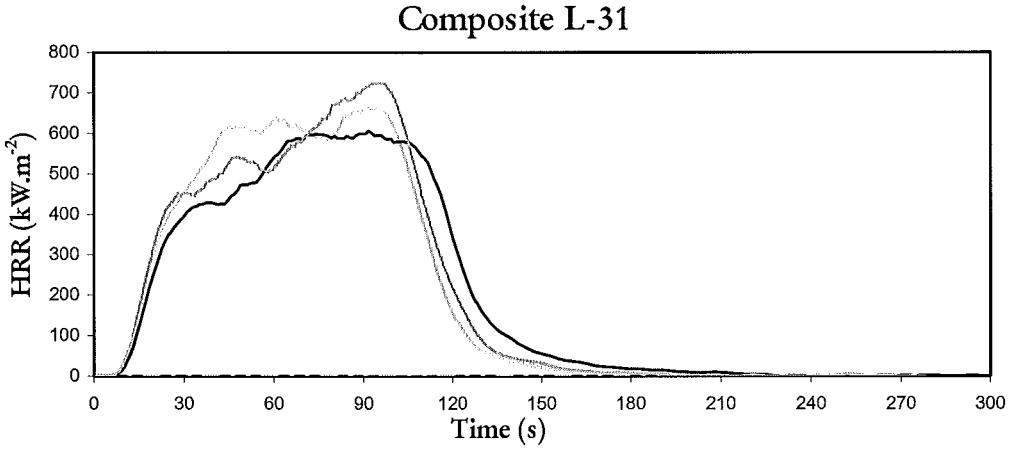

Fabric 33:

Composition: 60% Polypropylene, 40% Polyester

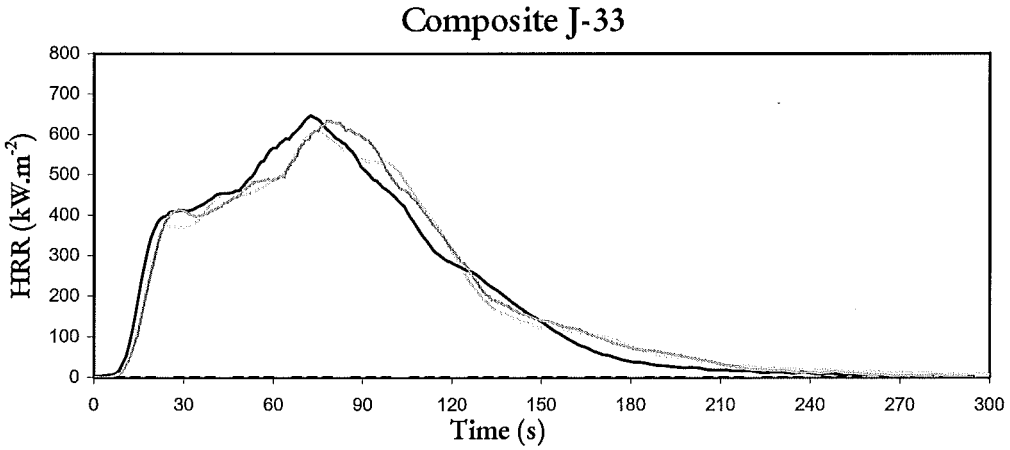

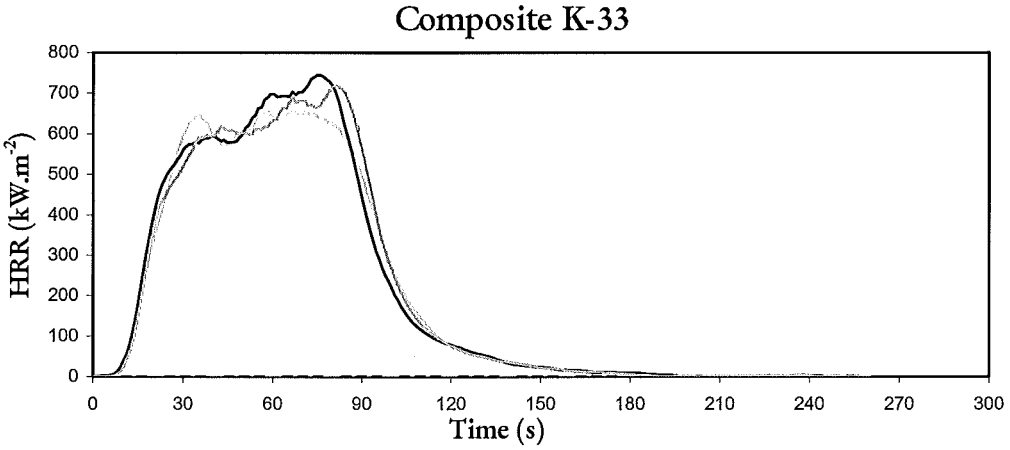

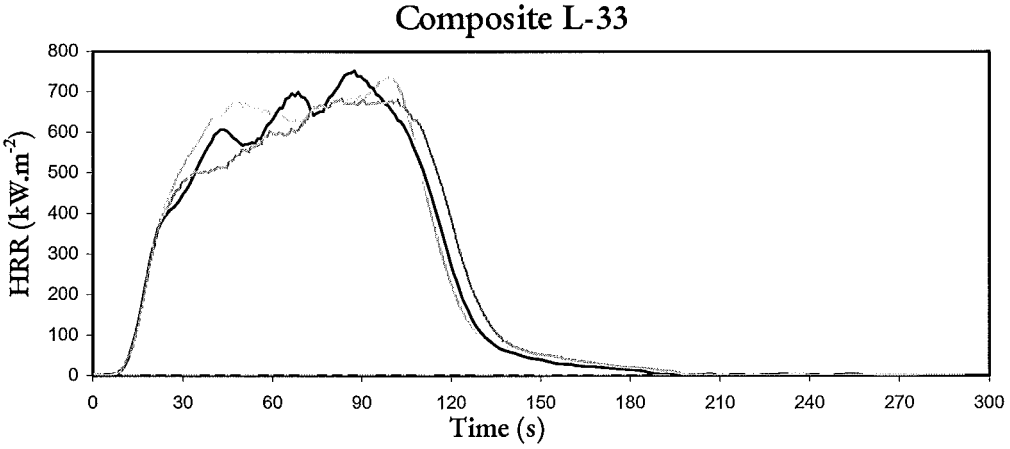

Fabric 35:

Composition: 43% Polyester, 41% Acrylic, 16% Olefin

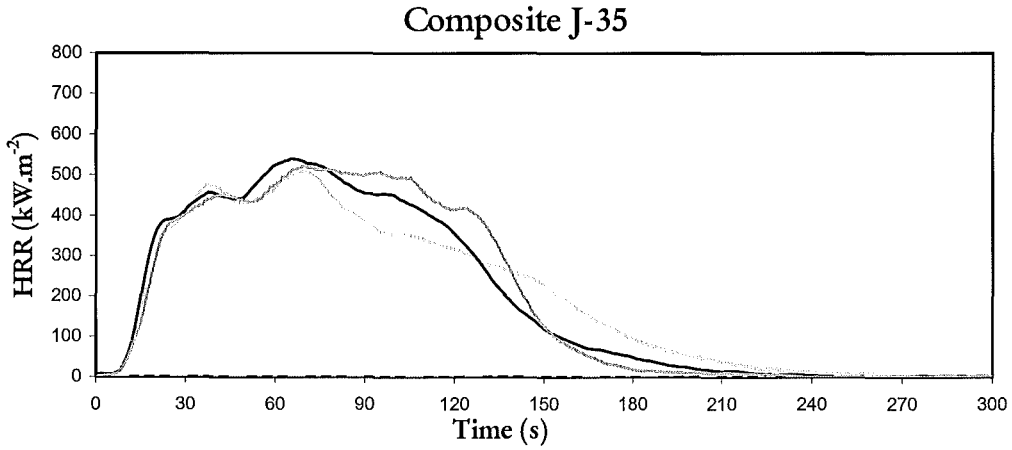

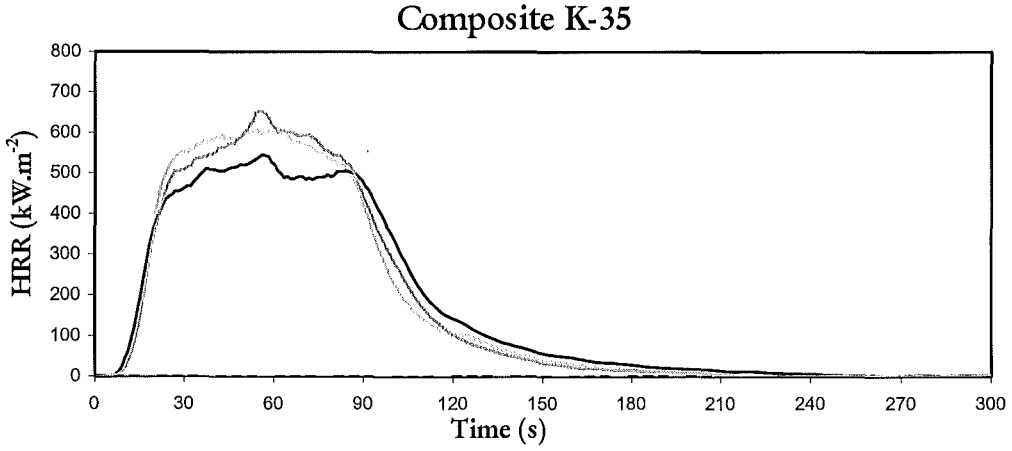

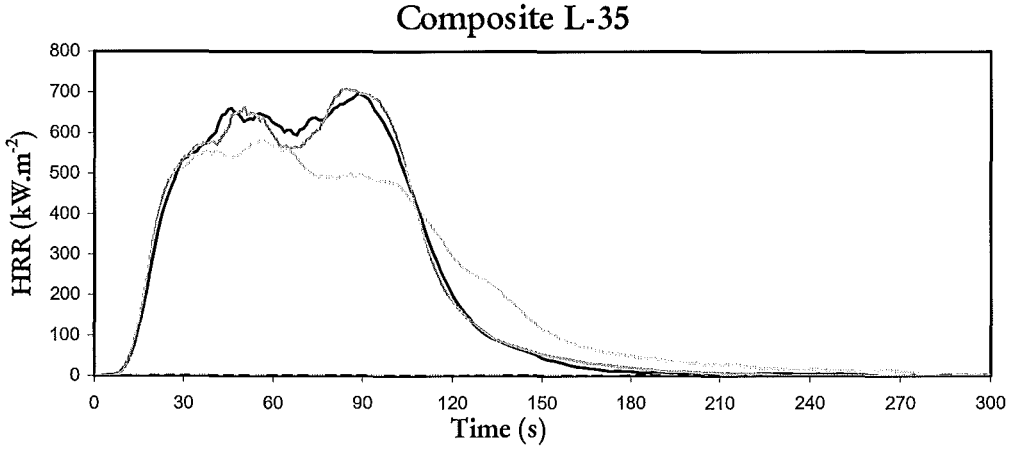

Charring fabrics

Fabric 27:

Composition: 100% Nylon Pile

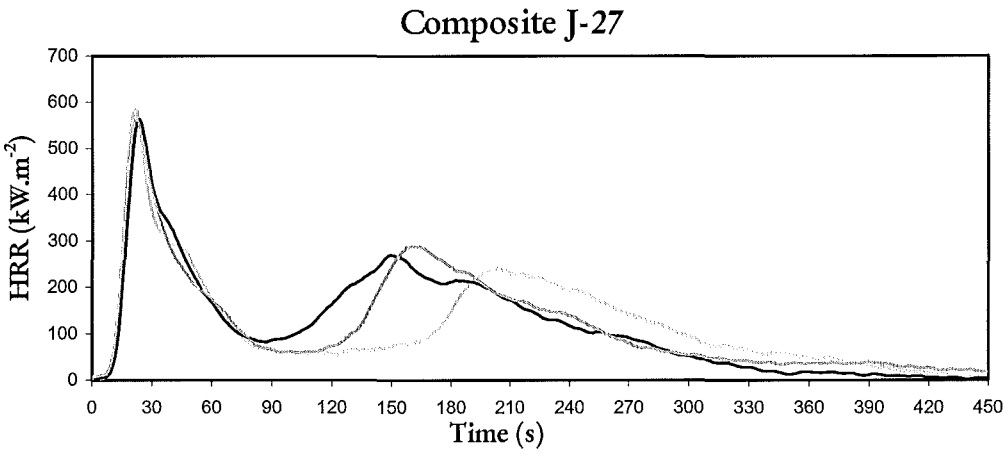

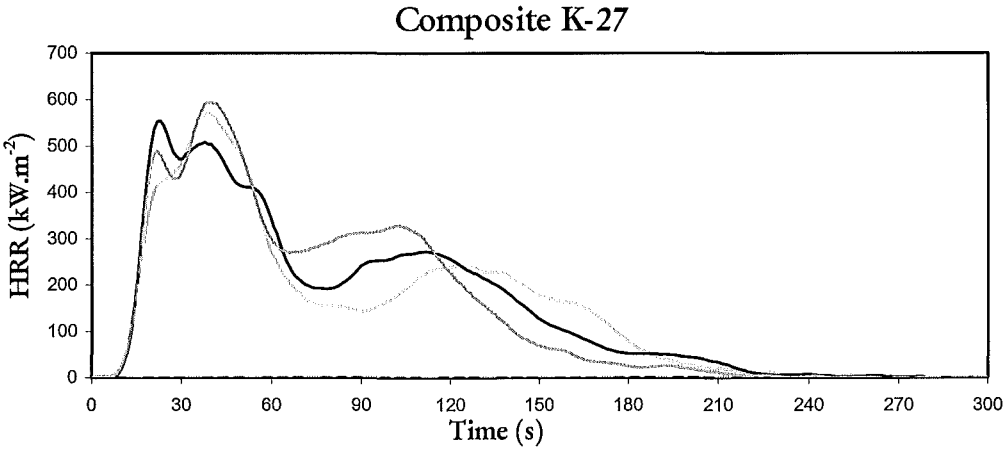

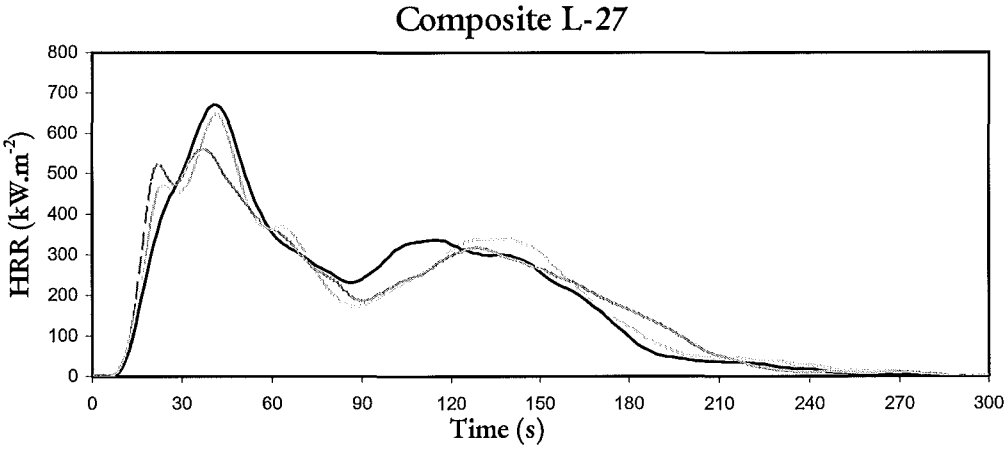

Fabric 28:

Composition: 100% Cotton

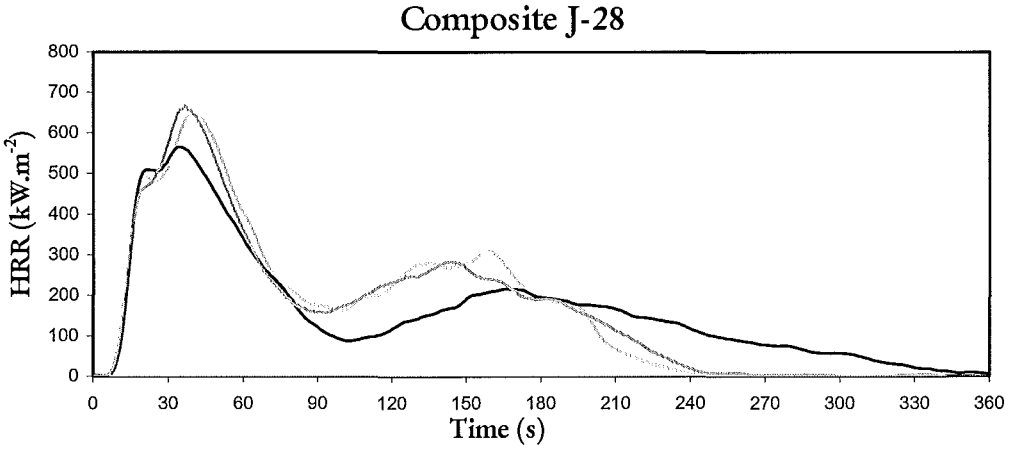

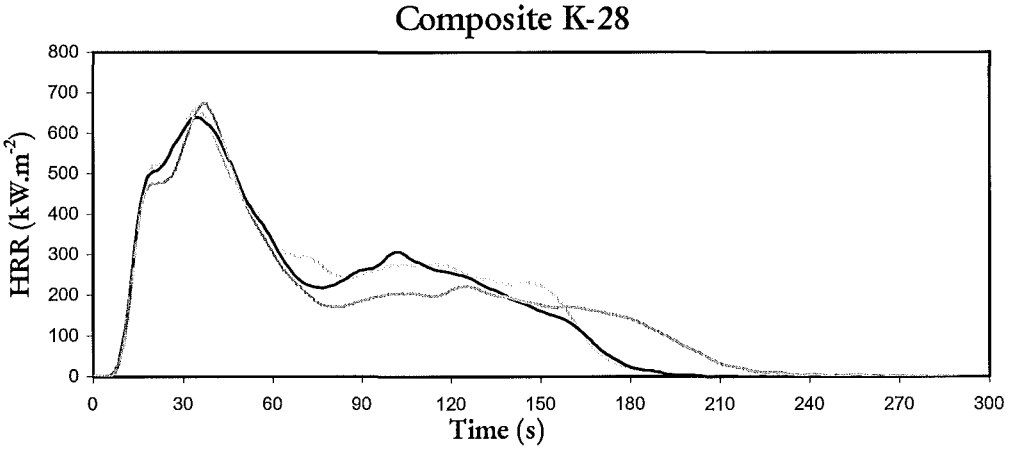

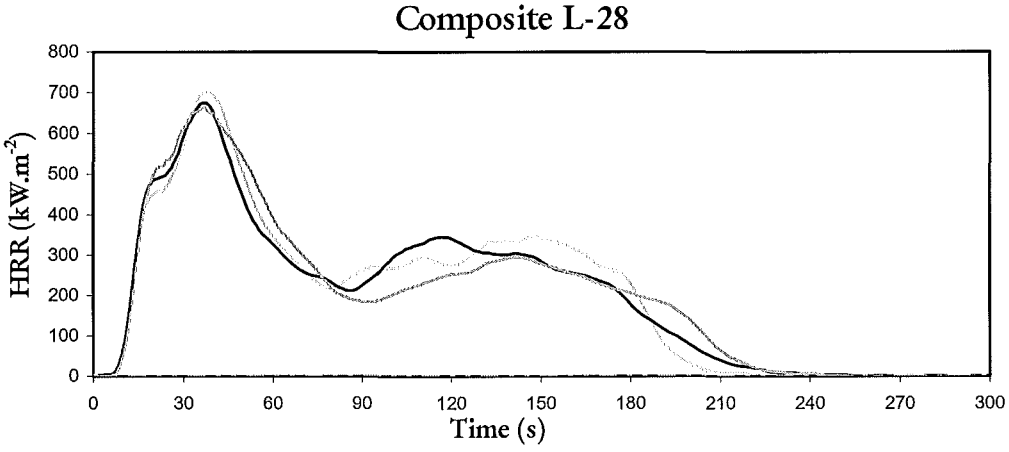

Charring/melting fabrics

Fabric 30:

Composition: 51% Polyester, 49% Cotton

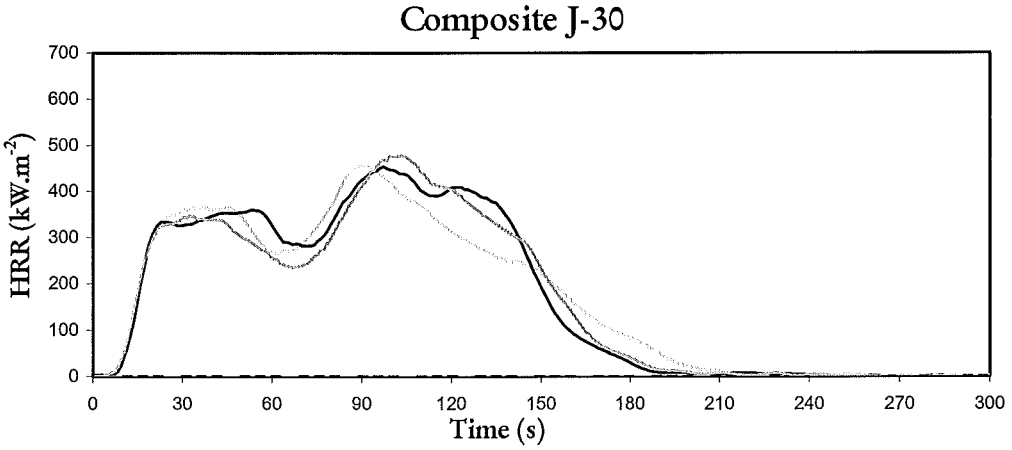

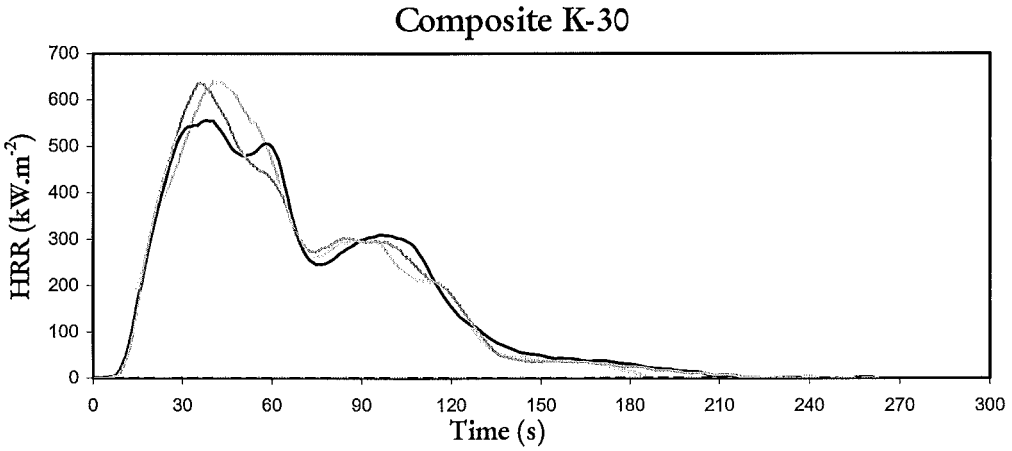

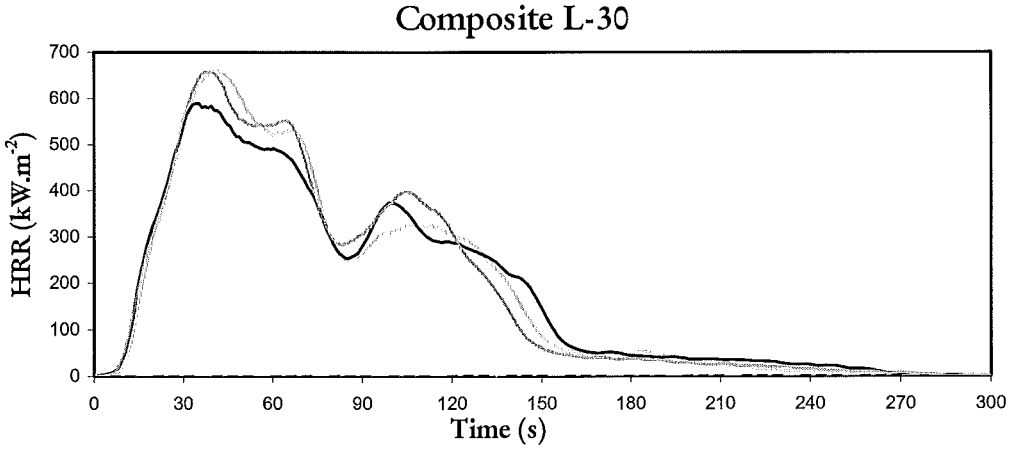

Fabric 32:

Composition: 51% Polyester, 49% Viscose

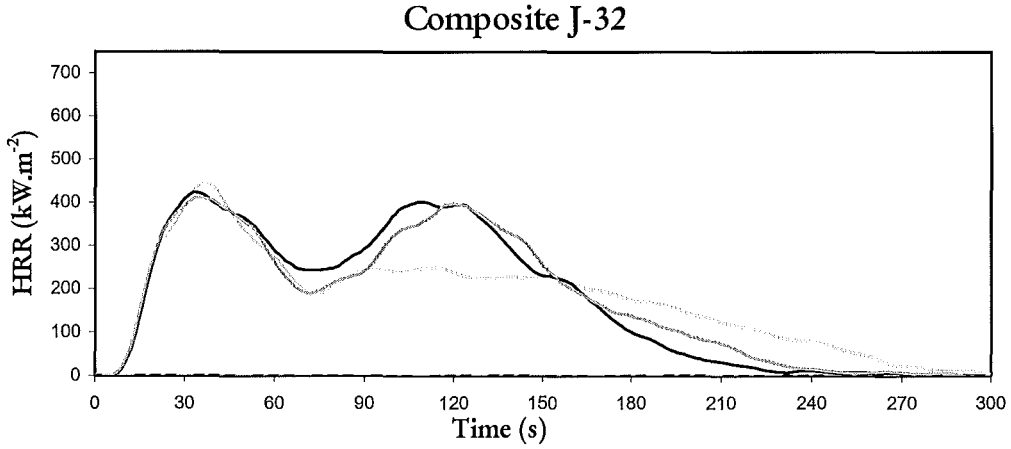

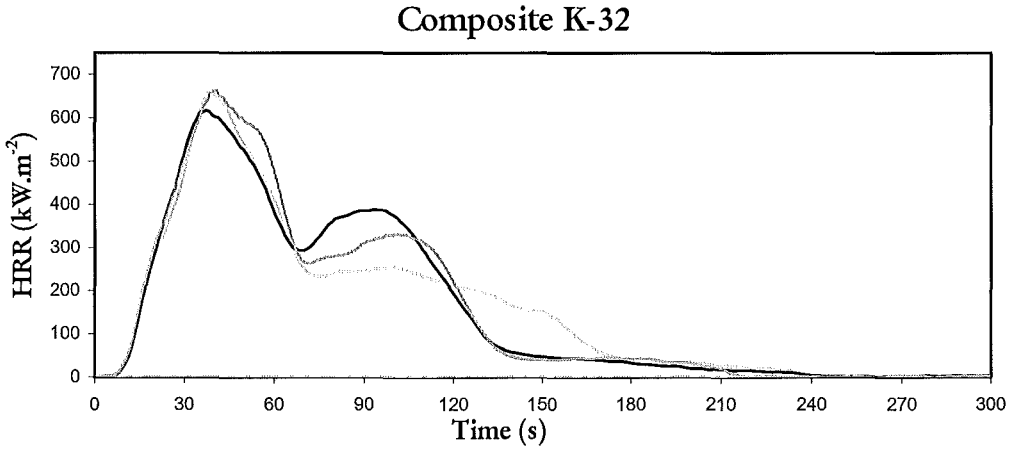

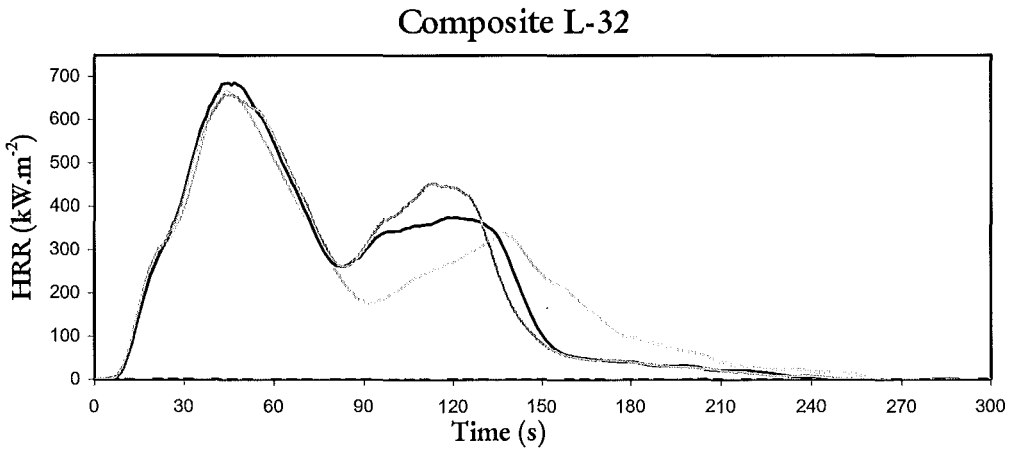

Fabric 34:

Composition: 31% Polyester, 21% Acrylic, 48% Cotton

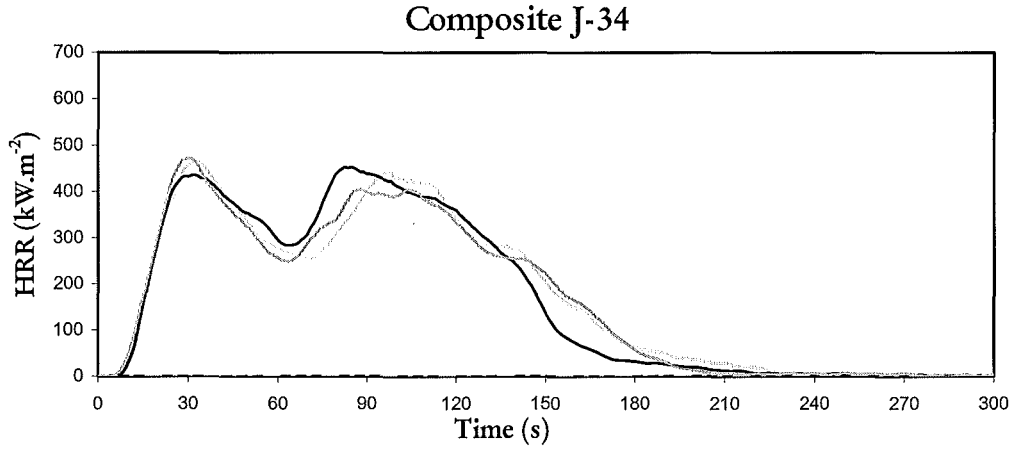

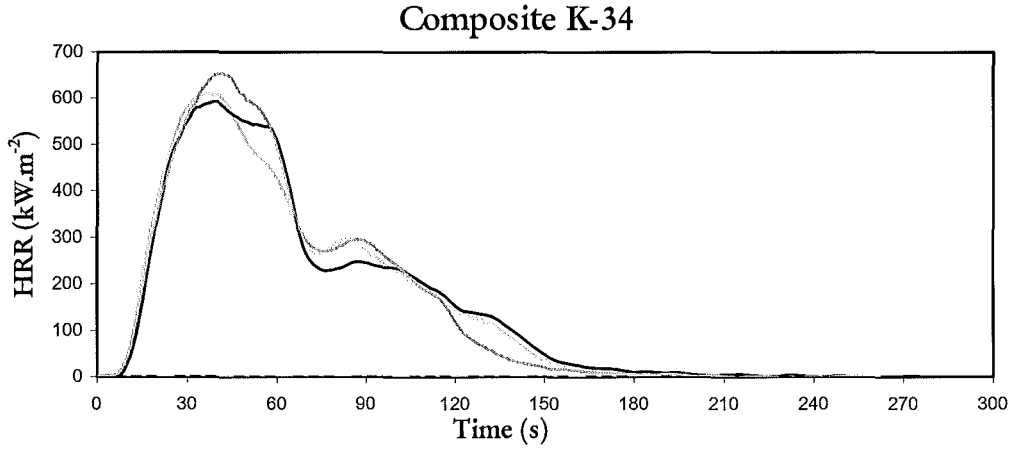

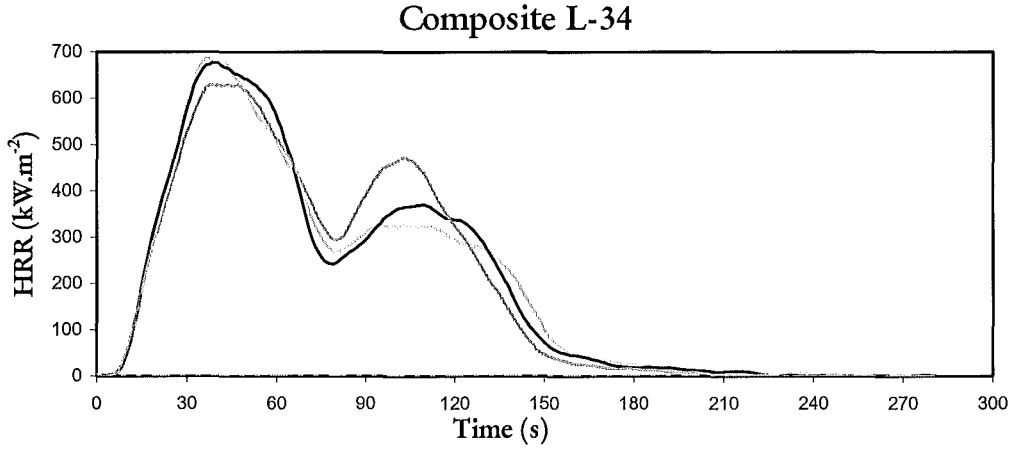

Fabric 36:

Composition: 39% Polyester, 40% Cotton, 21% Viscose

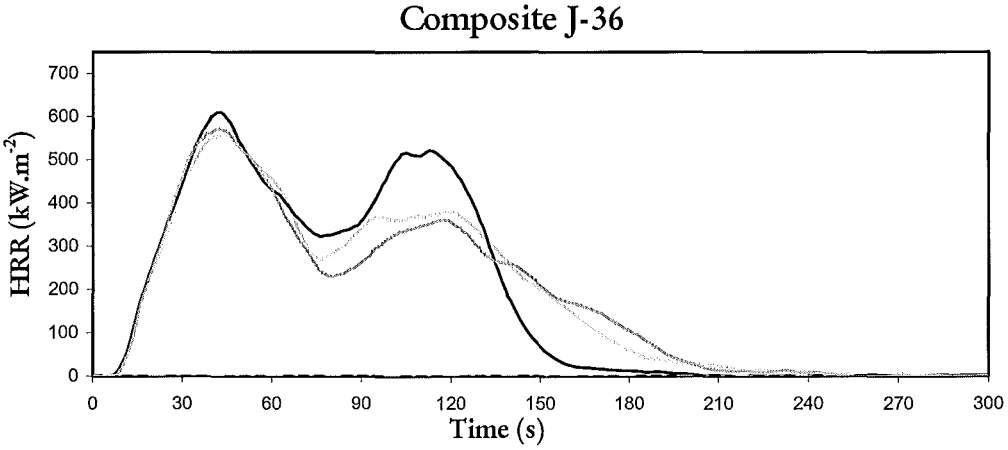

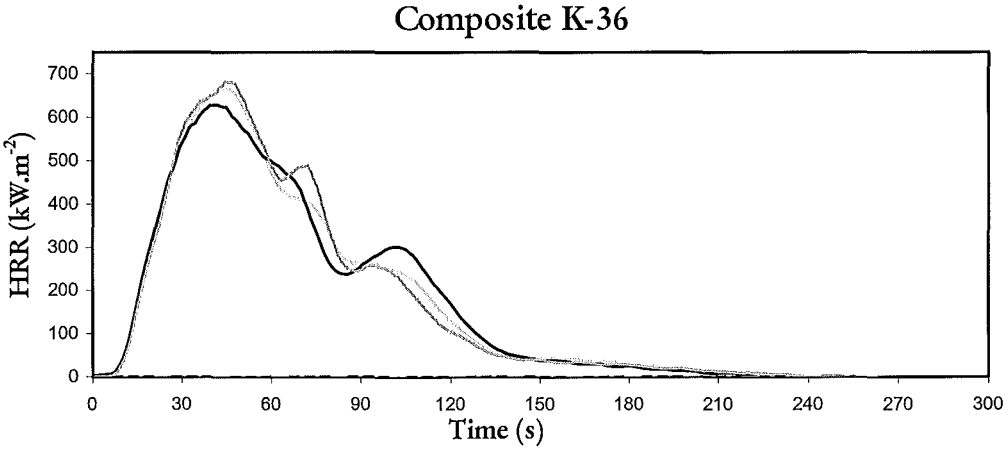

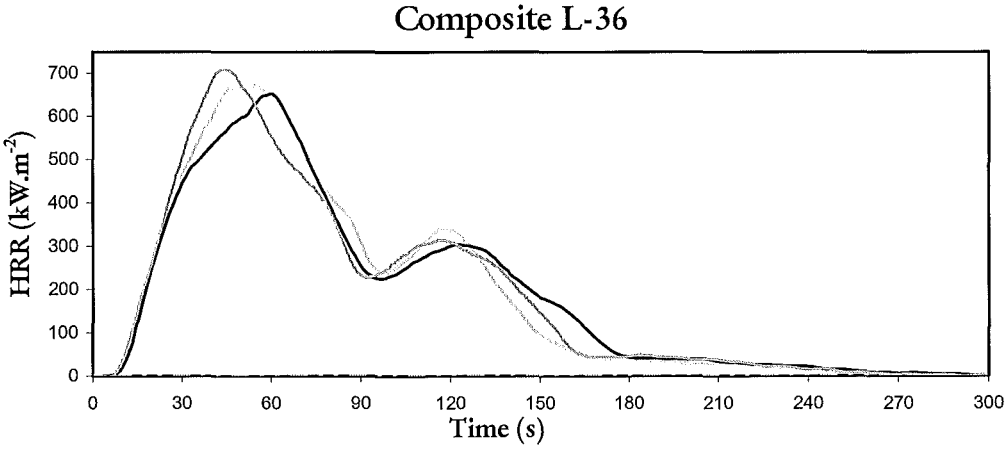

APPENDIX C: AVERAGING TRIPLICATE RUNS

Table C-1 shows the summarised reduced data for composite J-26 individual specimens and the mean values for the three runs. ISO 5660-1 and CBUF protocol require that the 180 second HRR average be within ± 10% of the arithmetic mean otherwise a further three runs are required (Clause 11.2.9, ISO 5660-1: 1993).

It is important to note that for some of the specimens the 300 second average HRR is not listed. This is because the length of the burning period and the time allowed for conditions to return to ambient conditions did not span this duration. This is indicated in the tabulated data in Appendix D as a dash in the corresponding column.

Table C-1: Tabulated data for composite K-27.

Parameter	*Units*	*Spec. 1*	*Spec. 2*	*Spec. 3*	*Mean*
m	g	24.4	25.0	24.6	24.67
t ig	s	16	16	16	16
q"	MJ/m^2	44.0	45.0	45.0	45
q" dot pk	kW/m^2	570	554	593	573
q" dot trough	kW/m^2	143	191	271	202
q" dot pk#2	kW/m^2	241	271	328	280
q" dot 60	kW/m^2	346	344	353	347
q" dot 120	kW/m^2	265	293	324	294
q" dot 180	kW/m^2	236	241	245	241
q" dot 300	kW/m^2	147	151	150	150
t pk, t=0	s	55	39	56	50
t pk, ign	s	39	23	40	34
dHc eff	MJ/kg	19.1	19.0	19.3	19.1
q" dot % diff	%				2%

APPENDIX D: AVERAGED DATA

Table D-1: Averaged Cone Calorimeter data

Specimen		J	K	L	J-23	K-23	L-23	J-24	K-24	L-24	J-25	K-25	L-25	J-26	K-26	L-26
m	(g)	23.84	15.02	21.11	32.88	24.29	30.67	35.32	30.25	33.06	35.06	26.58	32.19	30.99	22.92	28.50
ρ_{com}	(kg/m^3)	45	28	40	64.5	47.6	60.1	69.3	59.3	64.8	68.7	52.1	63.1	60.8	44.9	55.9
t_{ig}	(s)	18.7	4.0	5.0	16.0	9.7	11.7	16.0	12.0	12.7	26.7	13.7	13.0	17.7	10.7	9.7
t_{melt}	(s)		-			6			8			8			5	
q''_{ext}	(MJ m^{-2})	41	31	44	69	52	67	55	46	60	54	47	58	61	53	65
$\dot{q}''_{pk}$	(kW m^{-2})	489	578	655	709	742	730	384	729	742	520	676	642	576	714	781
$\dot{q}''_{pk\#1}$	(kW m^{-2})		-			N/A			N/A			N/A			N/A	
$\dot{q}''_{trough}$	(kW m^{-2})		-			N/A			N/A			N/A			N/A	
$\dot{q}''_{pk\#2}$	(kW m^{-2})		-			N/A			N/A			N/A			N/A	
$\dot{q}''_{60}$	(kW m^{-2})	131	310	291	293	386	347	224	377	382	321	457	423	231	392	343
$\dot{q}''_{120}$	(kW m^{-2})	260	255	348	433	435	511	279	384	481	376	385	460	361	434	504
$\dot{q}''_{180}$	(kW m^{-2})	221	172	243	358	298	372	253	263	335	292	259	323	324	299	365
$\dot{q}''_{300}$	(kW m^{-2})	137	-	-	230	-	226	183	-	-	181	-	-	203	-	-
$t_{pk,t=0}$	(s)	94.4	62.4	80.7	89.8	80.8	117.1	114.7	84.6	93.1	87.5	57.8	79.8	90.5	69.7	88.9
$t_{pkcalc=0}$	(s)	75.7	58.4	75.7	73.8	71.1	105.4	98.7	72.6	80.4	60.8	44.2	66.8	72.9	59.0	79.3
$\Delta h_{...}$	(MJ kg^{-1})	18.6	20.9	21.1	22.3	22.0	22.3	17.4	18.2	19.0	17.6	19.8	20.0	20.9	23.6	23.0
$\dot{q}''_{...}$	%	6%	1%	1%	13%	1%	0%	5%	0%	1%	1%	1%	0%	2%	1%	1%
diff (max)																

Table D-1 (Continued)

Specimen		J-27	K-27	L-27	J-28	K-28	L-28	J-29	K-29	L-29	J-30	K-30	L-30	J-31	K-31	L-31
m	(g)	33.37	24.67	30.56	36.10	28.19	33.41	32.75	24.75	30.39	32.00	24.11	29.53	30.59	22.71	28.34
ρ_{com}	(kg/m^3)	65	48	60	70.8	55.3	65.5	64.2	48.5	59.6	62.8	47.3	57.9	60.0	44.5	55.6
t_{ig}	(s)	31.0	16.0	17.3	19.0	17.7	18.7	14.7	11.3	11.7	16.0	11.3	14.7	10.7	9.0	12.7
t_{melt}	(s)		10			10			8			8			8	
q''_{tot}	(MJ m^{-2})	48	45	56	58	50	61	53	43	55	50	41	52	57	46	58
$\dot{q}''_{pk}$	(kW m^{-2})	570	573	626	624	658	681	604	603	657	462	611	637	650	660	664
$\dot{q}''_{pk\#1}$	(kW m^{-2})	570	573	626	624	658	681		N/A		354	305	366		N/A	
$\dot{q}''_{trough}$	(kW m^{-2})	66	202	197	139	210	413		N/A		261	260	262		N/A	
$\dot{q}''_{pk\#2}$	(kW m^{-2})	266	280	332	269	267	338		N/A		462	611	637		N/A	
$\dot{q}''_{60}$	(kW m^{-2})	261	347	361	399	401	413	291	389	401	253	377	393	247	346	350
$\dot{q}''_{120}$	(kW m^{-2})	176	294	313	297	324	338	386	353	442	311	327	375	386	370	454
$\dot{q}''_{180}$	(kW m^{-2})	175	241	293	274	271	318	291	239	305	276	237	293	311	255	320
$\dot{q}''_{300}$	(kW m^{-2})	166	150	188	194	167	204	178	-	-	169	-	-	191	-	-
$t_{pk,t=0}$	(s)	53.3	49.8	57.4	56.1	53.0	55.7	93.3	61.1	79.9	112.6	49.6	53.4	88.9	82.5	105.6
$t_{peak=0}$	(s)	22.3	33.8	40.1	37.1	35.3	37.0	78.7	49.7	68.3	96.6	38.3	38.7	78.3	73.5	93.0
$\Delta h_{...}$	(MJ kg^{-1})	16.6	19.1	19.3	18.2	19.5	19.7	18.4	19.3	19.9	16.9	17.2	17.7	20.3	21.1	21.1
$\dot{q}''_{...}$ %		17%	2%	2%	11%	4%	4%	2%	1%	0%	1%	1%	1%	2%	1%	1%
diff (max)																

Table D-1 (Continued)

Specimen		J-32	K-32	L-32	J-33	K-33	L-33	J-34	K-34	L-34	J-35	K-35	L-35	J-36	K-36	L-36
m	(g)	34.38	26.72	31.85	31.94	24.40	29.84	30.55	23.14	28.53	34.62	27.57	32.60	33.42	26.50	31.66
ρ_{com}	(kg/m^3)	67	52	62	62.6	47.8	58.5	59.9	45.4	55.9	67.9	54.1	63.9	65.5	52.0	62.1
t_{ig}	(s)	16.0	13.0	14.3	12.7	11.0	9.7	13.0	10.3	12.3	22.3	14.7	14.7	12.7	15.3	14.7
t_{melt}	(s)		10			7			8			10			10	
q''_{tot}	(MJ m^{-2})	52	45	55	60	52	64	51	41	53	58	50	61	54	43	54
$\dot{q}''_{pk}$	(kW m^{-2})	426	645	671	629	706	723	463	619	664	523	602	661	580	659	678
$\dot{q}''_{pk\ \#1}$	(kW m^{-2})	426	645	671		N/A		463	619	664		N/A		580	659	678
$\dot{q}''_{trough}$	(kW m^{-2})	206	263	233		N/A		263	255	269		N/A		345	248	232
$\dot{q}''_{pk\ \#2}$	(kW m^{-2})	349	325	388		N/A		434	280	390		N/A		351	274	319
$\dot{q}''_{60}$	(kW m^{-2})	268	376	386	319	418	385	279	398	419	321	392	397	345	405	395
$\dot{q}''_{120}$	(kW m^{-2})	271	335	360	411	422	500	322	325	387	385	385	458	351	348	375
$\dot{q}''_{180}$	(kW m^{-2})	260	252	301	322	291	356	276	234	297	316	275	334	296	249	301
$\dot{q}''_{300}$	(kW m^{-2})	175	156	187	201	-	-	170	-	-	199	167	204	182	-	-
$t_{pk,\ t=0}$	(s)	51.2	51.5	59.2	87.9	85.7	99.6	62.0	49.4	51.3	90.6	71.9	91.5	55.7	58.5	67.2
$t_{pk,adj\ t=0}$	(s)	35.2	38.5	44.8	75.3	74.7	89.9	49.0	39.0	39.0	68.2	57.2	76.9	43.0	43.2	52.5
Δh_{comb}	(MJ kg^{-1})	16.5	17.2	17.7	20.4	22.3	22.2	17.8	18.2	18.8	19.3	20.3	20.5	17.3	16.3	17.1
$\dot{q}''_{t=tig}$	%	8%	1%	3%	1%	1%	1%	0%	0%	1%	2%	1%	2%	2%	0%	0%
diff (max)																

APPENDIX E: MODEL I FRAME AND SOFT MASS CALCULATIONS.

A qualitative description is provided on how the chair frames mass and volume of the foam/fabric is obtained. Tabulated data from Enright's research was used to provide estimates of fabric volume on the chair and frame mass.

Table E-1: Summary of non-cone calorimeter input data required by CBUF Model I, adopted from Enright's research data (Table 8 and Table 9).

Foam/fabric	A1	A2	A3	A4	A5	B6	C7	D8
m_{cone} (g)	30	16.2	17.7	19.4	22.7	28.1	21	20.4
ρ_{avg} (kg/m^3)	60	32.4	35.4	38.8	45.4	56.2	42	40.8
Single armchairs								
m_{soft} (kg)	5.13	4.8	5.1	5.09	5.23	5.39	5.34	7.13
V_{soft} (m^3)	0.086	0.148	0.144	0.131	0.115	0.096	0.127	0.175
$m_{comb.\ tot}$ (kg)	25	24.67	24.97	24.96	25.1	21.46	22.1	25.04
m_{frame} (kg)	19.87	19.87	19.87	19.87	19.87	16.07	16.76	17.91
Style code	{1}	{1}	{1}	{1}	{1}	{4}	{4}	{1}
Style fac. A	1.0	1.0	1.0	1.0	1.0	0.9	0.9	1.0
Style fac. B	1.0	1.0	1.0	1.0	1.0	0.9	0.9	1.0
Two-seat sofas								
m_{soft} (kg)	7.65	7.16				8.04	7.96	10.63
V_{soft} (m^3)	0.128	0.221				0.143	0.190	0.261
$m_{comb.\ tot}$ (kg)	32.38	32.38				28.17	32.96	37.34
m_{frame} (kg)	24.73	25.22				20.13	25	26.71
Style code	{2}	{2}				{2}	{2}	{2}
Style fac. A	1	1				1	1	1
Style fac. B	0.8	0.8				0.8	0.8	0.8

Table E-1 provides a summary of the foam and fabric composites used in the production of the chairs in Enright's research. The first row represents the foam and fabric that was used. Letters indicate the foam code and the numeric value the fabric code. Row 2 is the total mass of the small-scale specimen and hence row 3 is the average specimen density.

For each respective chair style, (ie armchair or two-seat sofa) m_{soft} is the mass of the soft combustible products on the chair frame. V_{soft} is the volume of the soft combustibles, which is found using the average composite density. The total mass of the chair is represented by $m_{comb.\ tot}$. The mass of the chair frame, m_{frame} is the difference between the total mass of the chair and mass of the soft combustibles. The style codes are the CBUF styles assigned to each char style with the corresponding style factors.

FIRE ENGINEERING RESEARCH REPORTS

95/1	Full Residential Scale Backdraft	I B Bolliger
95/2	A Study of Full Scale Room Fire Experiments	P A Enright
95/3	Design of Load-bearing Light Steel Frame Walls for Fire Resistance	J T Gerlich
95/4	Full Scale Limited Ventilation Fire Experiments	D J Millar
95/5	An Analysis of Domestic Sprinkler Systems for Use in New Zealand	F Rahmanian
96/1	The Influence of Non-Uniform Electric Fields on Combustion Processes	M A Belsham
96/2	Mixing in Fire Induced Doorway Flows	J M Clements
96/3	Fire Design of Single Storey Industrial Buildings	B W Cosgrove
96/4	Modelling Smoke Flow Using Computational Fluid Dynamics	T N Kardos
96/5	Under-Ventilated Compartment Fires - A Precursor to Smoke Explosions	A R Parkes
96/6	An Investigation of the Effects of Sprinklers on Compartment Fires	M W Radford
97/1	Sprinkler Trade Off Clauses in the Approved Documents	G J Barnes
97/2	Risk Ranking of Buildings for Life Safety	J W Boyes
97/3	Improving the Waking Effectiveness of Fire Alarms in Residential Areas	T Grace
97/4	Study of Evacuation Movement through Different Building Components	P Holmberg
97/5	Domestic Fire Hazard in New Zealand	KDJ Irwin
97/6	An Appraisal of Existing Room-Corner Fire Models	D C Robertson
97/7	Fire Resistance of Light Timber Framed Walls and Floors	G C Thomas
97/8	Uncertainty Analysis of Zone Fire Models	A M Walker
97/9	New Zealand Building Regulations Five Years Later	T M Pastore
98/1	The Impact of Post-Earthquake Fire on the Built Urban Environment	R Botting
98/2	Full Scale Testing of Fire Suppression Agents on Unshielded Fires	M J Dunn
98/3	Full Scale Testing of Fire Suppression Agents on Shielded Fires	N Gravestock
98/4	Predicting Ignition Time Under Transient Heat Flux Using Results from Constant Flux Experiments	A Henderson
98/5	Comparison Studies of Zone and CFD Fire Simulations	A Lovatt
98/6	Bench Scale Testing of Light Timber Frame Walls	P Olsson
98/7	Exploratory Salt Water Experiments of Balcony Spill Plume Using Laser Induced Fluorescence Technique	E Y Yii
99/1	Fire Safety and Security in Schools	R A Carter

99/2	A Review of the Building Separation Requirements of the New Zealand Building Code Acceptable Solutions	J M Clarke
99/3	Effect of Safety Factors in Timed Human Egress Simulations	K M Crawford
99/4	Fire Response of HVAC Systems in Multistorey Buildings: An Examination of the NZBC Acceptable Solutions	M Dixon
99/5	The Effectiveness of the Domestic Smoke Alarm Signal	C Duncan
99/6	Post-flashover Design Fires	R Feasey
99/7	An Analysis of Furniture Heat Release Rates by the Nordtest	J Firestone
99/8	Design for Escape from Fire	I J Garrett
99/9	Class A Foam Water Sprinkler Systems	D B Hipkins
99/10	Review of the New Zealand Standard for Concrete Structures (NZS 3101) for High Strength and Lightweight Concrete Exposed to Fire	M J Inwood
99/12	An Analytical Model for Vertical Flame Spread on Solids: An Initial Investigation	G A North
99/13	Should Bedroom Doors be Open or Closed While People are Sleeping? - A Probabilistic Risk Assessment	D L Palmer
99/14	Peoples Awareness of Fire	S J Rusbridge
99/15	Smoke Explosions	B J Sutherland
99/16	Reliability of Structural Fire Design	JKS Wong
99/17	Heat Release from New Zealand Upholstered Furniture	T Enright
00/1	Fire Spread on Exterior Walls	FNP Bong
00/2	Fire Resistance of Lightweight Framed Construction	PCR Collier
00/3	Fire Fighting Water: A Review of Fire Fighting Water Requirements (A New Zealand Perspective)	S Davis
00/4	The Combustion Behaviour of Upholstered Furniture Materials in New Zealand	H Denize
00/5	Full-Scale Compartment Fire Experiments on Upholstered Furniture	N Girgis
00/6	Fire Rated Seismic Joints	M James
00/7	Fire Design of Steel Members	K R Lewis
00/8	Stability of Precast Concrete Tilt Panels in Fire	L Lim
00/9	Heat Transfer Program for the Design of Structures Exposed to Fire	J Mason
00/10	An Analysis of Pre-Flashover Fire Experiments with Field Modelling Comparisons	C Nielsen
00/11	Fire Engineering Design Problems at Building Consent Stage	P Teo
00/12	A Comparison of Data Reduction Techniques for Zone Model Validation	S Weaver
00/13	Effect of Surface Area and Thickness on Fire Loads	H W Yii
00/14	Home Fire Safety Strategies	P Byrne
00/15	Accounting for Sprinkler Effectiveness in Performance Based Design of Steel Buildings in Fire	M Feeney

00/16	**A Guideline for the Fire Design of Shopping Centres**	**J M McMillan**
01/1	**Flammability of Upholstered Furniture Using the Cone Calorimeter**	**A Coles**
01/2	**Radiant Ignition of New Zealand Upholstered Furniture Composites**	**F Chen**
01/3	**Statistical Analysis of Hospitality Industry Fire Experience**	**T Y A Chen**
01/4	**Performance of Gypsum Plasterboard Assemblies Exposed to Real Building Fires**	**B H Jones**
01/5	**Ignition Properties of New Zealand Timber**	**C K Ngu**
01/6	**Effect of Support Conditions on Steel Beams Exposed of Fire**	**J Seputro**
01/7	**Validation of an Evacuation Model Currently Under Development**	**A Teo**
01/8	**2-D Analysis of Composite Steel - Concrete Beams in Fire**	**R Welsh**
01/9	**Contribution of Upholstered Furniture to Residential Fire Fatalities in New Zealand**	**C R Wong**
01/10	**The Fire Safety Design of Apartment Buildings**	**S Wu**

School of Engineering
University of Canterbury
Private Bag 4800, Christchurch, New Zealand

Phone 643 364-2250
Fax 643 364-2758

10 September 2001

New Zealand Immigration Service
Department of Labour
P O Box 22-111
CHRISTCHURCH

Dear Sir/Madam

Dr Kurt Paterson has been offered a position as Visiting Lecturer in the Department of Civil Engineering at the University of Canterbury for a period commencing 15 January 2002 to 15 August 2002. This position involves the teaching the course "Environmental Monitoring and Measurement Analysis" to our postgraduate engineering students.

Appended is the information that we surmise you need to consider the request for his visit to New Zealand. I hope that this provides you with necessary information. Should you require any further information, please contact me.

Yours sincerely

Dr A H Buchanan
Head of Civil Engineering

c.c. Dr M Milke

INFORMATION ON APPLICATION OF DR KURT PATERSON

1. **Employer**

Department of Civil Engineering
University of Canterbury
Private Bag 4800
Christchurch, New Zealand
Tel: 03-364-2259; Fax: 03-364-2758

2. **Employee's Name**

Dr Kurt Paterson
Department of Civil and Environmental Engineering
Michigan Technological University
Houghton MI 49931-1295
USA

3. **Job Description**

(a) *Title*
Lecturer

(b) *Type of Work*
Lecturing, providing tuition, setting and marking assignments and tests

(c) *Details of Salary and Conditions*
Salary: $NZ5,000 (12 weeks duration and has 36 hours of lectures)
Other University conditions

(d) *Qualifications required*
Postgraduate lecturing experience in environmental engineering
Research experience

(e) *Duration of Position*
15 January 2002 - 15 August 2002

(f) *Attempts to recruit from within New Zealand*
Limited professionals available world-wide, none available in New Zealand.

10 September 2001

Dr Kurt Paterson
Department of Civil and Environmental Engineering
Michigan Technological University
Houghton MI 49931-1295
USA

Dear Dr Paterson

I would like to offer you a position as Visiting Lecturer in the Department of Civil Engineering at the University of Canterbury for a six month period commencing in February 2002. This letter should provide the details needed by the New Zealand Immigration Service and you should include this letter along with your application for a work visa.

Should you accept this offer, the position involves the teaching of a postgraduate course on"Environmental Monitoring and Measurement Analysis". We would like your visa to extend from 1 February 2002 to 1 August 2002 to allow us some flexibility in terms of your starting and ending dates. As a Visiting Lecturer you would be expected to prepare course material, deliver lectures and laboratories, and set/mark tests and assignments. In addition, you would be expected to interact with our students and staff to allow a full interchange of ideas. Your salary would be $NZ5,000

We look forward to hearing from you concerning this offer.

Yours sincerely

A H Buchanan
Head of Department